SCUOLA DI DOTTORATO
UNIVERSITÀ DEGLI STUDI DI MILANO-BICOCCA

Department of Earth and Environmental Sciences (DISAT)

PhD program in Chemical, Geological, and Environmental Sciences
Cycle XXXVIII

Curriculum in Terrestrial and Marine Environmental Sciences

CLIMATE CHANGE EFFECTS ON GROUNDWATER BUDGET AT REGIONAL AND BASIN SCALES

Surname: Redaelli Name: Agnese

Registration number: 808938

Tutor: Prof. Pasquero Claudia

Supervisor: Dott. Rotiroti Marco

Dott. Zanotti Chiara

Coordinator: Prof. Malusà Marco Giovanni

ACADEMIC YEAR 2024/2025

Table of Contents

Abstract

Groundwater systems are complex domains where multiple natural and anthropogenic processes interact, determining the various inputs and outputs of the systems. Current trends in climate change constitute a major threat to groundwater availability. The major concerns are usually related to the direct effects of climate change on groundwater recharge, driven by changes in temperature and precipitation patterns. Also, human activities often exert strong control over the groundwater budget, meaning that human responses to climate change can significantly affect groundwater resources.

The primary objective of this Ph.D. project is to examine the key processes governing the groundwater budget in a highly anthropized and intensively cultivated system, in order to identify and quantify the primary drivers of its vulnerability to climate change. To achieve this goal, the study focuses on an area of approximately 4,000 km^2 in the province of Brescia (N Italy). This area is considered representative of complex hydrogeological settings under strong human influence and includes two morainic amphitheaters, an alpine area, and a plain area that can be further subdivided into higher, middle, and lower plains.

The work was structured into two consecutive phases: an initial data-driven analysis followed by a model-based investigation. In the first phase, high-frequency data collected by online sensors in active drinking wells were exploited to explore the main processes governing the groundwater budget. Particularly, after a pre-processing aimed at extracting time series representative of static conditions from dynamic data, a time series analysis was carried out, with a particular focus on the seasonal patterns and on a comparative analysis of the system's dynamics under baseline conditions vs critical conditions (i.e., the 2022 meteorological drought).

In the second phase, a three-dimensional numerical model was developed to allow for the quantitative assessment of the main processes identified in the first phase, by simulating the key features of the system, including surface water bodies, springs, and human-driven processes such as irrigation practices and abstractions. Successively, two scenarios were run to compare the effects of potential climate change related-stressors

on the system. Results of the first phase clearly indicate that the two main potential stressors related to climate change are meteorological drought and changes in irrigation practices resulting from reduced surface water availability. Human processes play a significant role in the equilibrium of the aquifer system, and therefore human response to climate change in terms of water management can exacerbate the effects of climate change, in some cases exceeding the magnitude of the direct climatic impacts on groundwater resources. Particularly, results of the second phase reveal that in the study area, irrigation return flow from surface-water-fed irrigation constitutes the major component of aquifer recharge. Results reveal that a reduction in the irrigation return flow volumes over a two-year time frame, associated with potential changes in irrigation practices driven by surface water scarcity, may lead to significant aquifer depletion (corresponding to a total groundwater storage loss of 2.77×10^5 m^3/d over the simulated period), with repercussions on surface water bodies, springs, and groundwater-dependent ecosystems, effects that may exceed those directly induced by climatic variability.

Graphical Abstract

Chapter 1: Introduction

Groundwater constitutes a key resource and represents the largest reservoir of drinking water (UNESCO, 2022). Groundwater resource plays a crucial role in sustaining both human and ecological needs, supporting groundwater-dependent ecosystems, such as surface water bodies, springs, and wetlands that directly and indirectly depend on it. (Bhakar and Singh, 2019; Rohde et al., 2024; Saito et al., 2025).

Groundwater aquifers are complex systems whose equilibrium depends on several factors, with different processes governing the inputs (recharge) and the outputs (discharge). Groundwater recharge is a complex process fundamental for the system's sustainability and balance (Atawneh et al., 2021; Cook and Brunner, 2025). This process is determined by a combination of natural and anthropic inputs, including local precipitation, snowmelt, lateral recharge, interactions with surface water bodies, irrigation return flow, and managed aquifer recharge (Jasechko et al., 2014; Stigter et al., 2023). Conversely, the outputs of the groundwater system may include lateral groundwater flow between aquifers, human abstraction, springs discharge, and interactions with surface water bodies (Arce et al., 2023; Cook and Brunner, 2025; Davamani et al., 2024).

Each groundwater system represents a unique combination of these inputs and outputs, with each component playing a specific role in maintaining the system's overall balance. Each input and output responds differently to varying meteorological and climate forcings, exacerbating or mitigating its effects on groundwater systems (Amanambu et al., 2020a; Meixner et al., 2016). While natural processes can be thoroughly investigated and their response to variations in climate patterns can be simulated and, to a certain extent, forecasted, human activities can introduce additional modifications to the system that are difficult to define or anticipate a priori (Davamani et al., 2024; McNamara et al., 2025).

In this context, the only key to a comprehensive assessment of the climate change effects on groundwater is to reach a complete knowledge of the main processes governing the groundwater budget under the present conditions. This involves identifying and quantifying all the natural and anthropogenic factors in order to evaluate how they may

change under future climate change scenarios (Amanambu et al., 2020a; Pool et al., 2021; Taylor et al., 2013).

Most of the aquifers worldwide are located beneath highly anthropized territories, which have been intensively modified by urban or agricultural land use (Ndehedehe et al., 2023; Van der Gun, 2022). Therefore, considering only the meteoclimatic variables could lead to an incomplete representation of the systems' responses (Davamani et al., 2024). For this reason, socioeconomic response to the climatic changes must also be taken into account, and its potential effects on the groundwater budget must be identified and quantified (Söller et al., 2024; Stigter et al., 2023).

Recent projections highlight that surface temperature will increase until at least mid-century under all emissions scenarios, leading to drastic changes in the climate system, resulting in increased frequency and intensity of extreme events such as agricultural and ecological droughts (IPCC, 2023; Stigter et al., 2023). Historical records show an increasing trend in the severity of agricultural and ecological droughts worldwide in the last 120 years, as a consequence of amplified atmospheric evaporative demand (Vicente-Serrano et al., 2022). As reported in Vicente-Serrano et al. (2022), an increased drought severity is expected in areas in which advanced earth system models project reduced precipitation (e.g., southern North America and Central America, the Mediterranean region, western and southern Africa, and South Australia) but, more generally, in water-limited regions due to increasing temperature and atmospheric evaporative demand. Moreover, climate change is expected to severely affect groundwater storage globally. These impacts are not only related to predicted changes in precipitation but also involve other hydrological processes (e.g., evapotranspiration and snowmelt), worsened by over-pumping that could easily exceed the natural replenishment (Davamani et al., 2024; Wu et al., 2020).

These changes in natural hydrologic processes may not only lead to a reduction in natural recharge but also force significant changes in human water management (Vicente-Serrano et al., 2022). Human changes can, in turn, drive further impacts on the groundwater budget, creating a feedback loop between climate effects and human

responses (Amanambu et al., 2020a; Davamani et al., 2024; Taylor et al., 2013). All these considerations highlight the importance of understanding the influence of possible variation of meteorological and climate forcings, and the related human-mediated drivers on the groundwater budget using past meteoclimatic contexts as proxy for the future. This is crucial for long-term water resources management, with implications not only for the groundwater resource but also for the interconnected surface water system (Meixner et al., 2016; Scanlon et al., 2023).

References

Amanambu, A.C., Obarein, O.A., Mossa, J., Li, L., Ayeni, S.S., Balogun, O., Oyebamiji, A., Ochege, F.U., 2020. Groundwater system and climate change: Present status and future considerations. J. Hydrol. 589, 125163. https://doi.org/10.1016/j.jhydrol.2020.125163

Arce, M., Orellana-Macías, J.M., Causapé, J., Ramajo, J., Galè, C., Rossetto, R., 2023. Model-based assessment of interbasin groundwater flow in data scarce areas: the Gallocanta Lake endorheic watershed (Spain). Sustain. Environ. Res. 33. https://doi.org/10.1186/s42834-023-00192-9

Atawneh, D. Al, Cartwright, N., Bertone, E., 2021. Climate change and its impact on the projected values of groundwater recharge: A review. J. Hydrol. https://doi.org/10.1016/j.jhydrol.2021.126602

Bhakar, P., Singh, A.P., 2019. Groundwater Quality Assessment in a Hyper-arid Region of Rajasthan, India. Nat. Resour. Res. 28, 505–522. https://doi.org/10.1007/s11053-018-9405-4

Cook, P., Brunner, P., 2025. Quantification of Groundwater Recharge, Quantification of Groundwater Recharge. https://doi.org/10.62592/baus7081

Davamani, V., John, J.E., Poornachandhra, C., Gopalakrishnan, B., Arulmani, S., Parameswari, E., Santhosh, A., Srinivasulu, A., Lal, A., Naidu, R., 2024. A Critical Review of Climate Change Impacts on Groundwater Resources: A Focus on the Current Status, Future Possibilities, and Role of Simulation Models. Atmosphere (Basel). 15. https://doi.org/10.3390/atmos15010122

Intergovernmental Panel on Climate Change (IPCC), 2023. Climate Change 2021 – The Physical Science Basis. Cambridge University Press. https://doi.org/10.1017/9781009157896

Jasechko, S., Birks, S.J., Gleeson, T., Wada, Y., Fawcett, P.J., Sharp, Z.D., McDonnell, J.J., Welker, J.M., 2014. The pronounced seasonality of global groundwater

recharge. Water Resour. Res. 50, 8845–8867. https://doi.org/10.1002/2014WR015809

McNamara, I., Wolters, T., König, B., Rugen, A.L., Toro, M., Flörke, M., Wendland, F., 2025. Modelling the impacts of climate change on groundwater recharge patterns in northern Germany. J. Hydrol. Reg. Stud. 60. https://doi.org/10.1016/j.ejrh.2025.102507

Meixner, T., Manning, A.H., Stonestrom, D.A., Allen, D.M., Ajami, H., Blasch, K.W., Brookfield, A.E., Castro, C.L., Clark, J.F., Gochis, D.J., Flint, A.L., Neff, K.L., Niraula, R., Rodell, M., Scanlon, B.R., Singha, K., Walvoord, M.A., 2016. Implications of projected climate change for groundwater recharge in the western United States. J. Hydrol. 534, 124–138. https://doi.org/10.1016/J.JHYDROL.2015.12.027

Ndehedehe, C.E., Adeyeri, O.E., Onojeghuo, A.O., Ferreira, V.G., Kalu, I., Okwuashi, O., 2023. Understanding global groundwater-climate interactions. Sci. Total Environ. 904, 166571. https://doi.org/10.1016/j.scitotenv.2023.166571

Pool, S., Francés, F., Garcia-Prats, A., Pulido-Velazquez, M., Sanchis-Ibor, C., Schirmer, M., Yang, H., Jiménez-Martínez, J., 2021. From Flood to Drip Irrigation Under Climate Change: Impacts on Evapotranspiration and Groundwater Recharge in the Mediterranean Region of Valencia (Spain). Earth's Futur. 9, 1–20. https://doi.org/10.1029/2020EF001859

Rohde, M.M., Albano, C.M., Huggins, X., Klausmeyer, K.R., Morton, C., Sharman, A., Zaveri, E., Saito, L., Freed, Z., Howard, J.K., Job, N., Richter, H., Toderich, K., Rodella, A.S., Gleeson, T., Huntington, J., Chandanpurkar, H.A., Purdy, A.J., Famiglietti, J.S., Singer, M.B., Roberts, D.A., Caylor, K., Stella, J.C., 2024. Groundwater-dependent ecosystem map exposes global dryland protection needs. Nature 632, 101–107. https://doi.org/10.1038/s41586-024-07702-8

Saito, L., Byer, S., Munn, L., Badik, K., Provencher, L., McEvoy, D.J., Rohde, M.M., 2025. Strategies to Address Risks to Groundwater Dependent Ecosystems. Hydrol. Process. 39. https://doi.org/10.1002/hyp.70229

Scanlon, B.R., Fakhreddine, S., Rateb, A., de Graaf, I., Famiglietti, J., Gleeson, T., Grafton, R.Q., Jobbagy, E., Kebede, S., Kolusu, S.R., Konikow, L.F., Long, D., Mekonnen, M., Schmied, H.M., Mukherjee, A., MacDonald, A., Reedy, R.C., Shamsudduha, M., Simmons, C.T., Sun, A., Taylor, R.G., Villholth, K.G., Vörösmarty, C.J., Zheng, C., 2023. Global water resources and the role of groundwater in a resilient water future. Nat. Rev. Earth Environ. 4, 87–101. https://doi.org/10.1038/s43017-022-00378-6

Söller, L., Luetkemeier, R., Müller Schmied, H., Döll, P., 2024. Groundwater stress in Europe—assessing uncertainties in future groundwater discharge alterations due to water abstractions and climate change. Front. Water 6. https://doi.org/10.3389/frwa.2024.1448625

Stigter, T.Y., Miller, J., Chen, J., Re, V., 2023. Groundwater and climate change: threats and opportunities. Hydrogeol. J. 31, 7–10. https://doi.org/10.1007/s10040-022-02554-w

Taylor, R.G., Scanlon, B., Döll, P., Rodell, M., Van Beek, R., Wada, Y., Longuevergne, L., Leblanc, M., Famiglietti, J.S., Edmunds, M., Konikow, L., Green, T.R., Chen, J., Taniguchi, M., Bierkens, M.F.P., Macdonald, A., Fan, Y., Maxwell, R.M., Yechieli, Y., Gurdak, J.J., Allen, D.M., Shamsudduha, M., Hiscock, K., Yeh, P.J.F., Holman, I., Treidel, H., 2013. Ground water and climate change. Nat. Clim. Chang. https://doi.org/10.1038/nclimate1744

UNESCO, 2022. The United Nations World Water Development Report 2022: groundwater: making the invisible visible.

Van der Gun, J., 2022. Large Aquifer Systems Around the World, Large Aquifer Systems Around the World. https://doi.org/10.21083/978-1-77470-020-4

Vicente-Serrano, S.M., Peña-Angulo, D., Beguería, S., Domínguez-Castro, F., Tomás-Burguera, M., Noguera, I., Gimeno-Sotelo, L., El Kenawy, A., 2022. Global drought trends and future projections. Philos. Trans. R. Soc. A Math. Phys. Eng. Sci. 380. https://doi.org/10.1098/rsta.2021.0285

Wu, W.Y., Lo, M.H., Wada, Y., Famiglietti, J.S., Reager, J.T., Yeh, P.J.F., Ducharne, A., Yang, Z.L., 2020. Divergent effects of climate change on future groundwater availability in key mid-latitude aquifers. Nat. Commun. 11. https://doi.org/10.1038/s41467-020-17581-y

Chapter 2: Aims of the PhD project

The main aim of this work is to investigate the key processes governing the groundwater budget in a highly anthropized system within the province of Brescia (northern Italy), characterized by intensive agricultural activities, with the ultimate goal of identifying and quantifying the main drivers contributing to their vulnerability to varying meteoclimatic conditions. To reach this goal, two main approaches have been implemented. Firstly, a statistical time series approach was applied to perform, through a data mining of groundwater level time-series, a first assessment of the main processes governing the groundwater budget in different hydrogeological compartments. Successively, a modeling approach was applied to a pilot area to enable a precise quantification of the water volumes contributing to system inputs and outputs.

2.1 Data-driven approach

Several studies demonstrated how the analysis of groundwater level time series can be crucial in deepening the knowledge of hydrogeological systems and processes (e.g., (Anand et al., 2020; Bakker and Schaars, 2019; Colyer et al., 2021; Egidio et al., 2022; Fronzi et al., 2024; Lasagna et al., 2020; Meggiorin et al., 2021; Noori and Singh, 2021; Obergfell et al., 2019; Pathak and Dodamani, 2019; Ronchi et al., 2018; Sakizadeh et al., 2019; Sartirana et al., 2022; Treviño et al., 2023). Long and consistent time series of monitoring data are crucial for performing meaningful data mining and extracting useful information on the hydrogeological processes from recorded groundwater level data (Meggiorin et al., 2021; Taylor and Alley, 2001; Yang et al., 2025). However, such datasets are often challenging to obtain, manage, and process.

Recently, groundwater monitoring networks worldwide have been improved and are still under improvement, but the consequent extension of available data requires specific and reproducible procedures to manage all the stored data effectively (Fronzi et al., 2024; Yihdego and Khalil, 2017). Furthermore, regional monitoring networks managed by environmental agencies can hardly have the resolution needed to capture the complex heterogeneity of a territory (examples are reported in Asgharinia and Petroselli, 2020; Retike et al., 2022; Zaadnoordijk et al., 2019).

For groundwater studies, time series of static data (i.e., measurements taken after the well has been shut down long enough for the piezometric level to reach equilibrium) are normally required for extracting hydrogeological information. However, the collection of such data requires the drilling of ad hoc piezometers or measurements from active wells that need to be completely shut down for a time span that can last even several hours. Furthermore, one or more operators are required to measure the level in the well directly, limiting the number of monitoring wells that can be measured simultaneously. On the other hand, water suppliers often register for managing purposes long time series of groundwater levels and abstraction rates from online sensors recording in active drinking wells, which, if properly preprocessed, could become a valuable source of information on the hydrogeological processes. The data stored by water suppliers often have a high temporal resolution (e.g., one-minute temporal resolution) and are densely distributed over space, reaching even small aquifers and difficult areas frequently neglected by regional monitoring networks. Nevertheless, this data often lies unexploited due to a lack of a dedicated operating procedure that allows valuable information to be extracted. This issue was addressed in the first phase of this PhD project, through the definition of a dedicated procedure specifically proposed to extract meaningful time series from dynamic data collected from active wells, which could be considered representative of the natural conditions of the aquifers.

In most cases, when analyzing groundwater level time series, researchers worldwide focus on long-term trends of groundwater levels to identify signs of possible aquifer depletion or responses to long-term changes in precipitation patterns and climatic conditions. On the other hand, analyzing seasonal patterns has been proven effective in providing insights into the human and natural processes that influence the groundwater budget over time (Colyer et al., 2021; Lafare et al., 2016; Stahl et al., 2024; Wu et al., 2021). Indeed, many components of the groundwater budget exhibit pronounced seasonality. In this regard, Jasechko et al. (2014) pointed out that the recharge of groundwater systems by meteoric water worldwide has a strong seasonal feature. Similarly, anthropogenic processes influencing groundwater availability can also display marked seasonal variations. For example, agriculture, characterized by a strong seasonal

cyclicity, is considered one of the main human-driven factors affecting the groundwater balance: it has been proven to have multiple possible effects on groundwater worldwide, such as groundwater depletion in regions with primarily groundwater-fed irrigation or groundwater recharge from return flows where irrigation is fed by surface water (Dangar et al., 2021; Scanlon et al., 2023; Taylor et al., 2013). In this work, a procedure is proposed for evaluating seasonal patterns and their association with different processes governing the water budget and groundwater availability. The procedure is applied to investigate different hydrogeological contexts and water management practices.

In addition to understanding the processes that govern the groundwater budget under ordinary conditions, analyzing how groundwater responds to critical situations, such as hydrological droughts, can provide valuable information about the elements of the groundwater budget and how they respond to specific water management practices and policies.

Indeed, the analysis of critical situations can offer direct insights into what can be considered a plausible future in the context of climate change, not only through the analysis of the direct response of natural systems to variations in climate variables, but also through the study of the human response and the consequent adaptation measures taken to mitigate the effects of water scarcity (Ndehedehe et al., 2023; Stigter et al., 2023; Taylor et al., 2013). In fact, droughts have become frequent in recent decades and are projected to become much worse in the future as part of a warming world (Bevacqua et al., 2024; Montanari et al., 2023; Zhang et al., 2023). In this context, the year 2022 stood out for both temperature and precipitation anomalies. Intense and prolonged drought conditions affected several regions worldwide, resulting in devastating impacts on social, agricultural, and ecological sectors (Arias et al., 2024; Faranda et al., 2023; Liu et al., 2023; Weaver et al., 2023; Zhang et al., 2023). For this reason, in this work, the response to the 2022 meteorological drought is addressed, considering and disentangling all the possible aspects involved in the groundwater availability: a) direct effects of reduced precipitation and b) effects of the human response to surface water scarcity (i.e., increased abstraction and reduced surface-water-fed irrigation).

To summarize, the first phase of this PhD project was aimed at:

1. developing a procedure for the preprocessing of dynamic data resulting from online measurements in active drinking wells, to extract meaningful time series of groundwater levels;
2. analyzing the obtained groundwater level time series, with a focus on the seasonal patterns, to identify the main processes governing the groundwater budget under baseline conditions;
3. performing a comparative analysis of the seasonal dynamics during the 2022 hydrological drought against the baseline conditions (2013-2021) to get insights into the possible modifications induced by varying meteoclimatic forcings in the natural and human-mediated groundwater budget elements.

2.2 Model-based approach

Groundwater modeling is essential for managing water resources and constitutes a crucial tool for understanding complex subsurface hydrological systems. There are two main approaches to designing and solving groundwater models: the finite difference (FD) method and the finite element (FE) method. The FD method approximates the flow equation through differentiation, whereas the FE method adopts an integral approach. MODFLOW, developed by the United States Geological Survey (USGS), is the most-used and free FD code. FEFLOW, a proprietary, non-free numerical code, is the most-used FE code. In FD models, the differential equation is solved to calculate the unknown variable (e.g., hydraulic head) at the central points of the cells; in FE models, the hydraulic head solution is instead approximated using piecewise linear functions, with the distribution being approximated by a linear function for each element (Anderson et al., 2015; Spitz and Moreno, 1996; Wang and Anderson, 1982).

In this project, MODFLOW was selected as the numerical code to reconstruct a numerical groundwater flow model aimed at quantifying the main processes influencing the groundwater budget within the study area and investigating their feedback interconnections. This choice came as a consequence of MODFLOW's modular

structure, which allows flexibility in modeling and analyzing hydrogeological elements. In fact, it consists of a modular structure characterized by a main program supported by highly independent subroutines called 'packages'. Each package allows the simulation of a specific feature of a wide variety of hydrological systems, providing support in the analysis of their water budgets (Harbaugh, 2005; Kishor et al., 2025).

In a climate change context, numerical groundwater flow models have proven instrumental in predicting how aquifer systems respond to climate change perturbations, as they integrate climatic, hydrological, and hydrogeological data across spatial and temporal scales. In this way, a comprehensive quantitative understanding of groundwater-climate interactions can be obtained (Tsypin et al., 2025). In recent years, different authors have developed numerical models to investigate these interactions (Aslam et al., 2022; Christos et al., 2025; Das et al., 2024; Davamani et al., 2024; Dubois et al., 2021; Khadim et al., 2023; Mensah et al., 2022; Pool et al., 2021; Scibek et al., 2007). Dubois et al. (2021) provides an example of applying a regional-scale water-budget approach in a cold and humid climate, highlighting the complex responses of recharge, runoff, and evapotranspiration to warming and precipitation changes. Some scenarios were also simulated to analyze variations in groundwater levels and outflows in tropical regions (Khadim et al., 2023).

An important research gap concerns the adaptation of agricultural management systems to climate change, as these systems can significantly alter the groundwater budget. Globally, irrigation constitutes the largest consumer of freshwater resources, with 60-70% sourced from groundwater withdrawals, though local variations exist. (Amanambu et al., 2020b; Davamani et al., 2024; Guo and Li, 2024). Most of the world's large aquifer systems are located in regions with intensive agricultural activity, making them particularly vulnerable to both the direct effects of a changing climate and human-driven impacts related to changes in irrigation practices (Abd-Elaty et al., 2023; Ndehedehe et al., 2023). To preserve surface water and mitigate possible surface-water shortages, the transition from flood irrigation toward more efficient irrigation practices (e.g., drip-irrigation, sprinkler systems, or subsurface irrigation) is becoming widely applied

worldwide (Guo and Li, 2024; Pool et al., 2021). These methods can, in fact, reduce water consumption by up to 90% by delivering water directly to the plant's roots (Munir et al., 2018; Nikolaou et al., 2020). However, this change could significantly reduce the aquifer recharge. This highlights the need to consider irrigation-practice changes as one of the most relevant drivers of recharge variability to bear in mind while managing groundwater resources under changing climate conditions (Abd-Elaty et al., 2023; Pool et al., 2021; Van der Gun, 2022).

In this context, within this PhD project, the developed groundwater model was used to run two simulations specifically designed to investigate the aquifer's response to two hypothetical hydrological scenarios of practical interest. These scenarios, not intended to represent actual forecasts, were specifically designed to quantify and compare the effects of meteorological drought conditions and changes in irrigation management on the system. The main aim was to identify the primary driver of potential future aquifer depletion in a highly anthropized system with strong agricultural activity, thereby providing a useful tool for assessing system vulnerability.

To summarize, the second phase of this PhD project was aimed at:

1. developing and calibrating a numerical flow model of a complex hydrogeological system, representing not only the groundwater dynamics but also the main natural and anthropogenic processes influencing the water budget (i.e. surface water bodies, irrigation practices, human abstractions, lowland springs). This phase of the PhD project was carried out in cooperation with Prof. Daniel T. Feinstein from the University of Milwaukee-Wisconsin, and with Ph.D., P.H. Randall J. Hunt from the US Geological Survey in Madison;
2. exploiting the developed model to quantify the volumes of water exchanged within the system among its different components under baseline conditions;
3. designing and running two synthetic scenarios, aimed at quantifying the modifications induced on the water budget by the most important potential stressors, identified in the first phase of the work. The comparative analysis was

performed by quantifying storage losses as well as modifications in river and springs discharges.

References

Abd-Elaty, I., Fathy, I., Kuriqi, A., John, A.P., Straface, S., Ramadan, E.M., 2023. Impact of Modern Irrigation Methods on Groundwater Storage and Land Subsidence in High-water Stress Regions. Water Resour. Manag. 37, 1827–1840. https://doi.org/10.1007/s11269-023-03457-5

Amanambu, A.C., Obarein, O.A., Mossa, J., Li, L., Ayeni, S.S., Balogun, O., Oyebamiji, A., Ochege, F.U., 2020. Groundwater system and climate change: Present status and future considerations. J. Hydrol. 589, 125163. https://doi.org/10.1016/j.jhydrol.2020.125163

Anand, B., Karunanidhi, D., Subramani, T., Srinivasamoorthy, K., Suresh, M., 2020. Long-term trend detection and spatiotemporal analysis of groundwater levels using GIS techniques in Lower Bhavani River basin, Tamil Nadu, India. Environ. Dev. Sustain. 22, 2779–2800. https://doi.org/10.1007/s10668-019-00318-3

Anderson, M.P., Woessner, W.W., Hunt, R.J., 2015. Applied Groundwater Modeling. Elsevier. https://doi.org/10.1016/C2009-0-21563-7

Arias, P.A., Rivera, J.A., Sörensson, A.A., Zachariah, M., Barnes, C., Philip, S., Kew, S., Vautard, R., Koren, G., Pinto, I., Vahlberg, M., Singh, R., Raju, E., Li, S., Yang, W., Vecchi, G.A., Otto, F.E.L., 2024. Interplay between climate change and climate variability: the 2022 drought in Central South America. Clim. Change 177, 1–22. https://doi.org/10.1007/s10584-023-03664-4

Asgharinia, S., Petroselli, A., 2020. A comparison of statistical methods for evaluating missing data of monitoring wells in the Kazeroun Plain, Fars Province, Iran. Groundw. Sustain. Dev. 10, 100294. https://doi.org/10.1016/j.gsd.2019.100294

Aslam, R.A., Shrestha, S., Usman, M.N., Khan, S.N., Ali, S., Sharif, M.S., Sarwar, M.W., Saddique, N., Sarwar, A., Ali, M.U., Arshad, A., 2022. Integrated SWAT-MODFLOW Modeling-Based Groundwater Adaptation Policy Guidelines for Lahore, Pakistan under Projected Climate Change, and Human Development Scenarios. Atmosphere (Basel). 13. https://doi.org/10.3390/atmos13122001

Bakker, M., Schaars, F., 2019. Solving Groundwater Flow Problems with Time Series Analysis: You May Not Even Need Another Model. Groundwater 57, 826–833. https://doi.org/10.1111/gwat.12927

Bevacqua, E., Rakovec, O., Schumacher, D.L., Kumar, R., Thober, S., Samaniego, L., Seneviratne, S.I., Zscheischler, J., 2024. Direct and lagged climate change effects intensified the 2022 European drought. Nat. Geosci. 17, 1100–1107. https://doi.org/10.1038/s41561-024-01559-2

Christos, M., Stylianos, V., Sofia, F., Konstantinos, V., 2025. Assessment of future groundwater level using modflow code under different managerial scenarios in the Serres river basin, Greece. Earth Sci. Informatics 18, 465. https://doi.org/10.1007/s12145-025-01969-9

Colyer, A., Butler, A., Peach, D., Hughes, A., 2021. How groundwater time series and aquifer property data explain heterogeneity in the Permo-Triassic sandstone aquifers of the Eden Valley, Cumbria, UK. Hydrogeol. J. 30, 445–462. https://doi.org/10.1007/s10040-021-02437-6

Dangar, S., Asoka, A., Mishra, V., 2021. Causes and implications of groundwater depletion in India: A review. J. Hydrol. 596, 126103. https://doi.org/10.1016/j.jhydrol.2021.126103

Das, B., Singh, S., Thakur, P., Jain, S.K., 2024. Assessment of future groundwater levels using Visual MODFLOW in the Gomti River basin in India. Theor. Appl. Climatol. 155, 2917–2936. https://doi.org/10.1007/s00704-023-04795-5

Davamani, V., John, J.E., Poornachandhra, C., Gopalakrishnan, B., Arulmani, S., Parameswari, E., Santhosh, A., Srinivasulu, A., Lal, A., Naidu, R., 2024. A Critical Review of Climate Change Impacts on Groundwater Resources: A Focus on the Current Status, Future Possibilities, and Role of Simulation Models. Atmosphere (Basel). 15. https://doi.org/10.3390/atmos15010122

Dubois, E., Larocque, M., Gagné, S., Meyzonnat, G., 2021. Simulation of long-term spatiotemporal variations in regional-scale groundwater recharge: Contributions of

a water budget approach in cold and humid climates. Hydrol. Earth Syst. Sci. 25, 6567–6589. https://doi.org/10.5194/hess-25-6567-2021

Egidio, E., Lasagna, M., Mancini, S., De Luca, D.A., 2022. Climate impact assessment to the groundwater levels based on long time-series analysis in a paddy field area (Piedmont region, NW Italy): preliminary results. Acque Sotter. - Ital. J. Groundw. 11, 21–29. https://doi.org/10.7343/as-2022-576

Faranda, D., Pascale, S., Bulut, B., 2023. Persistent anticyclonic conditions and climate change exacerbated the exceptional 2022 European-Mediterranean drought. Environ. Res. Lett. 18. https://doi.org/10.1088/1748-9326/acbc37

Fronzi, D., Narang, G., Galdelli, A., Pepi, A., Mancini, A., Tazioli, A., 2024. Towards Groundwater-Level Prediction Using Prophet Forecasting Method by Exploiting a High-Resolution Hydrogeological Monitoring System. Water (Switzerland) 16, 1–19. https://doi.org/10.3390/w16010152

Guo, H., Li, S., 2024. A Review of Drip Irrigation's Effect on Water, Carbon Fluxes, and Crop Growth in Farmland. Water (Switzerland) 16. https://doi.org/10.3390/w16152206

Harbaugh, A.W., 2005. MODFLOW-2005, the US Geological Survey modular ground-water model: the ground-water flow process. US Department of the Interior, US Geological Survey Reston, VA.

Jasechko, S., Birks, S.J., Gleeson, T., Wada, Y., Fawcett, P.J., Sharp, Z.D., McDonnell, J.J., Welker, J.M., 2014. The pronounced seasonality of global groundwater recharge. Water Resour. Res. 50, 8845–8867. https://doi.org/10.1002/2014WR015809

Khadim, F.K., Dokou, Z., Lazin, R., Bagtzoglou, A.C., Anagnostou, E., 2023. Groundwater Modeling to Assess Climate Change Impacts and Sustainability in the Tana Basin, Upper Blue Nile, Ethiopia. Sustain. 15, 1–23. https://doi.org/10.3390/su15076284

Kishor, K., Aggarwal, A., Srivastava, P.K., Sharma, Y.K., Lee, J., Ghobadi, F., 2025. A Systematic Literature Review of MODFLOW Combined with Artificial Neural Networks (ANNs) for Groundwater Flow Modelling. Water (Switzerland) 17, 1–24. https://doi.org/10.3390/w17162375

Lafare, A.E.A., Peach, D.W., Hughes, A.G., 2016. Use of seasonal trend decomposition to understand groundwater behaviour in the Permo-Triassic Sandstone aquifer, Eden Valley, UK. Hydrogeol. J. 24, 141–158. https://doi.org/10.1007/s10040-015-1309-3

Lasagna, M., Mancini, S., De Luca, D.A., 2020. Groundwater hydrodynamic behaviours based on water table levels to identify natural and anthropic controlling factors in the Piedmont Plain (Italy). Sci. Total Environ. 716, 137051. https://doi.org/10.1016/j.scitotenv.2020.137051

Liu, Y., Yuan, S., Zhu, Y., Ren, L., Chen, R., Zhu, X., Xia, R., 2023. The patterns, magnitude, and drivers of unprecedented 2022 mega-drought in the Yangtze River Basin, China. Environ. Res. Lett. 18, 114006. https://doi.org/10.1088/1748-9326/acfe21

Meggiorin, M., Passadore, G., Bertoldo, S., Sottani, A., Rinaldo, A., 2021. Assessing the long-term sustainability of the groundwater resources in the Bacchiglione basin (Veneto, Italy) with the Mann–Kendall test: suggestions for higher reliability. Acque Sotter. - Ital. J. Groundw. 10, 35–48. https://doi.org/10.7343/as-2021-499

Mensah, J.K., Ofosu, E.A., Akpoti, K., Kabo-Bah, A.T., Okyereh, S.A., Yidana, S.M., 2022. Modeling current and future groundwater demands in the White Volta River Basin of Ghana under climate change and socio-economic scenarios. J. Hydrol. Reg. Stud. 41, 101117. https://doi.org/10.1016/j.ejrh.2022.101117

Montanari, A., Nguyen, H., Rubinetti, S., Ceola, S., Galelli, S., Rubino, A., Zanchettin, D., 2023. Why the 2022 Po River drought is the worst in the past two centuries. Sci. Adv. 9, 1–8. https://doi.org/10.1126/sciadv.adg8304

Ndehedehe, C.E., Adeyeri, O.E., Onojeghuo, A.O., Ferreira, V.G., Kalu, I., Okwuashi, O., 2023. Understanding global groundwater-climate interactions. Sci. Total Environ. 904, 166571. https://doi.org/10.1016/j.scitotenv.2023.166571

Noori, A.R., Singh, S.K., 2021. Spatial and temporal trend analysis of groundwater levels and regional groundwater drought assessment of Kabul, Afghanistan. Environ. Earth Sci. 80, 1–16. https://doi.org/10.1007/s12665-021-10005-0

Obergfell, C., Bakker, M., Maas, K., 2019. Identification and Explanation of a Change in the Groundwater Regime using Time Series Analysis. Groundwater 57, 886–894. https://doi.org/10.1111/gwat.12891

Pathak, A.A., Dodamani, B.M., 2019. Trend Analysis of Groundwater Levels and Assessment of Regional Groundwater Drought: Ghataprabha River Basin, India. Nat. Resour. Res. 28, 631–643. https://doi.org/10.1007/s11053-018-9417-0

Pool, S., Francés, F., Garcia-Prats, A., Pulido-Velazquez, M., Sanchis-Ibor, C., Schirmer, M., Yang, H., Jiménez-Martínez, J., 2021. From Flood to Drip Irrigation Under Climate Change: Impacts on Evapotranspiration and Groundwater Recharge in the Mediterranean Region of Valencia (Spain). Earth's Futur. 9, 1–20. https://doi.org/10.1029/2020EF001859

Retike, I., Bikše, J., Kalvāns, A., Dēliņa, A., Avotniece, Z., Zaadnoordijk, W.J., Jemeljanova, M., Popovs, K., Babre, A., Zelenkevičs, A., Baikovs, A., 2022. Rescue of groundwater level time series: How to visually identify and treat errors. J. Hydrol. 605. https://doi.org/10.1016/j.jhydrol.2021.127294

Ronchi, B., Stassen, F., Drevet, J.-P., Frippiat, C.C., Berger, J.-L., Dingelstadt, C., Veschkens, M., 2018. Long-Term Time-Series Analysis to Understand Groundwater Flow in Abandoned Subsurface Mines with Application to a Coalfield in Liège, Belgium. Mine Water Environ. 37, 470–481. https://doi.org/10.1007/s10230-018-0528-y

Sakizadeh, M., Mohamed, M.M.A., Klammler, H., 2019. Trend Analysis and Spatial Prediction of Groundwater Levels Using Time Series Forecasting and a Novel

Spatio-Temporal Method. Water Resour. Manag. 33, 1425–1437. https://doi.org/10.1007/s11269-019-02208-9

Sartirana, D., Rotiroti, M., Bonomi, T., De Amicis, M., Nava, V., Fumagalli, L., Zanotti, C., 2022. Data-driven decision management of urban underground infrastructure through groundwater-level time-series cluster analysis: the case of Milan (Italy). Hydrogeol. J. 30, 1157–1177. https://doi.org/10.1007/s10040-022-02494-5

Scanlon, B.R., Fakhreddine, S., Rateb, A., de Graaf, I., Famiglietti, J., Gleeson, T., Grafton, R.Q., Jobbagy, E., Kebede, S., Kolusu, S.R., Konikow, L.F., Long, D., Mekonnen, M., Schmied, H.M., Mukherjee, A., MacDonald, A., Reedy, R.C., Shamsudduha, M., Simmons, C.T., Sun, A., Taylor, R.G., Villholth, K.G., Vörösmarty, C.J., Zheng, C., 2023. Global water resources and the role of groundwater in a resilient water future. Nat. Rev. Earth Environ. 4, 87–101. https://doi.org/10.1038/s43017-022-00378-6

Scibek, J., Allen, D.M., Cannon, A.J., Whitfield, P.H., 2007. Groundwater-surface water interaction under scenarios of climate change using a high-resolution transient groundwater model. J. Hydrol. 333, 165–181. https://doi.org/10.1016/j.jhydrol.2006.08.005

Spitz, K., Moreno, J., 1996. A practical guide to groundwater and solute transport modeling. John Wiley and sons.

Stahl, M.O., Mar, T., Jameel, Y., 2024. Seasonal Groundwater Level Dynamics in Unconfined Aquifers across the United States. Groundwater 62, 876–888. https://doi.org/10.1111/gwat.13422

Stigter, T.Y., Miller, J., Chen, J., Re, V., 2023. Groundwater and climate change: threats and opportunities. Hydrogeol. J. 31, 7–10. https://doi.org/10.1007/s10040-022-02554-w

Taylor, C.J., Alley, W.M., 2001. Ground-water-level monitoring and the importance of long-term water-level data, US Geological Survey Circular.

Taylor, R.G., Scanlon, B., Döll, P., Rodell, M., Van Beek, R., Wada, Y., Longuevergne, L., Leblanc, M., Famiglietti, J.S., Edmunds, M., Konikow, L., Green, T.R., Chen, J., Taniguchi, M., Bierkens, M.F.P., Macdonald, A., Fan, Y., Maxwell, R.M., Yechieli, Y., Gurdak, J.J., Allen, D.M., Shamsudduha, M., Hiscock, K., Yeh, P.J.F., Holman, I., Treidel, H., 2013. Ground water and climate change. Nat. Clim. Chang. https://doi.org/10.1038/nclimate1744

Treviño, J., Rodríguez-Rodríguez, M., Montes-Vega, M.J., Aguilera, H., Fernández-Ayuso, A., Fernández-Naranjo, N., 2023. Wavelet Analysis on Groundwater, Surface-Water Levels and Water Temperature in Doñana National Park (Coastal Aquifer in Southwestern Spain). Water (Switzerland) 15. https://doi.org/10.3390/w15040796

Tsypin, M., Nguyen, V.D., Cacace, M., Blöcher, G., Scheck-Wenderoth, M., Luijendijk, E., Krawczyk, C., 2025. Influence of groundwater recharge projections on climate-driven subsurface warming: insights from numerical modeling. https://doi.org/10.5194/egusphere-2025-4335

Van der Gun, J., 2022. Large Aquifer Systems Around the World, Large Aquifer Systems Around the World. https://doi.org/10.21083/978-1-77470-020-4

Wang, H.F., Anderson, M.P., 1982. Introduction to groundwater modeling: finite difference and finite element methods. Freeman, San Francisco.

Weaver, S.M., Guinan, P.E., Semenova, I.G., Aloysius, N., Lupo, A.R., Hunt, S., 2023. A Case Study of Drought during Summer 2022: A Large-Scale Analyzed Comparison of Dry and Moist Summers in the Midwest USA. Atmosphere (Basel). 14, 1448. https://doi.org/10.3390/atmos14091448

Wu, R.S., Hussain, F., Lin, Y.C., Yeh, T.Y., Yu, K.C., 2021. Characterization of regional groundwater system based on aquifer response to recharge–discharge phenomenon and hierarchical clustering analysis. Water (Switzerland) 13. https://doi.org/10.3390/w13182535

Yang, Y.S., Yeh, H.F., Huang, C.C., Mackay, J.D., Bloomfield, J.P., Hsu, K.C., Chen, S.T., 2025. Assessing groundwater dynamics in data-scarce mountainous regions using a lumped parameter groundwater model. Terr. Atmos. Ocean. Sci. 36. https://doi.org/10.1007/s44195-025-00112-x

Yihdego, Y., Khalil, A., 2017. Groundwater resources assessment and impact analysis using a conceptual water balance model and time series data analysis: Case of decision making tool. Hydrology 4. https://doi.org/10.3390/hydrology4020025

Zaadnoordijk, W.J., Bus, S.A.R., Lourens, A., Berendrecht, W.L., 2019. Automated Time Series Modeling for Piezometers in the National Database of the Netherlands. Groundwater 57, 834–843. https://doi.org/10.1111/gwat.12819

Zhang, L., Yu, X., Zhou, T., Zhang, W., Hu, S., Clark, R., 2023. Understanding and Attribution of Extreme Heat and Drought Events in 2022: Current Situation and Future Challenges. Adv. Atmos. Sci. 40, 1941–1951. https://doi.org/10.1007/s00376-023-3171-x

Chapter 3: Study Area

The study area of this PhD project covers approximately 4000 km^2 within the province of Brescia, northern Italy (Fig. 1). In particular, in the first phase of the work (i.e., data-driven approach), the entire broader area was considered, whereas the second phase (i.e., model-based approach) focused on a narrower pilot area. In Fig.1, the broader study area of the first phase is represented with a black rectangle, while a red rectangle represents the numerical model pilot area of the second phase.

Based on the Köppen classification, the study area is categorized in the "Cfa" climate group, denoting a temperate continental climate with cold winters and humid, hot summers. The average temperature is 12.5°C, and the area is characterized by a bimodal rainfall regime with two maxima (autumn and spring) and two minima (winter and summer), and a mean annual precipitation of around 900 mm (1951-2005) (Faquseh & Grossi, 2023; Rotiroti et al., 2019).

This area is characterized by a heterogeneous geological and hydrogeological setting, including an alpine area in the north, a plain area (part of the Po Plain) in the south, and two morainic amphitheaters along lakes Garda and Iseo (Marchetti, 2002; Vercesi, 1994; Zanotti et al., 2019). Lakes Garda and Iseo are two of the main Italian lakes in the subalpine lakes district, which has been dam-regulated since the second half of the twentieth century, mainly for hydropower and agriculture (Hinegk et al., 2022).

In the study area, six main aquifer systems can be identified: i) Alpine area, ii) Lake Iseo and iii) Lake Garda morainic amphitheater, and a plain area which can be further divided into iv) higher plain, v) middle plain, and vi) lower plain (Fig. 1b). The transition from the higher to the lower plain is marked by the so-called "spring belt", a narrow area characterized by numerous (semi)natural lowland springs, which crosses the entire plain in a transverse direction located in the middle plain (Bartoli et al., 2012; De Luca et al., 2014). The Alpine area hosts alluvial river valley aquifers and mountain-blocked fractured aquifers, mainly recharged via precipitation and snowpack melt (Somers and McKenzie, 2020; Vercesi, 1994). The Iseo and Garda lakes morainic aquifer systems host local unconfined aquifers of limited potential and deeper confined aquifers, whose recharge mechanisms are difficult to determine due to the extreme structural complexity

of the aquifer systems. The land use is largely devoted to vineyards and as residential use, with intense summer tourism (Bini and Zuccoli, 2004; Vercesi, 1994; Zanotti et al., 2022) (Fig. 1c). The higher plain (north) hosts a monolayer unconfined aquifer up to 100 m below ground surface (b.g.s), mainly composed of coarse sediments (sands and gravels). In the middle plain, the thickness of the gravelly-sandy deposits becomes progressively finer while the silty-clayey layers become more continuous in thickness and extent, giving rise to semi-confined aquifers that become confined in the lower plain. The lower plain hosts a multi-layer system of confined sandy aquifers separated by a vertical alternation of several layers of fine material (silt and clay) (Bonomi et al., 2014; Rotiroti et al., 2019; Vercesi, 1994; Zanotti et al., 2022) (Fig. 3.2). The land use in the plain area is mostly agricultural (crop/arable land), where corn cultivation, especially for cattle and pig feeding, dominates (Fig. 1c). Here, irrigation demand is met through two sources: a) Subalpine lakes (lakes Iseo, Idro, and Garda) and Alpine rivers (i.e., Oglio, Mella, and Chiese rivers) water, and b) groundwater. Surface-water-irrigation is used in the northern part of the plain, where diverted water is distributed through an extensive network of centuries-old irrigation canals that serve multiple irrigation districts. In contrast, groundwater-fed irrigation is mainly used in the northernmost sector and in the southern part of the plain, supported by hundreds of irrigation wells (Rotiroti et al., 2019; Zanotti et al., 2022).

In the higher surface-water-fed irrigated plain, aquifer recharge occurs via (1) surface-water-fed irrigation return flow during the growing season, (2) local precipitation, (3) losing rivers and canals, and (4) surface mountain-front recharge (Markovich et al., 2019) in the northernmost sector, while discharge is primarily related to outflow to the lower plain aquifers, outflows through the springs belt, well abstraction, and the gaining portion of rivers (Bonomi et al., 2008; Rotiroti et al., 2023). In the middle plain, the aquifer recharge is strongly connected to the irrigation excess in the higher plain (Bartoli et al., 2012; Fumagalli et al., 2017). Groundwater recharge to the lower plain aquifer system mainly occurs through groundwater inflow from the higher plain aquifer, due to superficial confining low-permeability layers that limit surface infiltration. However, vertical recharge may also occur as a result of local discontinuities or incomplete

confinement. Discharges occur through gaining rivers and wells withdrawal (Rotiroti et al., 2023, 2019; Vercesi, 1994; Zanotti et al., 2022).

A prevalent NS direction characterizes groundwater flow in the higher plain, while interactions with surface water bodies cause NW-SE local deviations, especially in the shallow portion of the lower plain (Fig. 1b). The depth of the water table decreases from north to south, ranging from over 40 meters in the northernmost sector to less than 5 meters in the medium-low plain.(Bartoli et al., 2012; Delconte et al., 2014; Regione Lombardia, 2016; Rotiroti et al., 2019).

For the second phase of the PhD project (the model-based approach), the study focused on a narrower pilot area of approximately 2000 km² within the Oglio River basin (N Italy), located between the outflow of Lake Iseo and the river's confluence with the Mella River. In particular, the pilot area was selected to represent two of the most important and productive compartments that characterize the Brescia province: the surface-water-fed irrigated plain and the lower groundwater-fed irrigated plain.

Moreover, in this area, extensive datasets from previous projects were available, including data on rivers' discharges, which are pivotal to model development. Indeed, developing a robust model requires a large amount of reference data, including not only piezometric level measurements but also river and main canal stage and discharge data, as well as spring discharge records (Anderson et al., 2015; Hunt et al., 2006). These data are essential, as their absence would increase the model's uncertainty. Such data are extremely valuable for model construction and are typically difficult to obtain from institutional monitoring networks.

The choice of focusing on a narrower pilot area was driven by the need to reduce computational time (which increases with the size of the simulated domain) and by the availability of additional data required for the development of a numerical model, which go beyond the simple piezometric levels.

Furthermore, generally, the model's extent is expanded outward from the area of interest, both vertically and horizontally. This is because, especially in transient models, the effects of simulated transience should depend primarily on internal boundary conditions rather than conditions at the perimeter, which are usually less well constrained and subject to greater uncertainty and potential errors (Anderson et al., 2015; Reilly and Harbaugh, 2004). For these reasons, a buffer outside the interest domain of the Oglio Mella basin was included in the study area of the second phase.

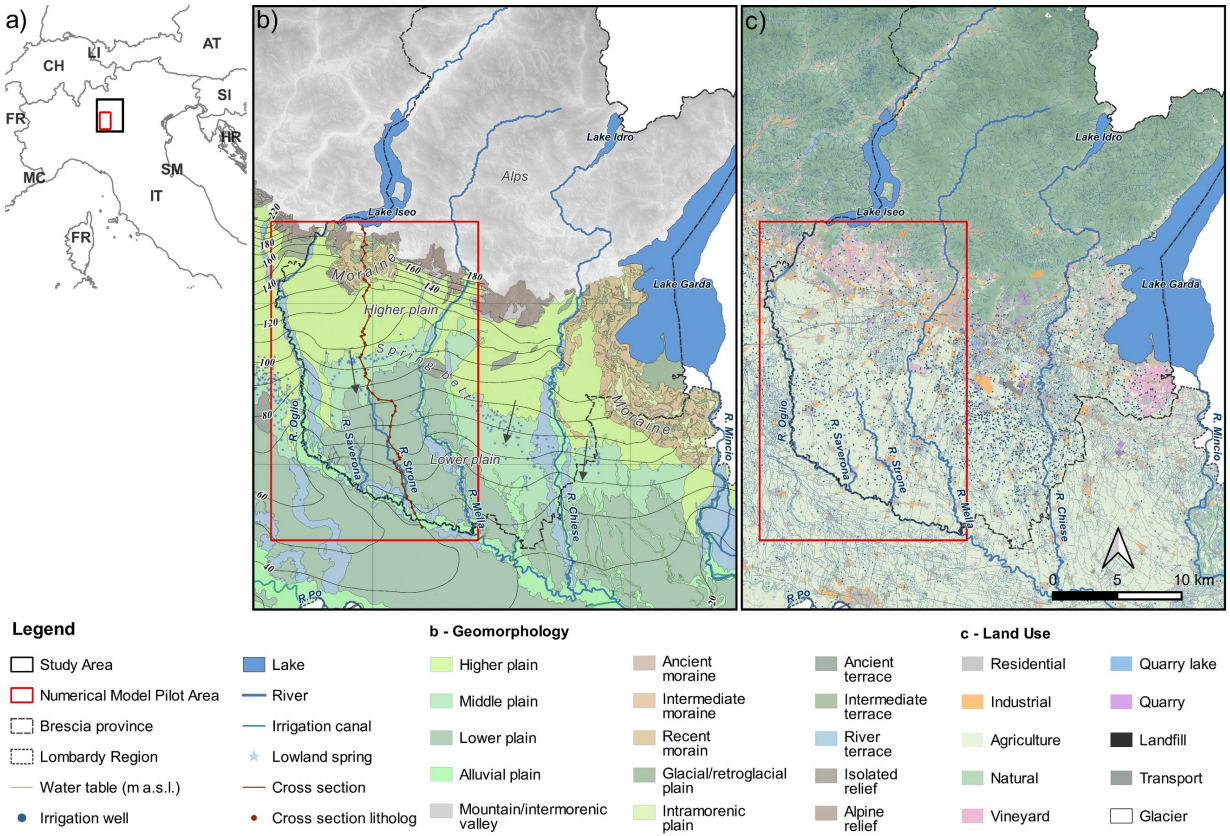

Figure 3.1 – a) *Study area (Black rectangle) and Numerical model pilot area (Red rectangle);* ***b)*** *Geomorphology (Regione Lombardia 2007), water table contour map (September 2014;* (Regione Lombardia, 2016)*) with flow directions, and cross-section trace. The cross-section is visible in Fig. 3.2;* ***c)*** *Land use (Land use classes have been represented from the geographic database Dusaf 7.0 (Regione Lombardia 2023)).*

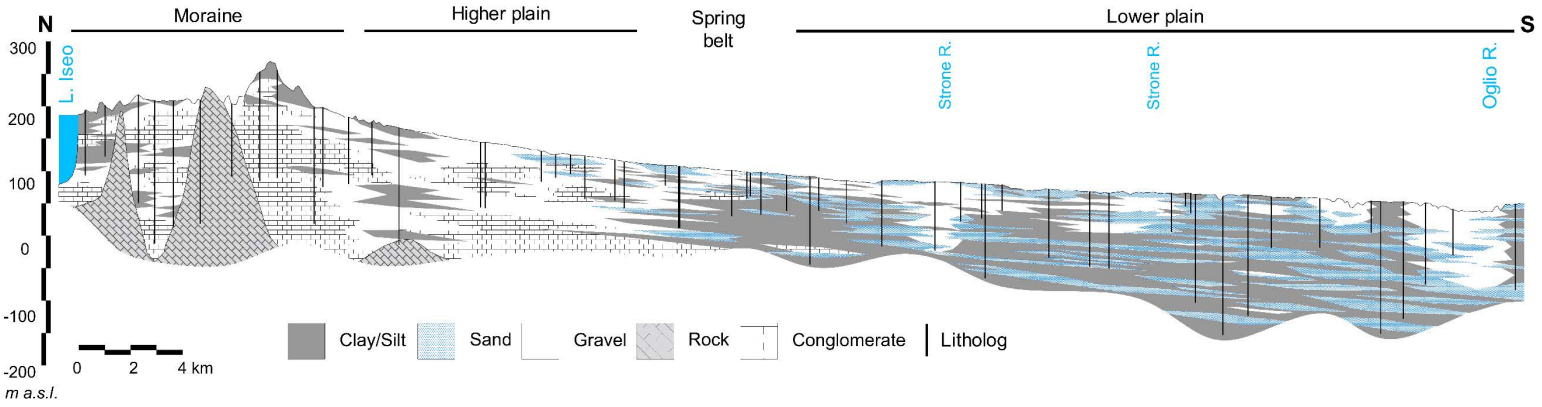

Figure 3.2 *– Cross-section (modified from Zanotti et al., 2022). The cross-section trace is visible in Fig. 3.1.*

References

Anderson, M.P., Woessner, W.W., Hunt, R.J., 2015. Applied Groundwater Modeling. Elsevier. https://doi.org/10.1016/C2009-0-21563-7

Bartoli, M., Racchetti, E., Delconte, C.A., Sacchi, E., Soana, E., Laini, A., Longhi, D., Viaroli, P., 2012. Nitrogen balance and fate in a heavily impacted watershed (Oglio River, Northern Italy): In quest of the missing sources and sinks. Biogeosciences 9, 361–373. https://doi.org/10.5194/bg-9-361-2012

Bini, A., Zuccoli, L., 2004. Anfiteatro morenico del Lago di Garda 17, 333–342.

Bonomi, T., Canepa, P., Del Rosso, F., Rossetti, A., 2008. Relazioni temporali pluridecennali di dati pluviometrici, idrologici e piezometrici nella pianura lombarda tra Ticino e Oglio. G. di Geol. Appl. 9, 227–248. https://doi.org/https://dx.doi.org/10.1474/GGA.2008-02.2-12.0242

Bonomi, T., Fumagalli, L., Rotiroti, M., Bellani, A., Cavallin, A., 2014. The hydrogeological well database TANGRAM©: a tool for data processing to support groundwater assessment. Acque Sotter. - Ital. J. Groundw. 3, 35–45. https://doi.org/10.7343/AS-072-14-0098

De Luca, D.A., Destefanis, E., Forno, M.G., Lasagna, M., Masciocco, L., 2014. The genesis and the hydrogeological features of the Turin Po Plain fontanili, typical lowland springs in Northern Italy. Bull. Eng. Geol. Environ. 73, 409–427. https://doi.org/10.1007/s10064-013-0527-y

Delconte, C.A., Sacchi, E., Racchetti, E., Bartoli, M., Mas-Pla, J., Re, V., 2014. Nitrogen inputs to a river course in a heavily impacted watershed: A combined hydrochemical and isotopic evaluation (Oglio River Basin, N Italy). Sci. Total Environ. 466–467, 924–938. https://doi.org/10.1016/j.scitotenv.2013.07.092

Faquseh, H., Grossi, G., 2023. The effect of climate change on groundwater resources availability: a case study in the city of Brescia, northern Italy. Sustain. Water Resour. Manag. 9, 1–15. https://doi.org/10.1007/s40899-023-00892-5

Fumagalli, N., Senes, G., Ferrario, P.S., Toccolini, A., 2017. A minimum indicator set for assessing fontanili (lowland springs) of the Lombardy Region in Italy. Eur. Countrys. 9, 1–16. https://doi.org/10.1515/euco-2017-0001

Hinegk, L., Adami, L., Zolezzi, G., Tubino, M., 2022. Implications of water resources management on the long-term regime of Lake Garda (Italy). J. Environ. Manage. 301, 113893. https://doi.org/10.1016/j.jenvman.2021.113893

Hunt, R.J., Feinstein, D.T., Pint, C.D., Anderson, M.P., 2006. The importance of diverse data types to calibrate a watershed model of the Trout Lake Basin, Northern Wisconsin, USA. J. Hydrol. 321, 286–296. https://doi.org/10.1016/j.jhydrol.2005.08.005

Marchetti, M., 2002. Environmental changes in the central Po Plain (northern Italy) due to fluvial modifications and anthropogenic activities. Geomorphology 44, 361–373. https://doi.org/10.1016/S0169-555X(01)00183-0

Markovich, K.H., Manning, A.H., Condon, L.E., McIntosh, J.C., 2019. Mountain-Block Recharge: A Review of Current Understanding. Water Resour. Res. https://doi.org/10.1029/2019WR025676

Regione Lombardia, 2007. Geoportal of the Lombardy Region, Italy. https://www.geoportale.regione.lombardia.it/en-GB/download-pacchetti?p_p_id=dwnpackageportlet_WAR_gptdownloadportlet&p_p_lifecycle=0&p_p_state=normal&p_p_mode=view&_dwnpackageportlet_WAR_gptdownloadportlet_metadataid=r_lombar%3A2318b9c5-f8f0-421f-97c0-6e4d912e2b93&_jsfBridgeRedirect=true. (accessed 10 May 2025).

Regione Lombardia, 2023. Geoportal of the Lombardy Region, Italy. https://www.geoportale.regione.lombardia.it/en-GB/metadati?p_p_id=detailSheetMetadata_WAR_gptmetadataportlet&p_p_lifecycle=0&p_p_state=normal&p_p_mode=view&_detailSheetMetadata_WAR_gptmetadataportlet_identifier=r_lombar%3A7cd05e9f-b693-4d7e-a8de-71b40b45f54e&_jsfBridgeRedirect=true. (accessed 4 June 2025).

Regione Lombardia, 2016. Programma di tutela e uso delle acque (PTUA 2016) "Programme for the protection and use of water."

Reilly, T.E., Harbaugh, A.W., 2004. Guidelines for Evaluating Ground-Water Flow Models: Scientific Investigations Report 2004-5038. USGS Sci. Investig. Rep. 2004-5038 1–30.

Rotiroti, M., Bonomi, T., Sacchi, E., McArthur, J.M., Stefania, G.A., Zanotti, C., Taviani, S., Patelli, M., Nava, V., Soler, V., Fumagalli, L., Leoni, B., 2019. The effects of irrigation on groundwater quality and quantity in a human-modified hydro-system: The Oglio River basin, Po Plain, northern Italy. Sci. Total Environ. 672, 342–356. https://doi.org/10.1016/j.scitotenv.2019.03.427

Rotiroti, M., Sacchi, E., Caschetto, M., Zanotti, C., Fumagalli, L., Biasibetti, M., Bonomi, T., Leoni, B., 2023. Groundwater and surface water nitrate pollution in an intensively irrigated system: Sources, dynamics and adaptation to climate change. J. Hydrol. 623, 129868. https://doi.org/10.1016/j.jhydrol.2023.129868

Somers, L.D., McKenzie, J.M., 2020. A review of groundwater in high mountain environments. Wiley Interdiscip. Rev. Water 7, 1–27. https://doi.org/10.1002/wat2.1475

Vercesi, P.L., 1994. Aspetti quali-quantitativi delle risorse idriche sotterranee del bresciano. Nat. Brescia. Ann. Mus. Civ. Sc. Nat. Brescia 21–52.

Zanotti, C., Rotiroti, M., Caschetto, M., Redaelli, A., Bozza, S., Biasibetti, M., Mostarda, L., Fumagalli, L., Bonomi, T., 2022. A cost-effective method for assessing groundwater well vulnerability to anthropogenic and natural pollution in the framework of water safety plans. J. Hydrol. 613, 128473. https://doi.org/10.1016/j.jhydrol.2022.128473

Zanotti, C., Rotiroti, M., Fumagalli, L., Stefania, G.A., Canonaco, F., Stefenelli, G., Prévôt, A.S.H., Leoni, B., Bonomi, T., 2019. Groundwater and surface water quality characterization through positive matrix factorization combined with GIS approach. Water Res. 159, 122–134. https://doi.org/10.1016/j.watres.2019.04.058

Chapter 4: PhD Activities

The PhD project was carried out through two successive phases, which are described in this thesis across three sections, according to the following structure:

- Phase 1: Data-driven approach:
    - Section I: Data Acquisition and Database Management: a Structured Approach (Chapter 5).
    - Section II: Time series analysis (Chapter 6).
- Phase 2: Model-based approach:
    - Section III: Implementation of the Groundwater Numerical Model and Results from Synthetic Scenarios (Chapter 7).

I) Data Acquisition and Database Management: a Structured Approach – Chapter 5

This first section is dedicated to data preprocessing, which was necessary to develop a structured database for the subsequent working phase. The work involved the acquisition, management, and standardization of heterogeneous datasets from the water supplier, *Acque Bresciane S.r.l. SB*, which were integrated into a unified database. Structural information on 107 wells and sensor installation depths was combined with groundwater level measurements to derive piezometric levels (m a.s.l.), where available. Particular attention was given to identifying and correcting anomalies in the time series, primarily due to installation errors, sensor displacement, or calibration issues. These steps provided not only a consistent and reliable dataset to support subsequent data-driven applications but also a powerful tool for the water supplier, useful for identifying situations potentially prone to future critical issues and for supporting the adaptation and improvement of the overall efficiency of the monitoring process.

II) Time series analysis – Chapter 6

This second section of the thesis describes the analyses carried out on the database obtained in the previous section to investigate groundwater dynamics in different hydrogeological settings. Specifically, a procedure was proposed to extract meaningful, noise-free information from dynamic data from active drinking water wells, minimizing

the influence of pumping. Of the 107 available wells, 61 were selected that had at least one complete year of data available prior to 2022. A cluster analysis was used to identify typical seasonal patterns under baseline conditions (2013-2021) in different hydrogeological contexts in the province of Brescia (Alpine area, Lake Iseo and Lake Garda morainic amphitheater, higher plain, middle plain, and lower plain). The resulting clusters were interpreted to identify the average seasonal patterns and the associated recharge and discharge processes. Subsequently, the 2022 data were compared with the data under baseline conditions to quantify the impact of the hydrological drought, analyzing precipitation and temperature anomalies that affect groundwater systems while differentiating between direct meteorological effects and indirect human responses to water scarcity. The analysis not only assessed the vulnerability of different hydrogeological systems to climate change but also supported researchers and water managers with tools for a more effective groundwater management in the context of climate change, particularly in regions where irrigation plays a central role.

The results of this section have been summarized in the following published paper, which is presented in Chapter 6 of this PhD thesis:

The Dual Role Of Irrigation In The Groundwater Budget Under Baseline Conditions versus The 2022 Drought: Lessons For Future Climate Adaptation

Agnese Redaelli[1], Tullia Bonomi[1], Davide Sartirana[1], Gianfranco Sinatra[2], Marco Rotiroti[1] and Chiara Zanotti[1],*

[1]Department of Earth and Environmental Sciences, University of Milano-Bicocca, Milan, Italy.

[2]Acque Bresciane S.r.l. SB, Via 25 Aprile, 18, 25038 Rovato, BS, Italy.

Journal of Hydrology, ***Volume 658,*** September 2025, 133211. https://doi.org/10.1016/j.jhydrol.2025.133211

Journal of Hydrology 658 (2025) 133211

Contents lists available at ScienceDirect

Journal of Hydrology

journal homepage: www.elsevier.com/locate/jhydrol

The dual role of irrigation in the groundwater budget under baseline conditions versus the 2022 drought: Lessons for future climate adaptation

Agnese Redaelli [a], Tullia Bonomi [a], Davide Sartirana [a], Gianfranco Sinatra [b], Marco Rotiroti [a], Chiara Zanotti [a,*]

[a] Department of Earth and Environmental Sciences, University of Milano-Bicocca, Milan, Italy
[b] Acque Bresciane S.r.l. SB, Brescia, Italy

* Corresponding author.
E-mail address: chiara.zanotti@unimib.it (C. Zanotti).

https://doi.org/10.1016/j.jhydrol.2025.133211
Received 10 August 2024; Received in revised form 27 March 2025; Accepted 28 March 2025
Available online 31 March 2025

III) Implementation of the Groundwater Numerical Model and Results from Synthetic Scenarios – Chapter 7

In the last section of the present thesis, the second phase of the PhD project is presented, concerning the development of a basin-scale numerical groundwater flow model for the Oglio River basin. The main goal of this model was to represent and quantify all inputs and outputs of the selected area as identified during the first phase, and to conduct a quantitative assessment of two synthetic scenarios of practical interest. To achieve this, a transient groundwater flow model was realized using MODFLOW-NWT as the numerical code, capturing the complexity of the study area through a combination of two MODFLOW packages. The model was first calibrated using a trial-and-error approach, followed by automatic calibration with the Parameter Estimation (PEST) software suite. Inflows and outflows of the system were quantified using MODFLOW's Hydrostratigraphic Unit (HSU) option. Subsequently, the calibrated model was used to run two synthetic scenarios designed to analyze the aquifer's response to two hypothetical hydrological scenarios of practical interest: (S1) a 2-year meteorological drought, using 2022 conditions as a reference, and (S2) a shift in irrigation practices

from surface-water irrigation to drip irrigation. The primary aim was to identify the main driver of potential future aquifer depletion in a highly human-influenced system with significant agricultural activity, providing a valuable tool for evaluating system vulnerability.

The results of this section are discussed in the following paper, submitted to the Journal of Hydrology, which is presented in Chapter 7 of the PhD thesis:

Changes in irrigation practices may bankrupt aquifers faster than meteorological droughts: a numerical modeling approach

Agnese Redaelli[1,*], Tullia Bonomi[1], Davide Sartirana[1], Gianfranco Sinatra[2], Daniel T. Feinstein[3], Randall J. Hunt[4], Marco Rotiroti[1], and Chiara Zanotti[1]

[1]Department of Earth and Environmental Sciences, University of Milano-Bicocca, Piazza della Scienza 1, 20126, Milan, Italy.

[2]Acque Bresciane S.r.l. SB, Via 25 Aprile, 18, 25038 Rovato, BS, Italy.

[3]Department of Geoscience, University of Wisconsin-Milwaukee, Lapham Hall, R 3209 North Maryland Avenue, Milwaukee, WI 53211, USA.

[4]Department of Geoscience, University of Wisconsin-Madison, Lewis G. Weeks Hall, 1215 West Dayton Street, Madison, WI 53706-1692, USA.

1 **Changes in irrigation practices may bankrupt aquifers faster than**

2 **meteorological droughts: a numerical modeling approach**

3 *Agnese Redaelli[1,*], Tullia Bonomi[1], Davide Sartirana[1], Gianfranco Sinatra[2], Marco Rotiroti[1], Daniel T.*

4 *Feinstein[3], Randall J. Hunt[4], and Chiara Zanotti[1]*

5 *[1]Department of Earth and Environmental Sciences, University of Milano-Bicocca, Milan, Italy.*

6 *[2]Acque Bresciane S.r.l. SB, Via 25 Aprile, 18, 25038 Rovato, BS, Italy.*

7 *[3]University of Wisconsin-Milwaukee, Lapham Hall, Geosciences Dept., Room 338, 3209 North Maryland*
8 *Avenue, Milwaukee, WI 53211, USA.*

9 *[4]University of Wisconsin-Madison, Lewis G. Weeks Hall, Geosciences Dept., 1215 West Dayton Street,*
10 *Madison, WI 53706-1692, USA.*

Chapter 5: Data Acquisition and Database Management: a Structured Approach

As part of this project, data from long-term monitoring operated by water manager Acque Bresciane S.r.l. SB on active wells were analyzed to identify situations most prone to possible future critical issues, support the planning of mitigation and adaptation strategies, and determine useful actions to enhance the efficiency of the monitoring process. The available data consists of groundwater levels and abstraction rates measured from active drinking wells. Typically, these data are collected by water suppliers for management purposes; however, especially in the past decades, the archiving and storage of such data in structured databases have not been a priority for most water suppliers. Therefore, in order to perform a meaningful data mining of the data, a first phase of data preprocessing was needed. The preprocessing procedure was implemented in the RStudio environment (R Core Team, 2021) to define an automatic system that allows for future data updates.

This phase of the PhD project involved the following tasks:

1. Acquisition, management, standardization of formats, and integration of the provided data into a single database.
2. Integration of structural data on wells and automatic sensor depths to determine piezometric levels (m a.s.l.) based on groundwater level data above the sensor (m).
3. Exclusion or correction of measurement anomalies in each time series related to problems connected with installation, movement, calibration, and measurement errors of the sensors.
4. Extraction of representative data, visualization, and exploratory analysis.

5.1 Groundwater online sensors

Continuous data is collected by the water supplier by means of online sensors installed in the drinking wells. These sensors (Fig. 5.1) are positioned below the typical groundwater level and measure the pressure of the overlying water column, which is then converted into the height (in meters) of the water between the sensor and the groundwater table.

Therefore, to obtain groundwater level data in m a.s.l. two auxiliary information are needed:

- Ground level data (m a.s.l.)
- Sensor depth data (m)

When these data are available, the groundwater level can be calculated with the following formula:

Groundwater level (m a.s.l.) = Well elevation (m a.s.l.)-Sensor depth (m)+Pressure Head above the sensor (m)

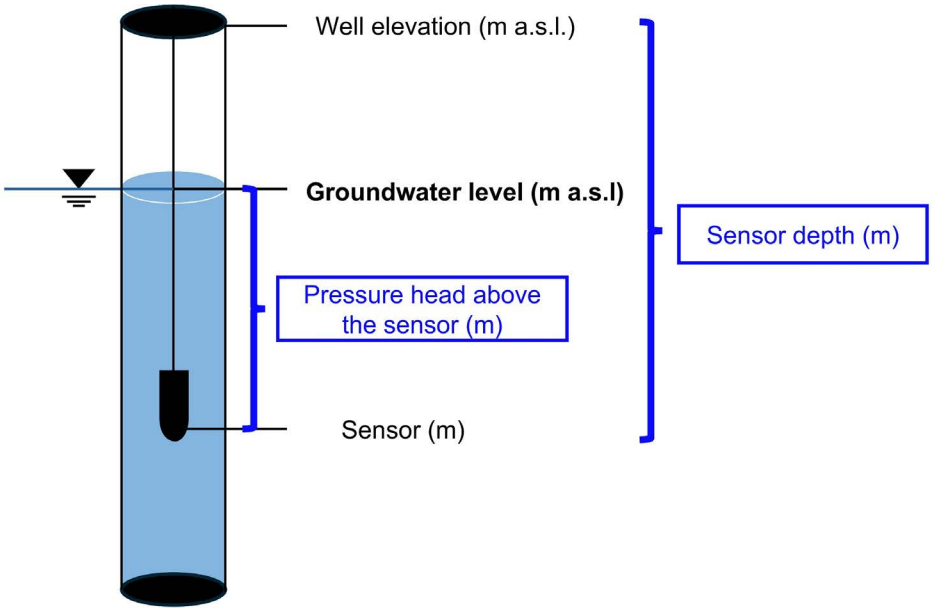

Figure 5.1 *– Schematic representation of a well and the main references used for the representation and correction of available level data.*

5.2 Acquisition, management, and integration of the provided data

The water supplier provided a total of 111 files containing:

- high-resolution (hourly data) static and dynamic groundwater level data above the sensor (m) and abstraction flow rates (L/s) data from automatic sensors extracted from the decommissioned data management system (maximum time range: 2013-2020);
- high-resolution (hourly data) static and dynamic groundwater level data above the sensor (m) and abstraction flow rates (L/s) from automatic sensors extracted from the current data management system (maximum time range: 2020-2023);
- static groundwater levels from manual measurements (m);
- supplementary structural information (e.g., well's elevation, well's depth, data logger depth, and geographic coordinates).

The provided data refer to 107 wells distributed in the province of Brescia, collected over nearly 11 years (2013-2023). Throughout the years, two different data management systems were implemented by the water supplier (a first system, decommissioned in 2020, and a second one implemented starting from 2020), leading to heterogeneous data archiving formats. Furthermore, data from online sensors were never integrated with information from the well structure or location (e.g., coordinates and screen depths), as these were managed by separate working groups within the water supplier organization. In this context, available data were not directly compatible or ready for use, and a reorganization of the data into a structured database was needed.

Firstly, all the available files were standardized into a common format and integrated into a single database specifically designed for graphical processing and comprehensive analysis. Specifically, identifying and defining a unique control code was essential to enable the joining of available measurements of the groundwater level above the sensor (m), the abstraction flow rates (L/s), and the available structural information of the wells. Where applicable, it also allowed for the merging of data series from the first decommissioned management system with those extracted from the current system.

Successively, the raw piezometric data, expressed as pressure head values above the sensor, were converted into piezometric levels (m a.s.l.) using, where available, the elevation values of the well reference point (m a.s.l.) and the sensor position (m a.s.l).

5.3 Dataset Cleansing

After merging the different files, a detailed analysis of the raw data from each historical series was performed to identify and exclude potential errors or malfunctions of the sensors, ensuring that only the most reliable data were maintained for subsequent analyses. First, all the possible data overlaps due to the transition from the decommissioned management system to the current one were removed, selecting the most reliable data. Particularly, the first phase of the new system installation often yielded a calibration phase with several missing data or malfunctions, leading to the exclusion of the new system data if the previous system data were available.

During the database analysis, data associated with measurement and/or sensor calibration errors have been registered in most time series. For this reason, a selection of data considered directly interpretable was made, excluding those associated with measurement errors and/or noise. For this initial selection, a detailed analysis of the raw data was carried out based on an attentive hydrogeological interpretation of the series trend. To discriminate between the effects of variable pumping rates and possible sensors' malfunctioning, each head measurement above the sensor, or piezometric level, was associated with the corresponding abstraction flow rate measured at the same time.

In particular, seven abstraction flow rate classes were defined for all 107 wells, each identified by a different color code. Thanks to this graphical representation, interpretable data and data clearly associated with measurement errors were differentiated for each well through the definition of:

- **a time window** to exclude data associated with an initial sensor calibration phase or data affected by a detection error not found in the remaining series;
- **threshold values** (in meters or meters above sea level) beyond which the measurement was not considered reliable.

These exclusion parameters were identified through expert-driven evaluation, supported by a graphical analysis aimed at identifying data that were clearly out of scale or indicative of obvious sensor errors.

In Figure 5.2 an example is shown of the exclusion of data below a threshold level: in this case the data highlighted with the red circle were static (abstraction rate = 0 L/s), but the resulting piezometric levels were significantly lower than dynamic data registered with abstraction rates up to 30 L/s, meaning that they were more plausibly associated with malfunctioning in the measurements or storage of the data than associated with actual hydrogeological processes.

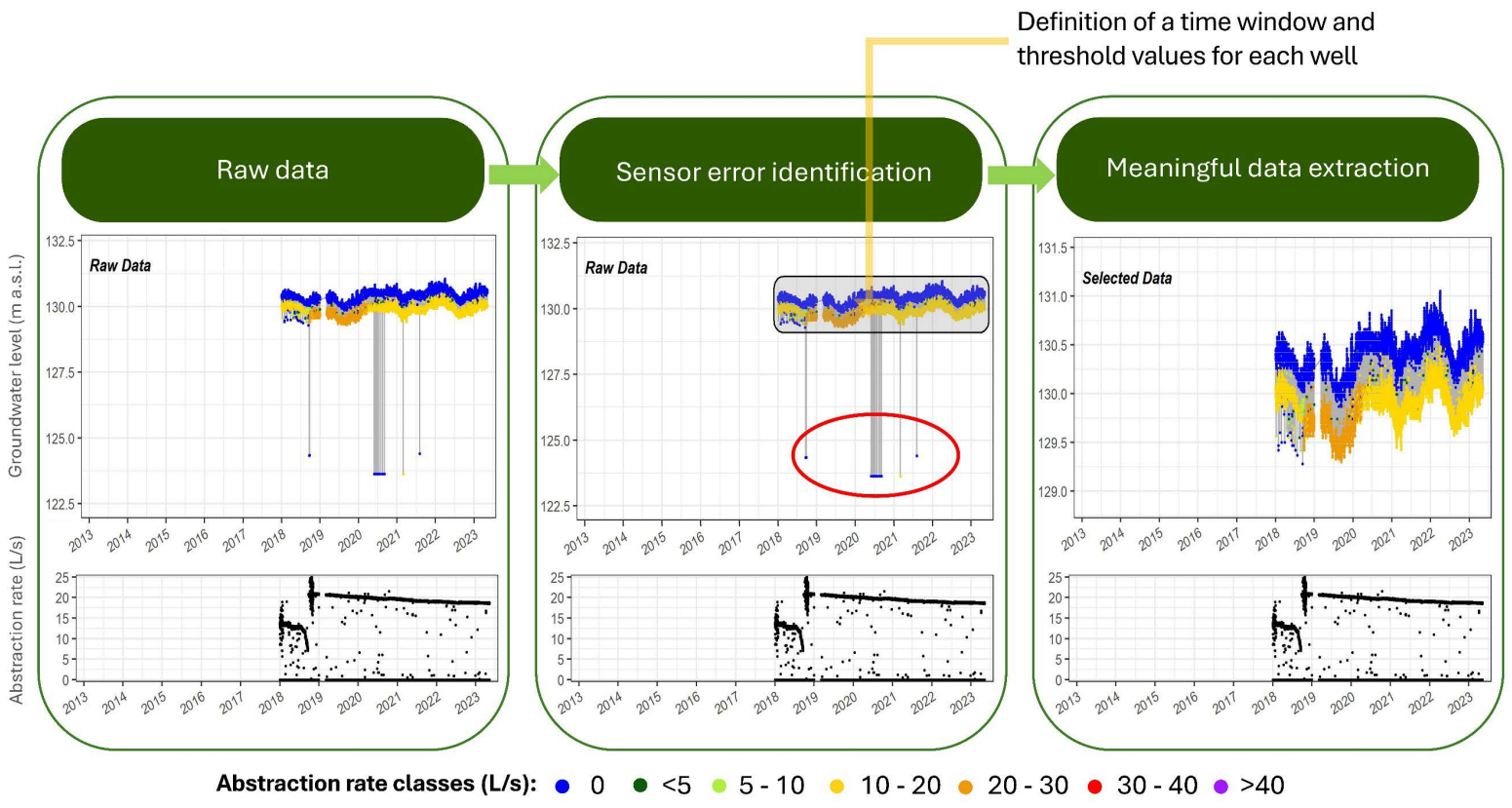

Figure 5.2 *– Schematic representation of the selection of interpretable data and exclusion of data associated with errors by visual inspection. Groundwater level data from automatic sensor are classified according to abstraction rate classes (L/s).*

After this first manual selection of the data, additional issues related to missing information were specifically addressed in order to minimize data loss and preserve as many available time series as possible. The most frequent problems were related to missing information, particularly to missing sensor depth data. Furthermore, a recurring issue was encountered, related to the displacement of the sensor throughout the years (e.g., due to maintenance, repositioning or sensor substitution), as previous sensor positions and depth information have not been retained, leaving only the most recent sensor location available. Therefore, several approaches were developed to address different issues:

- Missing sensor depth data.
- Sensor displacement associated with a sensor substitution.
- Sensor displacement not associated with a sensor substitution:
    - data from manual measurements available;
    - data from manual measurements not available.

As no specific metadata on sensor displacement was available, the displacement of each sensor was evaluated individually and discussed directly with the water supplier.

5.3.1 Missing sensor depth data

For some wells, the information regarding the depth of the sensor was lacking. In these cases, the elevation of the automatic sensor (in m a.s.l.) was determined by comparing the static groundwater level data manually measured (when available) with the average of the groundwater levels above the sensor associated with an abstraction rate of 0 L/s, measured on the same day. The average of the calculated values has been used to identify the position of the automatic sensor and to integrate the available manual measurements with the time series collected with the automatic sensor.

Example 1

Here is reported an example showing 1) the table containing the measurements used to identify the position of the automatic sensor in m a.s.l. (Table 5.1), 2) the comparison between the time series before and after the correction (Fig. 5.3), and 3) the calculated

position of the automatic sensor. For this well, the calculated position of the sensor is 93.882 m a.s.l..

Table 5.1 *– Comparison between manual static level measurements and groundwater level above the sensor, measured on the same day, used to calculate the position of the sensor in meters above sea level.*

Date	Static manual measurement (m a.s.l.)	Average of the groundwater level above the automatic sensor(m)	Calculated sensor elevation (m a.s.l.)
24/02/2014	115.15	21.266	**93.884**
20/05/2015	113.88	19.974	**93.906**
23/09/2015	115.36	21.469	**93.891**
19/09/2016	115.84	21.891	**93.949**
04/07/2018	114.03	20.25	**93.78**

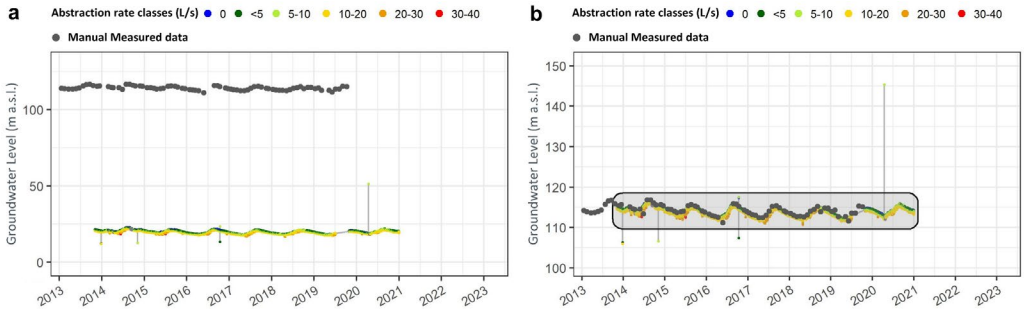

Figure 5.3 *– Time series correction:* ***a)*** *shows the time series before the correction (manual data are in m a.s.l., while the sensor's data are in m above the sensor), and* ***b)*** *shows the time series after the correction. Sensor data are classified according to abstraction rate classes (L/s), and manual data are represented in grey.*

5.3.2 Sensor displacement associated with a sensor substitution

For some wells, it emerged that the sensor's position referred only to the sensor of the current management system. However, this data did not apply to the sensor of the

decommissioned management system due to the displacement/substitution of the sensor over time, as clearly highlighted by sudden shifts between the series sections that cannot be justified or interpreted as actual drops.

In this case, the correction was made by comparing the manual static piezometric data with the average of the piezometric data (associated with an abstraction rate of 0 L/s) measured by the automatic sensor on the same date. The calculated average was then added to the sensor's altitude (m a.s.l.) provided by Acque Bresciane in order to obtain the correct sensor elevation for the time series section to be corrected.

Example 2

Here is reported an example showing 1) the table containing the measurements used to identify the position of the decommissioned sensor (Table 5.2), 2) the comparison between the time series before and after the correction (Fig. 5.4), and 3) the calculated position of the decommissioned management system sensor. The sensor's altitude (m a.s.l.) provided by Acque Bresciane was 94 m a.s.l., while the calculated altitude for the sensor of the decommissioned management system was 104.37 m a.s.l..

Table 5.2 *– Comparison between manual static level measurements (SMM) and static level recorded by the automatic sensor (MAS), measured on the same day, used to calculate the position of the decommissioned management system sensor.*

Date	Static manual measurement (SMM) (m a.s.l.)	Average of the measurements from the automatic sensor (MAS) (m a.s.l.)	Difference between SMM and MAS (m)	Average of differences (m)
02/03/2026	113.5	103.34	10.16	**10.37**
15/03/2016	113.36	102.48	10.88	
28/09/2016	115.39	105.32	10.07	

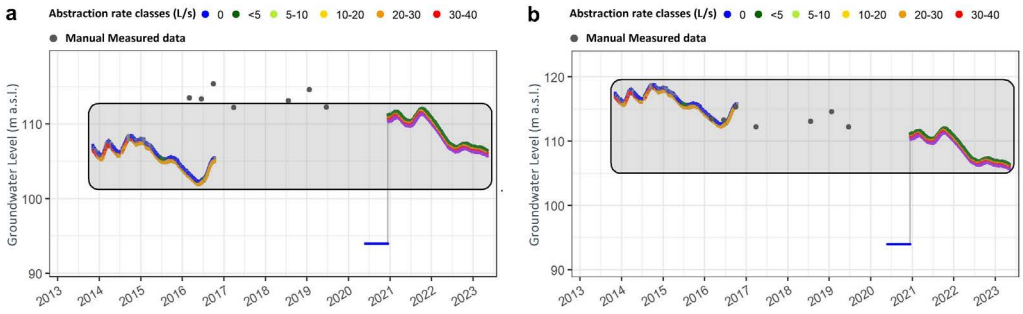

Figure 5.4 *– Time series correction:* ***a)*** *shows the time series before the correction, and* ***b)*** *shows the time series after the correction. Sensor data are classified according to abstraction rate classes (L/s), and manual data are represented in grey.*

5.3.3 Sensor displacement not associated with a sensor substitution – manual data available

For some wells, it was necessary to further divide the time series recorded by both decommissioned and actual management system sensors into multiple sections due to a sensor displacement over time. In these cases, it was necessary to identify the dates on which the sensor was moved and assign an identification code to each one.

The identified segments were corrected by comparing the available manual static values with the average static values (associated with a flow rate of 0 L/s) measured by the automatic sensor on the same date. The calculated averages were then added to the sensor altitude provided by Acque Bresciane in order to obtain the correct sensor position data for each section.

Example 3

Here is an example showing 1) the table containing the measurements used to identify the position of the time series section (Table 5.3 and Table 5.4), 2) the comparison between the time series before and after the correction (Fig. 5.5), and 3) the calculated position of the sensors for each section.

The time series measurements in the example were collected with three sensors. For the first sensor, the recorded data series had to be divided into four sections. The correction and realignment of the data were performed by comparing the manual static

measurements with the average of the static values (associated with a flow rate of 0 L/s) measured by the automatic sensor on the same date (Table 5.3). The average of the calculated values was then added to the automatic sensor elevation provided by Acque Bresciane.

Table 5.3 *– Comparison between manual static level measurements (SMM) and static level recorded by the automatic sensor (MAS), measured on the same day, used to calculate the position of the time series sections recorded with the first automatic sensor.*

Time series sections	Date	Static manual measurement (SMM) (m a.s.l.)	Average of the measurements from the automatic sensor (MAS) (m a.s.l.)	Difference between SMM and MAS (m)	Average of differences (m)
1 (04/11/2013 - 21/10/2016)	18/03/2014	112.95	125.79	-12.84	**-12.66**
	21/07/2014	114.36	127.16	-12.80	
	17/11/2014	113.48	126.17	-12.69	
	11/12/2014	113.36	126.20	-12.84	
	16/04/2015	111.79	124.25	-12.46	
	13/05/2015	111.24	124.02	-12.78	
	25/06/2015	111.66	124.03	-12.37	
	19/08/2015	113.07	125.45	-12.38	
	21/09/2015	113.06	125.97	-12.91	
	12/10/2015	112.71	123.99	-11.28	
	17/11/2015	111.63	124.44	-12.81	
	14/12/2015	110.93	123.76	-12.83	
	25/01/2016	110.44	123.23	-12.79	
	17/02/2016	110.11	122.92	-12.81	
	14/03/2016	109.74	122.47	-12.73	
	13/04/2016	109.28	122.06	-12.78	
	18/05/2016	109.42	122.23	-12.81	

Time series sections	Date	Static manual measurement (SMM) (m a.s.l.)	Average of the measurements from the automatic sensor (MAS) (m a.s.l.)	Difference between SMM and MAS (m)	Average of differences (m)
	26/08/2016	113.51	126.30	-12.79	
	19/09/2016	113.67	126.52	-12.85	
	11/10/2016	113.19	125.89	-12.70	
2 (13/10/2016 - 21/10/2016)	21/11/2016	111.94	109.38	2.56	**2.51**
	16/12/2016	111.18	108.73	2.45	
3 (21/10/2016 - 19/10/2017)	22/02/2017	109.91	109.27	0.64	**0.64**
	20/09/2017	112.63	111.98	0.65	
4 (19/10/2017 - 27/11/2018)	20/02/2018	111.74	122.63	-10.89	**-12.32**
	21/03/2018	109.38	122.07	-12.69	
	19/06/2018	109.83	122.62	-12.79	
	17/09/2018	112.43	125.74	-13.31	
	15/10/2018	112.62	125.30	-12.68	
	08/11/2018	112.30	124.98	-12.68	
	20/11/2018	112.16	123.35	-11.19	

The sensor's altitude (m a.s.l.) provided by Acque Bresciane was 94.93 m a.s.l., while the calculated altitude for the sensor was 82.26 m a.s.l. for section 1, 97.44 m a.s.l. for section 2, 95.57 m a.s.l. for section 3, and 82.61 m a.s.l. for section 4. The second sensor depth data was not available. To determine the elevation of the second sensor, the groundwater level above the sensor (m) (associated with a flow rate of 0 L/s) was subtracted from the manual measurement (m a.s.l.) (Table 5.4). The calculated altitude for the second sensor was 93.39 m a.s.l..

Table 5.4 *– Comparison between manual static level measurements (SMM) and static level recorded by the automatic sensor (MAS), measured on the same day, used to calculate the position of the second automatic sensor.*

Date	Static manual measurement (SMM) (m a.s.l.)	Average of the measurements from the automatic sensor (MAS) (m a.s.l.)	Sensor elevation (m a.s.l.)
22/05/2019	109.36	15.97	**93.39**

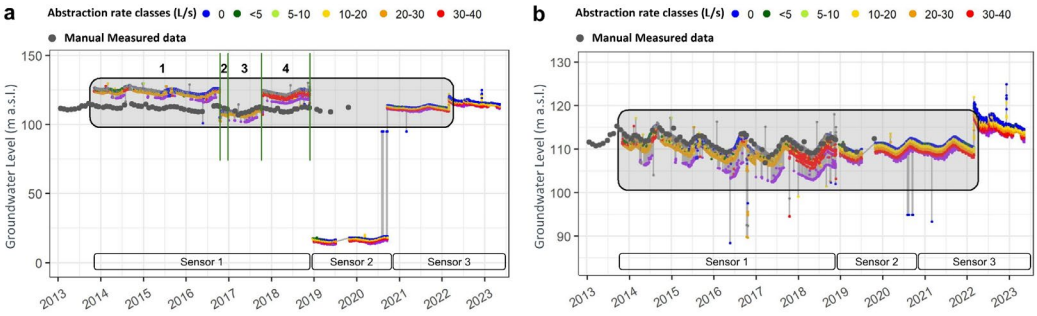

Figure 5.5 *– Time series correction:* ***a)*** *shows the time series before the correction, and* ***b)*** *shows the time series after the correction. Sensor data are classified according to abstraction rate classes (L/s), and manual data are represented in grey. Numbers from 1 to 4 refer to the four sections of the data series recorded by sensor 1.*

5.3.4 Sensor displacement not associated with a sensor substitution – manual data not available

For some wells, static manual data were not available. In these cases, the different segments of the historical series relating to the sensor displacement over time were corrected by comparing the last available data from the time series section to be realigned with the first available data from the reference series section. The data selected for correction were chosen based on the abstraction flow rate class. In these cases, an interval of up to two weeks has been considered acceptable for applying this correction method.

Example 4

Here is an example showing 1) the table containing the measurements used to identify the position of the time series sections (Table 5.5), 2) the comparison between the time series before and after the correction (Fig. 5.6), and 3) the calculated position of the sensors for each section.

The time series measurements in the example were collected with two sensors. For sensor 2, the recorded data series had to be divided into two sections. The correction of the time series from 04/11/2013 to 11/03/2021 was made using the second section from 12/03/2021 to 08/05/2023 as the reference. The data selected for correction were both associated with a withdrawal rate class <5 L/s. The sensor's altitude (m a.s.l.) provided by Acque Bresciane was 103.35 m a.s.l., while the calculated altitude for the first section was 112.8289 m a.s.l..

Table 5.5 *– Comparison between the last available data from the time series section to be realigned and the first available data from the reference section, used to calculate the position of the first time series section.*

Last available data from the time series section to be realigned (m a.s.l.)	First available data from the reference section (m a.s.l.)	Difference (m a.s.l.)
112.058	121.537	**9.4789**

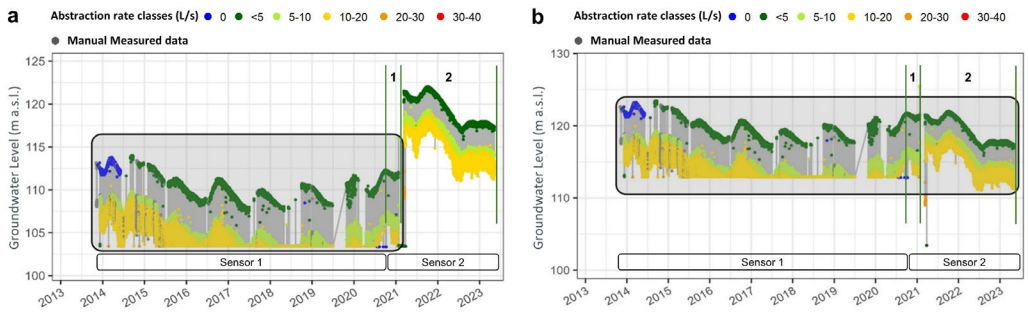

Figure 5.6 *– Time series correction:* ***a)*** *shows the time series before the correction, and* ***b)*** *shows the time series after the correction. Sensor data are classified according to abstraction rate classes (L/s), and manual data are represented in grey. Numbers 1 and 2 refer to the two sections of the data series recorded by sensor 2.*

References

R Core Team (2021) Development Core Team. (2021). R: A Language and Environment for Statistical Computing. In R Foundation for Statistical Computing (Vol. 3, p. https://www.R-project.org). R Foundation for Statistical Computing.

Chapter 6: Time Series Analysis

The Dual Role Of Irrigation In The Groundwater Budget Under Baseline Conditions versus The 2022 Drought: Lessons For Future Climate Adaptation

Agnese Redaelli[1], Tullia Bonomi[1], Davide Sartirana[1], Gianfranco Sinatra[2], Marco Rotiroti[1] and Chiara Zanotti[1],*

[1]Department of Earth and Environmental Sciences, University of Milano-Bicocca, Milan, Italy.

[2]Acque Bresciane S.r.l. SB, Via 25 Aprile, 18, 25038 Rovato, BS, Italy.

*corresponding author: chiara.zanotti@unimib.it

This chapter is largely based on the following paper: *Journal of Hydrology*, ***Volume 658,*** September 2025, 133211. https://doi.org/10.1016/j.jhydrol.2025.133211

Keywords: Groundwater level; Seasonality; Time Series; Dynamic data; Irrigation Water Management; Climate change

Highlights

- Surface-water-fed irrigation can recharge groundwater systems
- Groundwater-fed irrigation depletes groundwater
- 2022 drought determined significant changes in groundwater budget
- Surface-water-fed areas suffered a severe lack of recharge in 2022
- Groundwater-fed areas depletion increased by up to 100% more during 2022 summer

Abstract

Groundwater is facing shortage scenarios worldwide due to a changing climate, but systems governed by different recharge processes may react differently. Hence, understanding groundwater budget components is critical for sustainable resource management. This study analyzes seasonal groundwater level patterns from active drinking water wells, investigating different hydrogeological contexts and water management practices. In the first phase, data under baseline conditions (2013-2021) are

analyzed to identify the average seasonal patterns and the associated recharge and discharge processes. Successively, the 2022 data is compared with baseline data to quantify the effect of the hydrological drought. Results show that in surface-water-fed irrigation areas, the absence of surface water during the 2022 summer, related to winter snow scarcity in the Alps, caused significant disruption of the typical groundwater seasonal profile. The winter groundwater table decrease was more than twice the average decrease under baseline conditions, and the summer rise was the 30% of the average rise under baseline conditions. This is related to the missing recharge and the increased abstraction of groundwater to fill the lack of surface water for irrigation needs. Therefore, in a scenario of dryer summers linked to climate change, the plausible transition toward more efficient irrigation methods or groundwater irrigation could cause severe groundwater depletion and compensation measures will be needed. Conversely, in groundwater-fed irrigation areas, the increased irrigation needs during the 2022 summer determined a summer groundwater depletion 76% wider than the average summer depletion under baseline conditions. Here, mitigation actions to reduce abstracted volumes, such as transitioning to more efficient irrigation systems, could reduce groundwater vulnerability to climate change. On the other hand, aquifer systems governed by natural recharge and discharge processes showed a wider pluriannual variability associated with dry and wet years and resulted less vulnerable to single dry seasons than highly anthropic systems.

6.1 Introduction

Groundwater provides societies with tremendous social, economic, and environmental benefits and opportunities (UNESCO, 2022). Nevertheless, groundwater availability has been facing shortages worldwide in the last decades.

A recent study (Jasechko et al., 2024) highlighted that rapid groundwater-level declines are evident globally in the twenty-first century and that declines have accelerated over the past four decades in 30% of the world's regional aquifers. Although generally considered more resilient than surface water to meteorological conditions, concerns about groundwater availability in relation to climate change are rising worldwide

(Atawneh et al., 2021; Bierkens & Wada, 2019; Ndehedehe et al., 2023). More specifically, drought effect on water availability can have direct impacts on human activities and natural ecosystems (Stephan et al., 2021).

IPCC reports that Global surface temperature will increase until at least mid-century under all emissions scenarios, and this will lead to changes in the climate system, including increases in the frequency and intensity of hot extremes and agricultural and ecological droughts. Projected changes in extremes are larger in frequency and intensity with every additional increment of global warming (IPCC, 2023; Stigter et al., 2023).

In the last 120 years, an increasing trend in the severity of agricultural and ecological droughts emerged due to amplified atmospheric evaporative demand, and increased drought severity is expected in areas in which models project reduced precipitation (southern North America and Central America, northern South America and the Amazon basin, southwestern America, the Mediterranean region, western and southern Africa and South Australia) but, more generally, in water-limited regions everywhere due to enhanced atmospheric evaporative demand (Vicente-Serrano et al., 2022).

A recent study at a global scale demonstrated that climate change is expected to have severe impacts on groundwater storage under the business-as-usual scenario (RCP8.5), highlighting that these effects are not only linked to projected changes in precipitations but also controlled by other hydrological processes (e.g., evapotranspiration and snow-melt) worsened by the impacts of over-pumping that could easily far exceed the natural replenishment (Wu et al., 2020).

In these scenarios, understanding the elements of the groundwater budget in specific areas is the cornerstone of sustainable resource management (Di Giovanni et al., 2023). Indeed, different recharge mechanisms can respond differently to global warming (Meixner et al., 2016), and a region's sensitivity to climate change depends on the recharge mechanisms governing a given aquifer system (Amanambu et al., 2020).

The analysis of groundwater level time series demonstrated to be key in deepening the understanding of the groundwater's response to natural and anthropic factors (Anand et

al., 2020; Colyer et al., 2021; Egidio et al., 2022; Fronzi et al., 2024; Lasagna et al., 2020; Meggiorin et al., 2021; Noori & Singh, 2021; Obergfell et al., 2019; Pathak & Dodamani, 2019; Ronchi et al., 2018; Sakizadeh et al., 2019; Sartirana et al., 2022; Treviño et al., 2023).

More specifically, while most studies concentrate on long-term trends of groundwater levels, a focus on the seasonal patterns demonstrated to be able to provide precious insights into the anthropic and natural processes governing groundwater budget over time (Colyer et al., 2021; Lafare et al., 2016). Indeed, most of the groundwater budget elements can have a strong seasonality. In this regard Jasechko (2014) highlighted that the recharge of groundwater systems by meteoric water worldwide has a strong seasonal feature. On the other hand, also anthropogenic processes affecting groundwater can have strong seasonal differences. For example, agriculture, which has strong seasonal cyclicity, is regarded as one of the primary anthropogenic factors affecting the groundwater balance with multiple possible effects on groundwater worldwide, such as groundwater depletion in regions with primarily groundwater-fed irrigation or groundwater recharge from return flows where irrigation is fed by surface water (Dangar et al., 2021; Scanlon et al., 2023; Taylor et al., 2013).

Besides understanding the processes governing the groundwater budget under ordinary conditions, analyzing the groundwater response to critical situations, such as hydrological droughts, can provide valuable information on the groundwater budget elements and the response to water management policies. Hydrological droughts are defined as low-flow periods with streamflow or groundwater level deficits lower than “natural” conditions (Tramblay et al., 2020).

The year 2022 was one of the warmest years, with high temperatures in several regions worldwide. Many regions, such as the southwestern U.S., southern Europe, India and central South America suffered serious drought during that year, resulting in devastating impacts on social, agricultural, and ecological sectors (Liu et al., 2023; Weaver et al., 2023; Zhang et al., 2023).

In several European countries, 2022 was a critical year with a severe hydrological drought that resulted in enormous socioeconomic impacts (Faranda et al., 2023; Masseroni et al., 2024; Toreti et al., 2022). The drought conditions in Europe originated from a quasi-stationary high-pressure ridge extending from northern Africa to the British Islands and from the Azores to Italy, starting in winter 2021 (Avanzi et al., 2024). The simultaneous occurrence of dry and hot conditions during winter, as in 2022, generally causes the most severe snow droughts and, consequently, the most severe summer streamflow droughts (Dierauer et al., 2018, 2019).

Global projections emphasize the critical need to study the mechanisms of groundwater recharge and discharge and their changes under water scarcity conditions. This is essential for planning sustainable water resource management that accounts for potential future water scarcity. Nevertheless, several areas worldwide report a lack of monitoring data or monitoring networks that are scarce and unevenly distributed in both space and time (Bhatti et al., 2017; Haaf et al., 2023; Lall et al., 2020). In most cases, regional monitoring networks hardly reach the detail needed to deeply understand the water budget at local scales, especially in highly heterogeneous areas. On the other hand, water suppliers collect groundwater and abstraction rate data, which are often neglected as they are associated with pumping wells. To the best of our knowledge, no previous work specifically addressed the challenges in exploiting groundwater level data from pumping wells. Therefore, finding a way to exploit groundwater dynamic data from water suppliers can become the new key to investigate groundwater vulnerability to climate change with high spatial and temporal resolution.

This work aims to investigate first the water budget under baseline conditions through the analysis of groundwater levels over time with a specific focus on seasonality and, successively, to explore the system response to the 2022 drought, highlighting the direct effects of meteorological conditions and the indirect effects mediated by human response to water scarcity, and to evaluate the vulnerabilities of different hydrogeological systems to climate changes. Furthermore, this work aims to investigate the potential of exploiting groundwater dynamic data collected from active drinking water wells that are crucial

also for investigating areas such as the morainic amphitheaters, where no monitoring network is available, leading to a complete lack of data and previous knowledge of groundwater dynamics.

In this work, dynamic data from active drinking water wells are explored, and a preprocessing procedure is proposed aimed at extracting noiseless information from dynamic data representative of the aquifer conditions while discarding the effect of high pumping rates. The study area covers a wide range of hydrogeological settings and water management practices, including i) a plain area with intensive surface-water-fed irrigation, ii) a plain area with groundwater-fed irrigation, iii) two morainic amphitheaters with a multitude of small aquifers, and iv) alpine valleys.

To investigate the groundwater budget components, semi-static data under baseline conditions are analyzed through cluster analysis to extract seasonal patterns representative of recharge and discharge processes. To quantify the distortion from the typical seasonal patterns induced by meteorological conditions and water management, the effect of the 2022 drought is explored through a specific focus. Furthermore, 22 years of meteorological data are analyzed to quantify precipitation and temperature anomalies.

6.2 Materials and Methods

6.2.1 Study Area

The present study covers an area of ~ 4000 km^2 within the province of Brescia in northern Italy (Fig. 6.1).

According to the Köppen classification, the study area falls in the “Cfa” climate group, which is characterized by a temperate continental climate with cold winters and humid, hot summers and an average temperature of 12.5°C (Faquseh & Grossi, 2023). The rainfall regime, with a mean annual precipitation of ≅ 900 mm, is characterized by a bimodal trend with two maxima, with moderate prevalence of the autumn maximum over the spring one, and two minima, in winter and summer (Faquseh & Grossi, 2023).

The land use is mostly agricultural (Fig. 6.1c). The most commonly used irrigation method is the surface irrigation method, where farmers flow water down small trenches running through their crops, but this method is not practiced uniformly in the study area. In Figure 6.1d, the number of farms applying the surface irrigation method is shown for every municipality, standardized by the municipality area (n° of farms per hectare); it is evident that the surface irrigation method is widely applied in the south-central plain, while it is rarer in the northernmost sector of the plain and in the moraine amphitheaters, mostly devoted to vineyards.

This area is denoted by a heterogeneous geological and hydrogeological setting (Fig. 6.1b), including an alpine area in the north, a plain area (part of the Po Plain) in the south, and two morainic amphitheaters along lakes Garda and Iseo (Marchetti, 2002; Vercesi, 1994; Zanotti et al., 2019). Lakes Garda and Iseo, together with Lake Idro, represent three of the main Italian lakes of the subalpine lakes district whose regime is dam regulated since the second half of the twentieth century, mostly for hydropower and agricultural purposes (Hinegk et al., 2022).

In the study area, six main aquifer systems can be identified (Fig. 6.1b): i) Alpine area, ii) Lake Iseo morainic amphitheater, iii) Lake Garda morainic amphitheater, and a plain area which can be further divided into iv) higher plain, v) middle plain and, vi) lower plain. The transition from the higher to the lower plain is marked by a narrow area with numerous groundwater outflows (lowland springs), known as “the springs belt,” located in the middle plain (Bartoli et al., 2012; De Luca et al., 2014;).

From a hydrogeological point of view, the Alpine area hosts alluvial river valley aquifers, usually unconfined, and mountain-blocked fractured aquifers whose main recharge sources correspond to precipitation and snowpack melt (Somers & McKenzie, 2020; Vercesi, 1994). Almost all the coastal territories of Lake Iseo, Lake Idro and the northern portion of Lake Garda are included in the Alpine area. The Iseo and Garda lakes morainic aquifer systems constitute incredibly complex hydrogeological environments where moraine and fluvio-glacial/-lacustrine deposits overlap. Vineyards and residential destination are the two main land uses. In particular, the area along the shores of Lake

Garda is characterized by a strong summer tourist vocation. These systems include local unconfined aquifers of limited potential and deeper confined aquifers layered between silty/clayey aquitards with complex and long recharge mechanisms, which are difficult to determine due to the structural complexity of these aquifer systems (Bini & Zuccoli, 2004; Vercesi, 1994; Zanotti et al., 2022).

The higher plain (north) hosts a monolayer unconfined aquifer up to 100 m b.g.s, mainly composed of coarse sediments (sands and gravels – Fig. 6.2). The land use is mainly agricultural (Fig. 6.1c) (crop/arable land), where corn cultivation, especially for cattle and pig feeding, dominates. In this area, irrigation is mostly fed by surface water through an extensive network of centuries-old irrigation canals (Fig. 6.1c) whose water comes from Subalpine lakes (i.e., lakes Iseo, Idro, and Garda) and Alpine rivers (i.e., Oglio, Mella, and Chiese rivers). An exception is represented by the northernmost sector of the higher plain, where irrigation is rarely practiced using groundwater. In the higher plain, aquifer recharge occurs via irrigation return flow during the growing season, local precipitation, losing rivers and canals, and mountain-front recharge in the northernmost sector, while discharge is primarily related to outflows through the springs belt, well abstraction, gaining portion of Oglio River and outflow to the lower plain aquifers (Bonomi et al., 2008; Rotiroti et al., 2023). This sector constitutes the recharge area of both higher and lower plain aquifer system.

The presence of the springs belt at the transition between the higher plain and the downstream lower plain intercepts and discharges the summer excess groundwater, preventing the increase of groundwater heads in the higher plain caused by irrigation during the growing season from being transferred to the lower plain aquifer. The spring's increased discharge transfers this excess downstream without excessively altering the groundwater level in correspondence and downstream of the spring belt (Fumagalli et al., 2017; Rotiroti et al., 2019a).

The lower plain hosts a multi-layer system of confined sandy aquifers separated by a vertical alternation of several layers of fine material (silt and clay – Fig. 6.2) (Vercesi, 1994). This multilayer system can be subdivided into three aquifer sub-units: shallow

(depth <40 m below ground surface (b.g.s.)), intermediate (40–100 m b.g.s.), and deep (>100 m b.g.s.). The shallow aquifer can become locally semi-confined or unconfined due to local factors, such as the local absence of shallow confining layers. (Rotiroti et al., 2019b). As shown in Figure 6.2, irrigation wells (I) predominantly tap the shallow sub-unit, whereas drinking water supply wells (D) tap the intermediate and deep aquifer sub-units. Similarly to the higher plain, the land use in the lower plain is mainly agricultural, but here the main source for irrigation is the groundwater abstracted through irrigation wells (Rotiroti et al., 2019a; Zanotti et al., 2019). Groundwater recharge for the lower plain aquifer system occurs solely through groundwater inflow from the higher plain aquifer due to the presence of superficial confining low-permeability layers that reduce or completely prevent surface infiltration. Discharges from the lower plain aquifers occur through gaining rivers and well abstraction (Vercesi, 1994).

The groundwater flow in the plain area is characterized by a NS direction in the higher plain and NW to SE direction in the lower plain (Regione Lombardia, 2016). The water table depth (Fig. S.6.1a) decreases from north to south, ranging from more than 40 m in the northernmost sector to less than 5 m in the medium-low plain.

Climate studies for northern Italy indicate that this region is facing a concerning trend toward dry conditions (Baronetti et al., 2020). Projections for the twenty-first century (Baronetti et al., 2022) suggest this trend will persist and intensify. Most Global Climate Models (GCM) and Regional Climate Models (RCM) indicate an increase in drought severity, particularly under the high-emission scenario (RCP 8.5), with longer drought durations and a larger percentage of drought-affected areas expected by the latter part of the century (Baronetti et al., 2022; Raymond et al., 2019; Sofia et al., 2023). Significant temperature increases and escalating drought conditions will particularly impact the Alpine region, a crucial water source for the downstream plain areas.

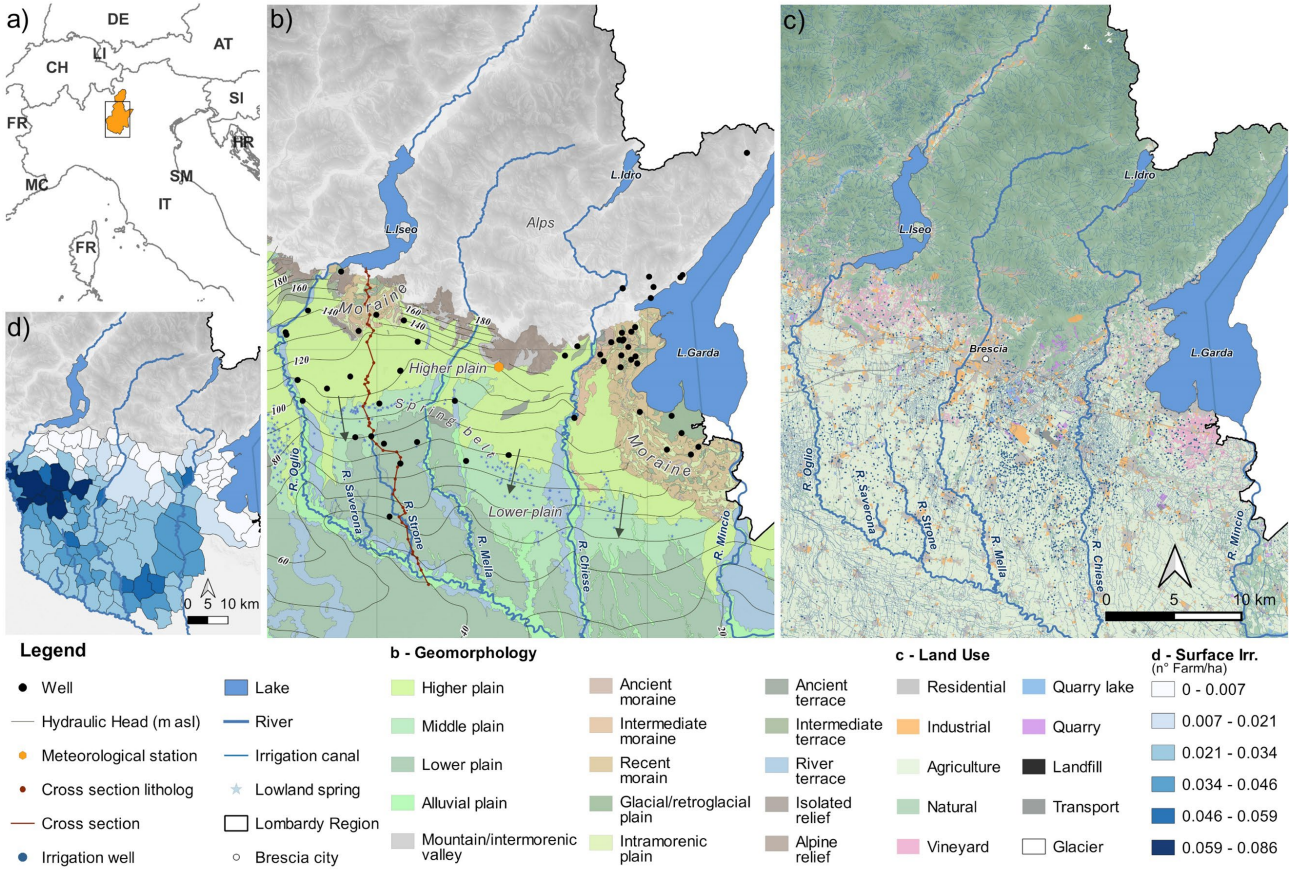

***Figure 6.1** – **a)** Study area; **b)** Geomorphology (Regione Lombardia, 2007), monitoring wells, meteorological monitoring station, water table contour map (September 2014; (Regione Lombardia, 2016)) with flow directions, and cross-section trace. The cross-section is visible in Fig.*

6.2; ***c)*** *Land use (land use classes have been represented from the geographic database Dusaf 7.0 (Regione Lombardia 2023));* ***d)*** *Application of the surface irrigation method (surface water or groundwater fed) - number of farms that apply the surface irrigation method per hectare (municipal data available from ISTAT - http://dati-censimentoagricoltura.istat.it/Index.aspx)).*

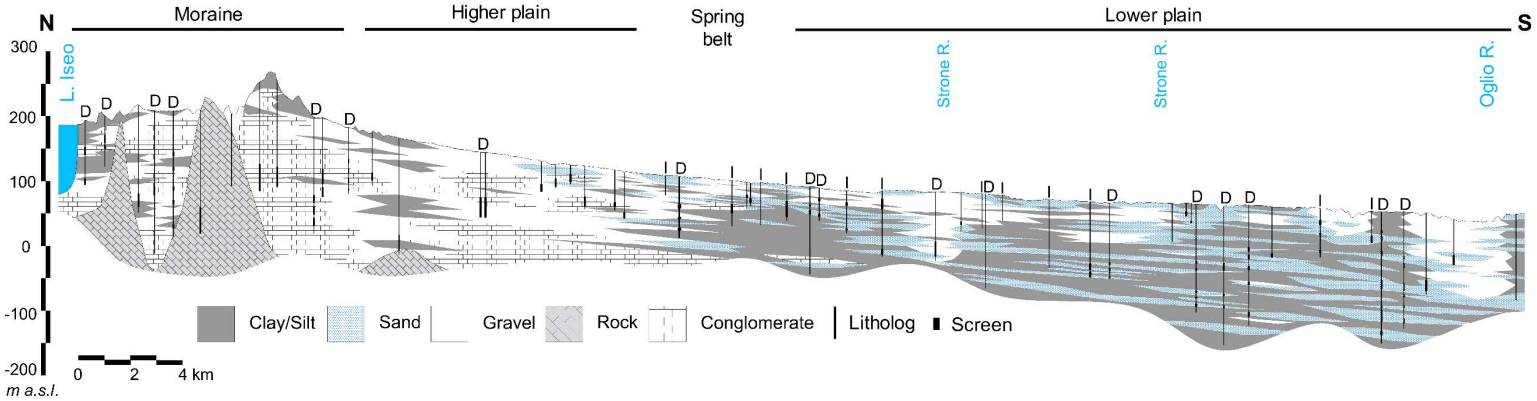

Figure 6.2 *– Cross-section (modified from Zanotti et al., 2022). The cross-section trace is visible in Fig. 6.1. Wells are classified according to their use: D = Drinking, I = Irrigation, while no label indicates other uses.*

6.2.2 Available data

The local water supplier Acque Bresciane S.r.l. provided hourly raw data of the water head above the data logger (meters) and withdrawal rate (L/s) for 107 drinking water supply wells. The total data covers a maximum period of 10 years, from 2013 to 2022. In addition, the dataset containing static groundwater level data manually collected between 2013 and 2021 was provided. Since the data come from wells used for public supply, and the integrated monitoring network is constantly being improved and expanded, the available time series are characterized by different time spans. Finally, available supplementary structural information such as the well's elevation, well's depth, and data logger depth were provided by the water supplier for each well.

In previous studies (Zanotti et al., 2022), the classification of the groundwater body tapped by each well (Confined, Semiconfined, and Unconfined) was performed, evaluating the depth and extension of the first screen, lithostratigraphic data, geological information from the area, detailed cross-sections, and groundwater depth data. For nine wells, this categorization was not available.

Daily water level data of Lake Garda were downloaded from the web portal of Regional Agency for Environmental Protection of Lombardy (ARPA Lombardy, https:///www.arpalombardia.it/Pages/Meteorologia/Requested-data-metered.aspx). In particular, the hydrometric observations recorded by the monitoring station of Manerba del Garda - Dusano (in the south-wester part of the Lake Garda) cover the period 2017–2022. Finally, from the same web portal, the datasets containing the historical series of daily precipitation and maximum and minimum temperature data from 2001 to 2022 were downloaded. These data were recorded by the gauging station in the city of Brescia (ITAS Pastori), where the longest time series were available.

6.2.3 Meteorological data analysis

Meteorological data were explored to identify the precipitation and temperature anomalies with a specific focus on 2022. The period 2001-2020 was considered as the reference period, and temperature and precipitation anomalies were expressed as

percentage variations from the reference period average. Yearly anomalies were evaluated on the hydrological years (December – November). Furthermore, monthly anomalies in the 2021 and 2022 periods were evaluated and compared with the minima, maxima, 25th, and 75th percentiles of the monthly anomalies in the reference period. The multi-annual variability of the seasonal data was calculated: for each season, the cumulative precipitation, the average temperature, and dry days were calculated for every hydrogeological year of the considered time window.

6.2.4 Groundwater level data preprocessing

Data preprocessing started with the exclusion of data associated with sensor errors (e.g., negative values). Of the 107 available wells, 61 were selected that had at least one complete year of data available prior to 2022. Successively, on the 61 selected wells, the identification and the extraction of the static and/or semi-static trends were carried out. A first analysis of the availability of groundwater level data associated with a 0 L/s abstraction rate (Q) value revealed that the selection of these sole data would result in a substantial loss of data and in the elimination of several wells from the dataset since, in several cases, the wells are rarely completely switched off. Consequently, the data associated with a minimum flow rate, identified by a threshold value of 5 L/s, were selected. This threshold was chosen as the value that would allow maximum continuity along the time series while preserving proximity to static conditions and avoiding the effects of higher pumping rates. To investigate the effect of using data associated with a <5 L/s discharge compared to the static data, a distribution analysis was performed on the daily maximum data through a Wilcoxon signed-rank test at a 95% significance level. The test showed that 78% of the wells had no significant difference between the distribution of static data and data associated with a <5 L/s discharge. The remaining 22% of the wells showed a maximum difference of 0.47 m, which accounted for less than 2% of the total range of the total variability of the single wells. Only for two wells, average differences of 5.6 m and 6.5 m emerged, which accounts for 14% and 15% of the two wells' total variability. These average differences are mostly associated with sporadic data, whose effect is overcome by the monthly median calculation in the

successive step. The procedure for the distribution analysis is thoroughly explained in the supplementary material (Section S.6.2).

Successively, to reduce the remaining noise in the data, the maximum daily values were extracted from the selected semi-static trend and the monthly medians were calculated. Monthly median groundwater levels were selected as robust values, less influenced by any possible remaining outlier and therefore considered representative of the static value. The figures in Section S.6.3 show several examples of the preprocessing on a variety of wells: from the raw data to daily maxima on data associated with an abstraction rate lower than 5 L/s and the monthly medians.

6.2.5 Groundwater level data analysis

As a first phase, the obtained time series were firstly standardized by subtracting the global mean for each well and then detrended by subtracting the yearly mean to remove the effect of interannual fluctuations, which could have masked seasonal variability, and to enable the comparison between time series with different time spans. Successively, seasonal profiles were extracted for each well as the twelve monthly medians. Figures in Section S.6.4 show examples of how subtracting the yearly mean allows for the extraction of meaningful seasonal profiles for a single well while using the original data could lead to noisy information.

To identify groups of wells with similar seasonal profiles and recurrent patterns, a hierarchical cluster analysis (HCA) was performed, considering the 12 monthly medians of the 61 available wells as different variables. Cluster analysis is an unsupervised pattern recognition technique that divides a large group of elements into smaller coherent groups, i.e., clusters (Triki et al., 2014; Zhou et al., 2007). Hierarchical clustering, in particular, was widely used for several groundwater analyses (Nourani et al., 2022; Pathak & Dodamani, 2019; Yin et al., 2022). In this study, HCA was performed using the Ward hierarchical method (Ward, 1963) with the squared Euclidean distance (Bloomfield et al., 2015) in the RStudio environment using the "*hclust*" function from the "*stats*" package (R Core Team (2021) Development Core Team, 2021).

Through the combined analysis of the groundwater level fluctuations, such as the seasonal minimum and maxima and the dynamic range (the difference between the maximum and minimum groundwater levels), the obtained clusters have been further grouped using a posteriori knowledge of the groundwater systems' hydrogeological conditions. This analysis was performed on data from 2013-2021, focusing specifically on years with baseline conditions representative of the natural seasonal trend of the groundwater level within the study area's meteoclimatic regime.

To investigate how the seasonal variability is related to the total variability of the data for each well, the standard deviation of the original data (as monthly medians), and the standard deviation of the detrended data (i.e., subtracted annual mean) were calculated. The ratio between these two values indicates how much of the total variability is associated with the seasonal variability. This analysis considered only wells with at least two years of data before 2022.

6.2.6 2022 drought effects evaluation

To identify the different hydrogeological systems' responses to 2022 extreme conditions, the groundwater level trends from years before 2022 and the 2022 trend were compared. This analysis was conducted on a subset of 51 wells with the 2022 measurement available.

For the wells that showed a clear seasonal profile, a detailed analysis was carried out to quantify the distortion of the seasonal profile of 2022 compared to the seasonal profile of the reference years. Specifically, minimum and maximum groundwater levels have been identified for each year, and the average increase and decrease were calculated; successively, the 2022 decreases and increases were compared with the average decrease and increase and expressed as percentage anomalies. For the wells where the pluriannual trend constitutes a major contribution to the total variability and seasonal patterns were less evident, a qualitative analysis through visual inspection was conducted.

6.3 Results

6.3.1 Meteorological data analysis

The year 2022 stood out for record-low precipitation and record-high air temperature, which resulted in a severe hydrological drought. Figure 6.3 and a focus in Section S.6.5 summarize the elaborations of meteorological data at the weather monitoring station (Fig. 6.1); a twenty-year time window (2001 – 2020) was considered as reference period.

Figure 6.3a combines the temperature and precipitation anomalies over the hydrological years (Dec-Nov) based on the reference period. Figure 6.3b shows the monthly precipitation and temperature values for the reference period (boxplots and black line, respectively) and the 2022 data (red triangle and red line). Figures 6.3c shows monthly precipitation anomalies as percentages: the grey bars indicate maxima, minima, 25^{th} and 75^{th} percentile of the percentage anomalies over the reference period, while red and blue bars indicate percentage anomalies of the 2021 and 2022 data. Figure 6.3d reports the seasonal count of dry days.

This elaboration highlights how the hydrological 2022 year constitutes an absolute anomaly for both temperature and precipitation with respect to the reference period. Specifically, as shown in Figures 6.3b and 6.3c, starting from December 2021 throughout the whole 2022, the precipitations were characterized by a severe negative rainfall anomaly and a deficit of precipitation of approximately - 48% that reached the highest value in October 2022 with a rainfall deficit of - 99% compared to the reference period. The driest season was spring, with a deficit equal to -75% (Fig. 6.3c, Fig. 6.3d, and Fig. S.6.18). In addition to the precipitation deficit, an annual temperature anomaly of about +1.5 ºC was recorded compared to the 2001-2020 average of 14.4 ºC (Fig. 6.3a). Positive temperature anomalies above 2 °C were recorded in February, May, June, October, and December, with a July peak of +3.6 °C (Fig. 6.3b, Fig. S.6.17, and Fig. S.6.19).

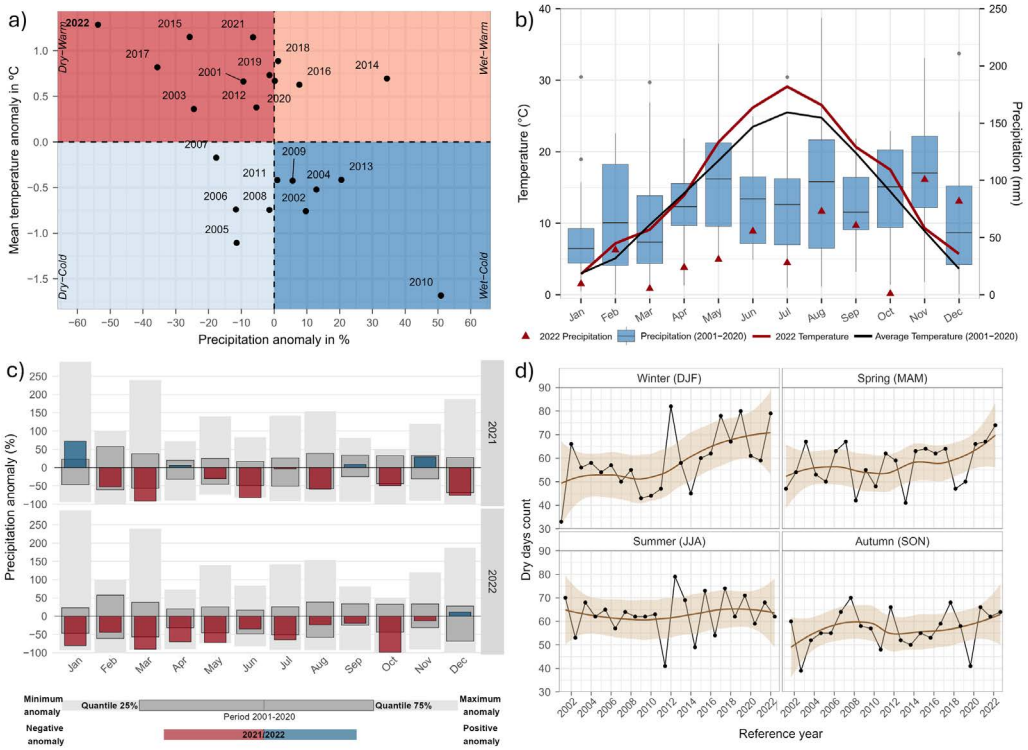

***Figure 6.3** – **a)** Precipitation and temperature anomalies over hydrological years (Dec – Nov) with respect to the reference period 2001-2020; **b)** Monthly precipitation and temperature over the reference period (boxplots and black line) and 2022 monthly precipitation and temperature (red triangles and red line); **c)** Precipitation anomalies (as percentages): grey bars indicate maxima and minima (light grey) and 25th and 75th percentile (dark grey) of precipitation anomalies over the reference period, while red and blue bars indicate 2021 and 2022 anomalies compared to the reference period; **d)** Seasonal count of dry days. The brown line represents the loess regression, while the light-brown area represents the confidence interval.*

6.3.2 Analysis of Groundwater levels under baseline conditions

The HCA resulted in the identification of 13 clusters. The spatial distribution and seasonal profiles are shown in Figure 6.4, while Figure 6.5 shows the monthly median of groundwater level for each well, color-coded by clusters. The 13 clusters have been grouped into 6 groups (A-F) based on similarities between seasonal maxima and minima. The areas where these groups are located can be considered hydrological units with

comparable characteristics and where the groundwater level reacts to recharge and discharge in comparable ways.

In Table 6.1, the ratios between the standard deviation of the detrended monthly median (i.e., subtracted annual mean) and the standard deviation of the original monthly medians are reported as average over the different clusters.

The characteristics of each group are listed below, while focuses on single clusters are available in the supplementary materials (Section S.6.6)

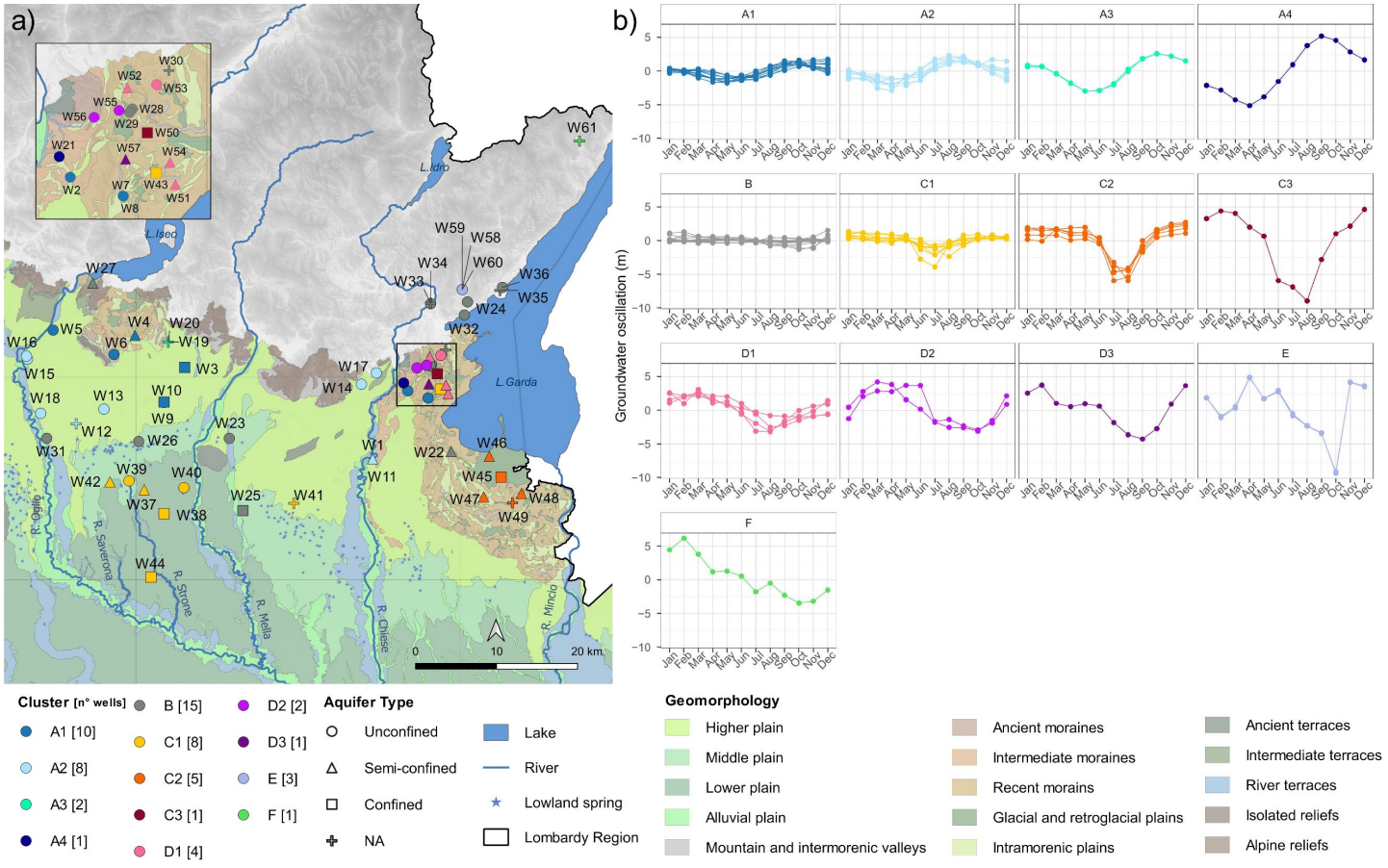

Figure 6.4 – a) *Spatial distribution of the wells color-coded by cluster over the geomorphological map (Regione Lombardia, 2007),* ***b)*** *Seasonal pattern of the wells, grouped by clusters.*

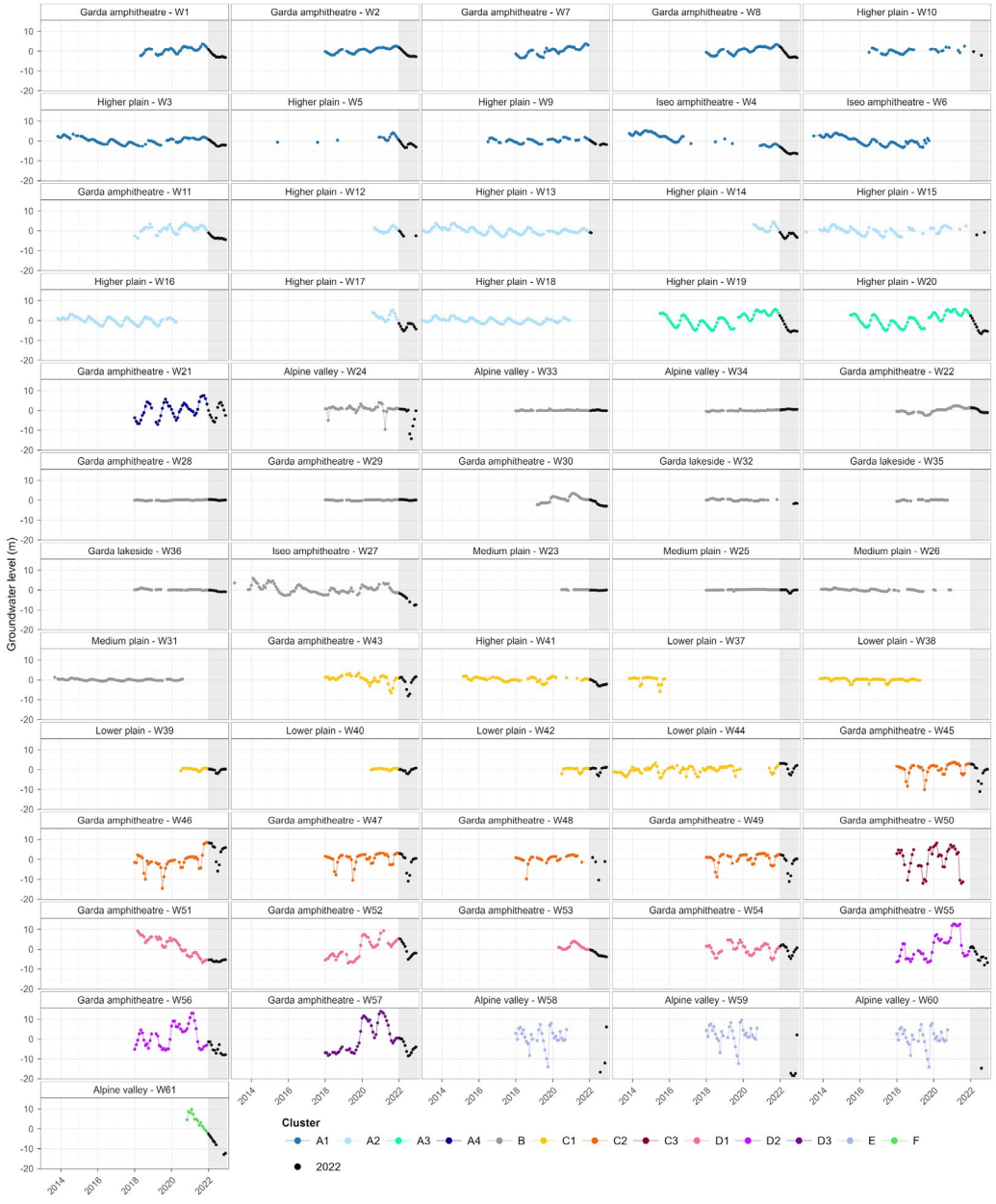

Figure 6.5 *– Groundwater level time series (monthly median) color-coded by cluster. Data for 2022, excluded from the cluster analysis, are represented as black dots over the grey-shaded area.*

***Table 6.1** – Average ratio between the seasonal variability and the total variability calculated, respectively, as the standard deviation of detrended data (annual mean subtracted) and the standard deviation of original data.*

Cluster	Average of sd. Detrended/ sd. Total
A1	62.81%
A2	84.70%
A3	63.88%
A4	92.63%
B	76.57%
C1	87.68%
C2	92.45%
C3	92.32%
D1	59.05%
D2	75.01%
D3	53.76%
E	99.24%
F	n.d.

Group A consists of 4 clusters, including 15 wells located in the higher plain, 4 wells in the intermorainic plains, and 2 wells located in the morainic deposits. All clusters exhibit a seasonal pattern with a minimum in Spring and a maximum during Autumn. The range of seasonal variability increases from A1 (2.6 m) to A4 (one well - 10.3 m).

The A group seasonal profile, with its summer rising, can be generally associated with recharge from surface water linked to irrigation processes: irrigation return flow or leakages from unlined irrigation canals. The clusters highlight a difference between wells located in the outer limit of the morainic aquifer systems and in the northern part of the higher plain (A1 and A3), where the surface irrigation method is rarely applied and irrigation canals are sparser, and the southern sector of the higher plain (Cluster A2) where the surface irrigation method is prevalent, and a dense canal network is evident.

More specifically, wells in the northern sector (A1 and A3) generally show a wider pluriannual oscillation, with the seasonal oscillation constituting ca. 60% of the total variability, while wells in the southern sector of the higher plain (A2) show a wider seasonal oscillation (3.8 m) constituting 85% of the total variability (Table 6.1).

Group B includes 1 cluster, grouping 15 wells spatially dispersed in the study area. This cluster groups wells with the minimum seasonal oscillation in the dataset. The pluriannual variability (Fig. 6.5) is different among the wells in the cluster, ranging from very narrow (e.g., W33 and W34) to wider oscillations (e.g., W22 and W30). Within group B, 3 cases can be identified, characterized by specific hydrogeological settings that determine this narrow range of seasonal oscillation: a) proximity to the spring belt (middle plain), b) proximity to the Lake Garda shores, and c) morainic compartment and alpine valleys.

Group C represents wells tapping from lower plain and morainic aquifers that show a seasonal trend disrupted by a summer lowering. Group C includes three clusters (C1-C3) with a total of 14 wells, where C1 groups all the wells in the lower plain and a single well in the morainic compartment, C2 groups a set of neighboring wells in the southern portion of the Garda Lake morainic amphitheater and C3 only one well located in the morainic compartment. The range of the seasonal variability increases from C1 (2.5 m) to C3 (13.6 m). All the wells of group C show reduced pluriannual variability, and seasonal variability constitutes about 90% of the total variability.

Group D (D1-D3) collects 7 wells in the morainic hills, showing a response to local precipitation. All group D clusters have a seasonal pattern with a maximum in Spring and a minimum in Summer or late Summer. All the wells in group D clusters show wide pluriannual variability (Fig. 6.5), and seasonal variability constitutes 54% (D3) to 65% (D1) of the total variability. For example, summer 2020, which was particularly wet, resulted in an average increase for most wells (Fig. 6.5). Well W51 appears to be the only exception since it is distinguished by a decreasing trend over all the available years dependent on local conditions.

Cluster E groups three wells tapping a small coarse aquifer in the Alpine valleys. The seasonal pattern, strictly correlated to the local geomorphological features, is characterized by the absence of an evident maximum but shows a minimum in October. Due to the relatively lower elevation of the tapped alpine aquifer, liquid precipitation constitutes the year-round primary driver of groundwater recharge.

Cluster F includes only one well located in a small Alpine valley. As cluster E, cluster F well tap a small coarse aquifer. However, its seasonal pattern, with no specific maxima or minimum, results mostly from a general decreasing trend, and due to the reduced amount of available data, a specific seasonal pattern does not emerge.

6.3.3 Analysis of groundwater level response to the 2022 drought

The different hydrogeological compartments have shown a peculiar response to the 2022 drought.

For group A, the analysis of the 2022 response was conducted on 17 wells having 2022 data (Fig. 6.6, focus in Section S.6.7). For each well, the 2022 spring decrease and summer increase were compared with the average decreases and increases in the previous years. It results that during 2022, over the whole A group, spring decrease was 111% higher than the average decrease measured in years before 2022, while the 2022 summer increase was 69% lower than the average increase (Fig. 6.6). More specifically, considering only the Higher Plain aquifer, the 2022 winter decrease was 89% wider than the usual decrease, while the 2022 summer increase was 71% lower than the usual increase.

Moreover, in the typical seasonal profile of group A, the spring minimum is reached in April-May, while in 2022, 60% of wells (9 wells) reach the minimum in summer (July-August) during the irrigation season (Fig. S.6.21). Differently, three wells (W5, W14, and W17) reach the minimum in the typical period, while they reach the maximum in July or August, i.e., 1-2 months before the typical maximum. For these three wells, the analysis was conducted using a reference period of one year (2021) since it was the only complete year available.

Well W21 (cluster A4) represents the only exception within group A; indeed, the 2022 increase was only 6% lower than the average measured in years prior to 2022, while the decrease was 44% wider than the average decrease. As described in Section S.6, well W21 taps a smaller and highly responsive aquifer, which plausibly shows a response even to a small amount of recharge. Therefore, this peculiar behavior compared to group A could be attributable to the local management of irrigation water, where even a small amount could determine the groundwater table rise, also sustained by August and September rain.

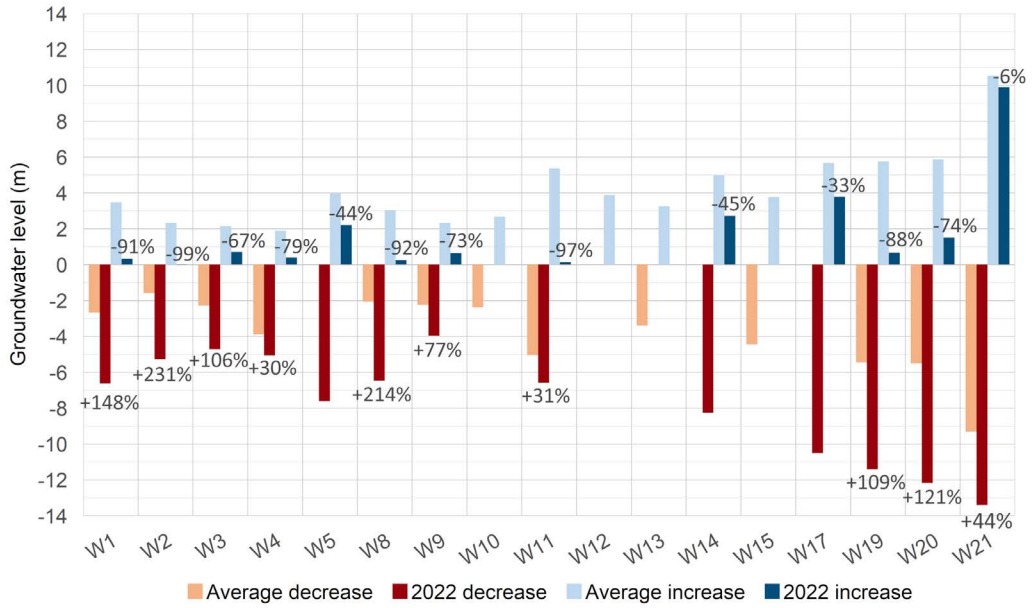

Figure 6.6 *– Average winter/spring groundwater level decrease (orange bar), and summer increase (light blue bar) compared to 2022 winter/spring decrease (red bar) and increase (blue bar).*

For group C, the 2022 response analysis was conducted on 11 wells with 2022 data. In 2022, group C displayed the typical profile but with an exacerbated summer minimum (Fig. 6.7, focus in Section S.6.7). The 2022 summer decrease and subsequent increase were compared to the average decreases and increases in previous years (Fig. 6.7 and Fig. S.6.22). Results show that, globally, the 2022 summer decrease was 76% higher than the average decrease (Fig. 6.7). As a result, the lowest groundwater level throughout

the available series was recorded in 9 wells. For most of the wells, the increase after the summer minimum led to the restoration of normal conditions, while for 2 wells (W41 and W44), the 2022 increase was lower than the average of the years before 2022.

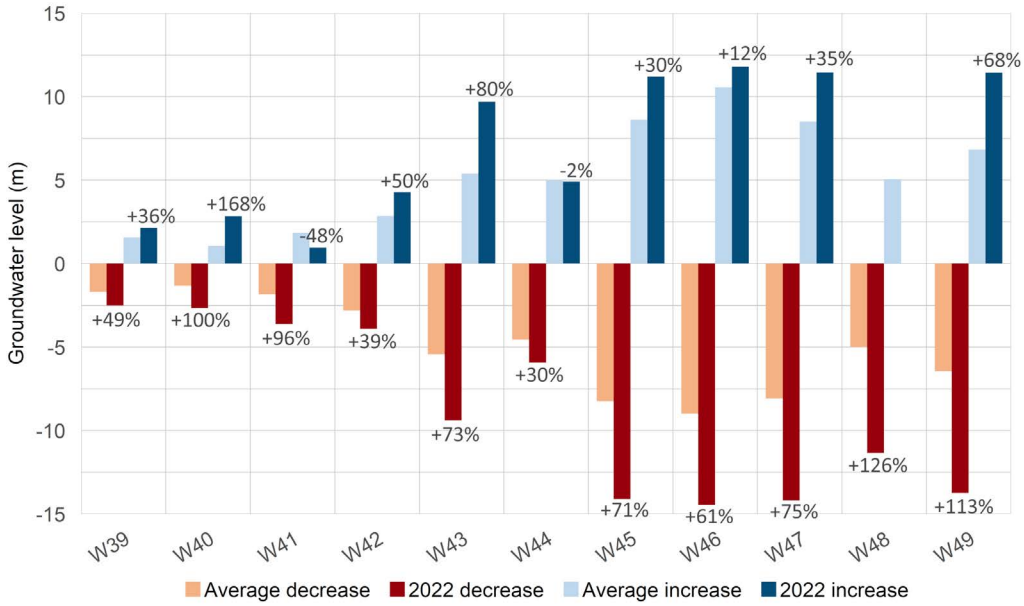

***Figure 6.7** – Average summer groundwater level decrease (orange bar), and autumn increase (light blue bar) compared to 2022 summer decrease (red bar) and increase (blue bar).*

For group B, 2022 data are available for 12 wells. Group B is characterized by a steady groundwater level with the narrowest groundwater level oscillation throughout the study area. The reduced amplitude of the oscillations is also confirmed in 2022. In the spring belt, 2022 data are available only for the eastern sector (W23 and W25), which shows a 2022 response comparable to group C. Their 2022 trend is characterized by a decrease during the summer period that determined an unprecedented minimum. As for group C, this response to the 2022 conditions is attributable to the increased summer groundwater demand.

Group B wells in the morainic compartment, primarily influenced by the recharge effect of rainy periods, exhibited different responses to the reduced amount of precipitation due to local hydrogeological factors. However, in 2022, a significant decrease in groundwater level was observed within all wells' trends, with 8 wells recording historical

groundwater level minima within the available time series (Fig. 6.5 and Fig. S.6.23). Wells in the alpine valleys constitute exceptions: in well W33 the level increased comparably to the previous years, and in well W34, the groundwater level growing trend started in 2020 is also maintained during 2022 (in both cases the range is limited to a few cm), while well W24 shows a marked decrease in 2022 (ca. 1 m).

W32, W35, and W36 wells, located along the Lake Garda shores, confirmed the pressure balance between these portions of the aquifer and the lake. The groundwater level trend of the three wells is indeed equal to the trend of the water level of Lake Garda, which showed a 2022 minimum typical of surface water bodies (Section S.6).

All 7 wells of Group D have 2022 data. During 2022, the effect of the drought period is highlighted by a general decrease in the groundwater level in all the wells. Group D's response to 2022 is not homogeneous (Fig. 6.5, focus in Section S.6.8). For wells W52, W53, W54 and W57 (assuming W53 to have a similar time series to his neighboring well W52) 2022 response does not determine an unprecedented condition, as opposite to Groups A and B, while for wells W55 and W56 the 2022 response induce a minimum which is respectively 1.4 m and 2.4 m lower than the minimum of the previous years. Well W51 is characterized by a decreasing trend in all the available years.

Due to a lack of data, analysis could not be performed for Cluster E and Cluster F (Fig. 6.5, focus in Section S.6.8).

6.4 Discussion

6.4.1 Groundwater recharge and discharge of the different aquifer systems under baseline conditions

6.4.1.1 Higher Plain Aquifer – Surface-water-fed irrigation areas

The higher plain aquifer system is characterized by a highly permeable unconfined aquifer mainly composed of coarse sediments. All the wells tapping this aquifer system fall into the A group, showing a groundwater level rise during summer, which is a dry season in terms of precipitation. The A group seasonal profile, with its summer rising,

can be generally associated with recharge from surface water linked to irrigation processes: irrigation return flow or leakages from unlined irrigation canals (Zucaro et al., 2011).

A narrower seasonal oscillation is evident in the north-western area and at the border of the morainic area (cluster A1 - 2.6 m), where irrigation canals are sparser than in the resto of the area (Fig. 6.1c), and irrigation methods rarely include the surface irrigation method (Fig. 6.1d). An exception is the well in cluster A3 which shows a wider variability, associated with the specific geological setting. For these wells, the seasonal variability only determines a portion of the total variability (ca. 60%), and wide pluriannual oscillations are evident. Therefore, in these areas, the contribution of local precipitation and recharge from upstream formations (mountain-front recharge) is significant and determines a wider pluriannual variability (Fig. 6.5, Table 6.1) compared to downstream wells. A narrow oscillation (cluster A1) is also evident for the confined and semi-confined wells of the higher plain (W3, W10), showing a seasonal pattern comparable to all wells in group A. The presence of fine material layers precludes aquifer direct contact with the surface, but their local extension does not prevent the interaction between these aquifer portions with the overlying unconfined aquifers of the higher plain.

Conversely, wells in the southern and eastern portions of the higher plain (cluster A2), where the canal network is denser (Fig. 6.1c) and where the most common irrigation method is surface irrigation (Fig. 6.1d), show wider seasonal oscillations (3.8 m). Here, the seasonal variability is much wider than the pluriannual variability, constituting 85% of the total variability. Therefore, results confirm that the recharge in the higher plain is primarily influenced by irrigation return flow and leakages from the surface water network, while the variability associated with dryer or wetter years is reduced. Indeed, the infiltration of excess irrigation water together with losses during the distribution of water flowing along the unlined irrigation canals network has been estimated, through an isotopic approach, to constitute around 60% of the groundwater's recharge in the area

while the remainder is from local precipitation and recharge from upstream (Rotiroti et al., 2019a, 2023).

6.4.1.2 Middle Plain Aquifer – Springs Belt

The wells at the transition between the higher plain and the lower plain show groundwater levels constant throughout the year and over different years (group B). In this area the decrease in grain size from coarse to fine sediments, and the consequent change in the aquifer transmissivity, force the groundwater level close to the ground level, constraining the groundwater head oscillations (De Luca et al., 2014). Therefore, the stability of the groundwater trend is mostly associated with the lower permeability of the aquifer system. In the western part of the area, downstream to the intensively irrigated areas, a seasonal pattern is associated with recharge from surface water irrigation, although the variability is significantly lower than upstream. In the eastern part, no seasonal pattern is evident.

6.4.1.3 Lower Plain Aquifer – Groundwater-fed irrigation areas

The lower plain aquifer system hosts a multilayer system of superimposed confined aquifers. All the wells in the lower plain fall into the C1 cluster, showing a constant pluriannual trend with significant summer decreases. Here, recharge is only from groundwater inflow from the higher plain, while irrigation water's and rainwater's infiltration is highly reduced due to diffuse sub-horizontal layers of clay and silt that preclude the aquifers from direct interaction with the surface. Contrary to the higher plain, the main source of irrigation comes from the groundwater extracted through the numerous irrigation wells displayed in the lower plain (Fig. 6.1c). Irrigation thus not only has minimal to no impact in recharging lower plain aquifer but, combined with the summer increase in domestic water demand, contributes significantly to the discharge from the aquifer system.

6.4.1.4 Morainic Aquifers

The morainic aquifer systems show a wide variety of seasonal patterns, strongly linked to the high heterogeneity of the geology settings.

South of Lake Garda, a group of wells marking a specific area and tapping confined and semiconfined aquifers that constitute cluster C2 is evident. These aquifers experience a significant drop in groundwater levels during the summer. The area is largely used for vineyards, which do not require intensive irrigation.

The summer decrease is plausibly associated with increased groundwater extraction for domestic use during hotter months, worsened by the increase in the population due to tourist flow for summer holidays in the locations close to Lake Garda and by the limited lateral extent of the aquifers, which result in significant fluctuations in groundwater levels.

Another group of wells is clearly evident, in the north-west portion of the Lake Garda amphitheater, and it constitutes group D. This group shows a direct response to local precipitations with a maximum during spring due to winter and spring precipitations and a minimum at the end of summer linked to dry summers and increased summer water demand. The reduced dimensions of the tapped aquifers and the fragmentation of the superficial impermeable layer determine a direct response of the aquifer to precipitations. The seasonal variability of these wells is only a small component of the total variability since pluriannual variations are higher than seasonal variations. This further supports the interpretation of group D as wells strongly linked to local precipitations, affected by rainy or dry months, but mainly by the cumulative effect of wet or dry years.

Several other wells in the morainic aquifers system show different behaviors, falling into the A, B, or C groups. Three wells fall in the A group (clusters A4 and A1), with a summer increase associated with a summer recharge. Also in this case, since summer is the dry season, this recharge could be associated with surface water and irrigation processes. These territories have agricultural land use, but no dense river network is present. In this case, further analysis, such as isotopic analysis, could provide a conclusive validation of the recharge by irrigation hypothesis.

Seven wells of the Lakes Garda and Iseo moraine fall in the B group. The reduced amplitude of the seasonal pattern oscillation is related to the limited thickness of the

tapped shallow aquifers, which are generally discontinuous and have low productivity. Despite local differences, aquifers with these characteristics are thereby affected by limited groundwater level oscillation that responds to particularly rainy periods (Severi et al., 1994). Local precipitation constitutes the main input of these systems (Bini & Zuccoli, 2004). This means that seasonality is not evident, while a wider variability is associated with pluriannual precipitation trends.

A peculiar situation emerges for the wells along the Lake Garda shores, which present a strong similarity with the Lake Garda hydrometric level as a result of the pressure balance between the aquifer and the lake (Fig. S.6.20).

Two moraine wells in clusters C1 and C3, with a marked summer groundwater level drop, tap confined aquifers in mostly residential areas. In this case, similarly to cluster C2, the increase in summer withdrawals is plausibly associated with domestic uses, also in relation to summer tourist flow, exacerbated by the reduced dimensions of the aquifer.

6.4.1.5 Alpine Aquifers

Wells in the alpine valleys show various behaviors: 3 wells in group E, 1 well in group F and 3 wells in group B (W24, W34 and W33), each characterized by a peculiar trend due to the geological and hydrogeological feature of the specific watershed (e.g. size and altitude) and aquifer (e.g. size, shape, lithology).

6.4.2 The 2022 hydrological drought

Results indicate that 2022 constitutes both a temperature and precipitation anomaly, showing: a) lack of winter precipitation, starting from December 2021, determining reduced local recharge, but mostly reduced snow accumulation in the Alps, which led to a water deficit in spring at the beginning of the irrigation season, and b) dry spring and summer, with anomalous high temperatures, which increased the irrigation needs and determined high evapotranspiration, reducing net recharge percentage. The combination of dry and hot conditions had significant repercussions on water reserves. Studies on the Italian Alps highlight that the warm and dry winter conditions caused a severe snow drought, with a snow water equivalent reported 88% lower than the 2011-2021 period

(Avanzi et al., 2024), with a March SWE anomaly in 2022 reaching the lowest value in the last century (Colombo et al., 2023).

Spring snow melting constitutes one of the main water sources of the subalpine lakes (ANBI Lombardia, 2023; Cochand et al., 2019; Crespi et al., 2021). Therefore, in 2022, the lack of winter snow in the alpine region led to a reduced inflow in the alpine lakes, leading to a water deficit of more than -30% in the lakes' water volumes (ANBI Lombardia, 2023).

The subalpine lakes constitute the reservoir for rivers and irrigation canals in the downstream plain during summer. Therefore, the reduced availability of surface water in the subalpine lakes and in the downstream rivers (-60% at the regional scale) led to a severe lack of surface water resources for irrigation purposes.

In addition, the particular meteoclimatic conditions of 2022, and particularly the high temperatures, have led to an increase in net irrigation needs that, at a regional level, has recorded an increase of 32% compared to the period 2016-2021 (ANBI Lombardia, 2023). Increased evapotranspiration has been proven to worsen storage anomalies during summer droughts (Teuling et al., 2013).

It was demonstrated (Montanari et al., 2023) that the 2022 hydrological drought in the Po plain (N Italy) was the worst event in the past two centuries (30% lower than the second worst), being part of an increasing trend in severe drought occurrence in the area. Bonaldo et al. (2023) highlight that persistent negative rainfall anomalies like the ones that characterized the 2022 event, though unlikely to become a typical feature of future climate, could remarkably increase their frequency, particularly in severe climate change conditions, and rising temperatures will magnify their impacts. Local studies on Northern Italy indicate that droughts are expected to increase by about 50% by the mid-21st century and by approximately 80% by the late 21st century under both Representative Concentration Pathway (RCP) 4.5 and RCP 8.5 (Sofia et al., 2024). More specifically for the city of Brescia, in the study area of the present study, climate change projections on groundwater resources indicate that a temperature increase has to be expected across all climate scenarios, while changes in precipitation patterns are

predicted with winter increase and summer decrease leading to water scarcity by the middle of the century (Faquseh & Grossi, 2023).

6.4.3 Groundwater recharge and discharge changes due to the 2022 drought

6.4.3.1 Higher Plain Aquifer – Surface-water-fed irrigation areas

In the higher plain, 2022 determined a drastic change in the typical seasonal pattern. All the wells tapping the higher plain aquifer system reached an unprecedented minimum and exhibited a wider spring decrease (up to +148%) and a narrower summer increase (up to -97%) and shifts in the time distribution of minima and maxima compared to the reference period. This modified seasonal pattern is also evident in the northwest area where, under normal conditions, wells show a reduced seasonality and a wider pluriannual variability.

Since the seasonal pattern is attributable mainly to recharge provided by surface water irrigation, it emerged that the vulnerability of this aquifer system is not directly linked to the lack of summer rainfall. Rather, the system's groundwater scarcity was determined by the winter conditions (reduced rain and snow precipitation and higher winter temperatures decreasing snow accumulation) that largely determine the availability of surface water resources, especially in the lake's reservoirs. Specifically, the reduced availability of surface water resources resulted in a significant reduction of the total derived volumes for irrigation purposes from the Oglio and Chiese rivers (-36% and -53%, respectively (ANBI Lombardia, 2022, 2023)).

Furthermore, irrigation management played a crucial role in groundwater recharge: the lack of surface water led to an increased abstraction of groundwater to fulfill irrigation needs. Indeed, data shows that, at the Lombardy region scale, the groundwater volume abstracted in 2022 for irrigational purposes was double the average volume of groundwater extracted in 2016-2021 (ANBI Lombardia, 2023). Therefore, 2022 modified seasonal patterns show the joint effect of surface water scarcity for irrigation and increased groundwater abstraction for irrigation purposes.

6.4.3.2 Lower and Middle Plain Aquifers – Groundwater-fed irrigation areas

In the lower plain, groundwater levels in 2022 showed a drastic increase in the typical summer lowering (from 30% to 100% - Fig. 6.7); in most cases, the successive rising led to the restoration of baseline conditions. Since the main driver of summer decrease is water abstraction for irrigation purposes, which in this area is mostly based on wells, the response to the 2022 climatic conditions could be linked primarily to the increased summer temperature, which led to an increased net irrigation need for crop yield. The same response is visible in the middle plain, where 2022 data show a significant decrease during summer, plausibly associated with increased demand and groundwater abstraction.

6.4.3.3 Morainic Aquifers

The southeast part of the morainic amphitheater (cluster C2), which has a seasonality similar to the lower plain, also shows a 2022 response similar to the one of the lower plain, with a significantly wider groundwater level decrease during the 2022 summer compared to previous years (from 61% to 113%) but in several cases, the autumn rising did not restore the groundwater level of the previous winter.

In the northern part of the morainic amphitheater (group D), the shorter time series limits the interpretation of the 2022 response due to high multi-annual variability. This contrasts with groups A, B, and C, where the seasonal pattern is the primary component of variability. In this case, longer time series would allow for a more solid comparison of 2022 effects with respect to a baseline calculated over several years. Nevertheless, group D’s 2022 response generally does not determine dramatic unprecedented conditions (Fig. 6.5, focus in Section S.6.8).

Morainic wells that showed seasonal profiles assimilable to those in the plain (groups A, B, and C) also show a general 2022 response similar to plain wells, but the limited amplitude of the aquifers determines some peculiarities. The well W43 with the C profile has a widened summer decrease, but it restores the original conditions during autumn; the well W21, in group A, shows a widened winter decrease, but the summer rise is

similar to the average rise of the previous years, which seems to indicate that even small amount of recharge can determine a rise in this small aquifer. The morainic wells in group B (W30, W28, W29 and, W22) confirm narrow oscillations and 2022 does not determine a global groundwater level minimum.

6.4.3.4 Alpine Valleys

In the alpine valleys, 2022 data are available only for wells falling in the B group. The two neighboring wells W34 and W33, showed increased groundwater levels in 2022 (less than 40 cm, compatible with the total variability of the wells). These wells tap an alpine valley aquifer with an ample watershed. Since no recharge from precipitation was available, this increased groundwater level can plausibly be associated with a mountain front recharge that was able to perdure for several dry months. Also in this case, chemical and isotopic analysis could provide more robust insights into the recharge processes of this valley.

Conversely, well W24, located in a small valley on the slopes towards the lake, shows an unprecedented minimum in 2022, 15 meters below the groundwater level at the beginning of 2022. Therefore, as for the data under baseline conditions, 2022 data also showed diverse responses in different alpine valleys; here, more data are needed to investigate local recharge and discharge, also based on watershed amplitude, altitude, and exposition.

6.4.4 Aquifer Vulnerability to climate change and adaptation measures

6.4.4.1 Higher Plain Aquifer – surface-water-fed irrigation areas

Results indicate that in areas with surface-water-fed irrigation, such as the higher plain, climate change adaptation strategies to preserve agricultural productivity will have a decisive impact on groundwater availability, plausibly stronger than climate change itself. Implementing actions to improve the efficiency of irrigation processes, like canal lining operations, and transitioning to more efficient irrigation techniques, such as sprinkling or micro irrigation, would lead to a drastic reduction in groundwater recharge.

Currently, in Italy, local authorities favor the transition from traditional surface irrigation systems to water-saving techniques such as spray, drip, or micro irrigation techniques in response to European and Italian directives. Previous studies (Fabbri et al., 2016; Pool et al., 2021, 2022) highlight that the infiltration due to irrigation could strongly decrease considering the climate changes, up to disappearance due to the complete transition to these irrigation systems. The potential decrease of the infiltration related to the joint effect of climate change and irrigation policies could represent a social, economic and environmental issue, including the decreased inflow of the middle plain springs related to the progressive recharge reduction.

Furthermore, results clearly demonstrate that, in the most extreme case, switching from surface water irrigation to groundwater irrigation would have the double effect of reducing recharge and introducing a new system output. Indeed, groundwater irrigation has been proven to exacerbate drought conditions' effects on groundwater storage (Liu et al., 2022).

In these scenarios, compensation measures will have to be implemented to restore groundwater recharge and guarantee the social and ecosystem services that it provides (such as the downstream springs). Examples of mitigation measures could be managed aquifer recharge systems, such as forested infiltration areas, exploiting the high flow conditions in wetter seasons.

6.4.4.2 Lower plain – Groundwater-fed irrigation areas

Conversely, in areas characterized by groundwater-fed irrigation, such as the lower plain, results indicate that vulnerability to climate change is mostly mediated by human abstractions: higher temperatures are expected to lead to increased water needs for irrigation and domestic purposes both in terms of extracted volumes and longer abstraction periods. Recent studies (Amanambu et al., 2020; Russo & Lall, 2017; Whittemore et al., 2016) have shown that groundwater levels can respond faster to changes in abstraction rates driven by human response to climate variability than to direct changes in recharge, also driven by climate variability. Unlike the high plain areas,

in the lower plain, mitigation actions such as the transition to more efficient irrigation methods or the reduction of aqueduct losses could contribute positively to the resilience of groundwater resources, reducing anthropic pressures and extracted volumes.

6.4.4.3 Middle plain

The transition zone in the middle plain shows recharge processes strongly connected to the irrigation excess in the higher plain. Still, results also indicated a summer decrease related to increased abstractions in 2022, similar to the lower plain. Therefore, in the middle plain, vulnerability in terms of water scarcity is linked to two aspects: 1) reduced recharge from upstream in case of changes in irrigation processes and surface water availability and 2) increased abstraction linked to increased irrigation and domestic needs due to higher temperatures. In this area, groundwater not only constitutes a valuable resource for human needs, but it also guarantees environmental services by feeding the multitude of springs vital for downstream agriculture and ecosystems.

6.4.4.4 Morainic Aquifers

Results in the southern sector of the Garda morainic amphitheater (cluster C2) indicate a water budget and a vulnerability profile similar to the one in the lower plain, governed by human abstractions. Similarly to the lower plain, in this area, the main driver of water scarcity during climate change could be increased abstractions for domestic use, exacerbated by the limited extension of the aquifers. Similarly, mitigation measures that reduce the extracted volumes in the future are necessary to preserve the water resource.

The wells in the northeast sector of the Lake Garda morainic amphitheater (group D), which show a wider pluriannual variability compared to the seasonality, seem to indicate that in a hydrogeological context where the main recharge and discharge components are natural, groundwater can be resilient to single dry seasons. This is the opposite of environments where the water budget is highly governed by human water resource management, where anthropic impacts can exacerbate the effects of dry seasons. Nevertheless, longer time series could produce more robust conclusions in this highly variable region.

As regards single aquifers with peculiar situations that resulted similar to plain regions (groups A, B, or C), vulnerability to climate change can be deduced by association with respect to the groups they belong to, with parallels to what was deduced for groups A, B, and C. A significant aspect, however, lies in the reduced extension and productivity of these aquifers, which can potentially make them more vulnerable as the volumes involved are much lower than those of plain systems.

6.4.4.5 Alpine Valleys

Data were insufficient to draw robust conclusions about alpine valleys, but they highlighted the importance of local studies since vulnerability profiles are strictly connected to the amplitude and altitude of the aquifers and their watershed, other than human consumption and the presence of surface water bodies.

6.4.5 Methodological approach pros and cons

This work is based on dynamic data collected from active wells. This is unconventional since, in most cases, hydrogeological investigations are based on static data, which are considered more representative of the aquifer conditions. Here, the authors propose a method for data preprocessing that led to the extraction of significant information from dynamic groundwater level data. Exploiting dynamic data from active wells could help fill the gaps in ordinary monitoring networks in other regions worldwide.

Indeed, data from water suppliers are usually monitored and archived for management purposes, and therefore, they can be used for research purposes without additional costs. These data usually have a high temporal resolution (hour/minutes), which means that the selection of static/semi-static data could lead to a lower resolution (days/months), which is still significant for hydrogeological evaluations.

Exploiting dynamic data allowed us to investigate territories where the lack of regional monitoring networks has always prevented any kind of hydrogeological characterization. In this case, for example, no previous data are reported on the moraine aquifer system, which still constitutes a strategic territory for Italian wine production, tourism, and a residential area.

In this case, the limitations of the work are mostly related to the data being scattered among the database time span: different time spans were available for different wells. This prevented the application of typical analyses, such as trend analysis, which would have led to results that were not comparable between different wells.

On the other hand, the evaluation of seasonal patterns was applied here by subtracting yearly means, which allowed data from different years to be compared both within the same well and different wells.

While most time series studies focus on long-term trends, the seasonal analysis applied here allowed for a detailed understanding of the groundwater budget and a more precise quantification of the drought effects. Indeed, in most cases, the drought effects were not evident as significant global minima over the time span, but they were most likely associated with dramatic changes in the seasonal patterns, showing the complete lack of seasonal recharge or the exacerbation of seasonal depletion.

6.5 Conclusions

The present work provides valuable support to researchers and water managers, offering tools for more effective groundwater management in the context of climate change, particularly in regions where irrigation plays a central role.

The analysis investigated groundwater levels across diverse hydrogeological settings, analyzing seasonal patterns to understand recharge and discharge dynamics under baseline conditions while assessing the response of groundwater resources to the 2022 drought with implications for similar contexts facing water scarcity challenges, which afflicted several countries.

The main outcomes of the study highlighted the dual role of irrigation on groundwater budget, based on the irrigation water source (i.e., surface water or groundwater-fed irrigation).

Indeed, in regions with surface-water-fed irrigation, surface water scarcity under hydrological droughts can rapidly induce a groundwater depletion related to a) the missing recharge from irrigation return flow and b) the increased groundwater

abstraction to compensate for the lack of surface water. In these regions, the transition toward efficient irrigation practices, such as sprinkling or micro irrigation, would determine a significant reduction of aquifer recharge and would require compensation measures such as managed aquifer recharge during wet seasons.

On the other hand, in regions with groundwater-fed irrigation, increased temperatures and the associated increased irrigation needs lead to increased groundwater depletion during irrigation season. In these regions, the aquifer balance could benefit from mitigation actions aimed at reducing groundwater abstractions, such as more efficient irrigation practices or consumption reduction.

Differently, aquifer systems governed by natural recharge and discharge processes can be more characterized by pluriannual variability associated with dry and wet years and, therefore, less sensitive to single dry seasons than highly anthropic systems.

The main limitations of this study arise from the varying time spans of the available data, which prevented the application of standard analyses, such as trend analysis, while still allowing for the comparison of seasonal patterns.

The results of this work highlighted that analyzing groundwater seasonal patterns provides a deep understanding of groundwater dynamics and enables precise quantification of drought season effects, offering new findings that long-term analyses like trend analysis cannot describe in such detail and that can be applied in any similar hydrogeological context.

Furthermore, if properly preprocessed, dynamic data from active wells can be valuable sources for investigating aquifer dynamics. They can also be useful for obtaining time series data in regions where monitoring networks are missing or insufficient.

CRediT authorship contribution statement: Agnese Redaelli: Data curation, Formal analysis, Visualization, Investigation, Writing – original draft. **Tullia Bonomi**: Conceptualization, Supervision, Validation, Resources, Funding acquisition, Project administration, Writing – review & editing. **Davide Sartirana**: Writing – review & editing, Visualization,

Conceptualization. **Gianfranco Sinatra**: Resources. **Marco Rotiroti**: Conceptualization, Supervision, Validation, Funding acquisition, Project administration, Writing – review & editing. **Chiara Zanotti**: Data curation, Formal analysis, Visualization, Investigation, Methodology, Conceptualization, Supervision, Validation, Funding acquisition, Project administration, Writing – original draft.

Funding: This research was financially supported by Acque Bresciane S.r.L. SB, water supplier, through the research contract no. 2021-ECO-0019.

Declaration of competing interest: The authors declare the following financial interests/personal relationships which may be considered as potential competing interests: Chiara Zanotti reports financial support was provided by Acque Bresciane S.r.l. SB. Marco Rotiroti is Associate Editor of the Journal of Hydrology. If there are other authors, they declare that they have no known competing financial interests or personal relationships that could have appeared to influence the work reported in this paper.

Acknowledgments: We thank dott. Letizia Fumagalli for her precious insights and scientific support.

Appendix A. Supplementary data: Supplementary data to this article can be found online at https://doi.org/10.1016/j.jhydrol.2025.133211.

References

Amanambu, A.C., Obarein, O.A., Mossa, J., Li, L., Ayeni, S.S., Balogun, O., Oyebamiji, A., Ochege, F.U., 2020. Groundwater system and climate change: Present status and future considerations. J. Hydrol. 589, 125163. https://doi.org/10.1016/j.jhydrol.2020.125163

Anand, B., Karunanidhi, D., Subramani, T., Srinivasamoorthy, K., Suresh, M., 2020. Long-term trend detection and spatiotemporal analysis of groundwater levels using GIS techniques in Lower Bhavani River basin, Tamil Nadu, India. Environ. Dev. Sustain. 22, 2779–2800. https://doi.org/10.1007/s10668-019-00318-3

ANBI Lombardia, 2022. Report sulla stagione irrigua in Lombardia 2021.

ANBI Lombardia, 2023. Report sulla stagione irrigua in Lombardia 2022.

Atawneh, D. Al, Cartwright, N., Bertone, E., 2021. Climate change and its impact on the projected values of groundwater recharge: A review. J. Hydrol. https://doi.org/10.1016/j.jhydrol.2021.126602

Avanzi, F., Munerol, F., Milelli, M., Gabellani, S., Massari, C., Girotto, M., Cremonese, E., Galvagno, M., Bruno, G., Morra di Cella, U., Rossi, L., Altamura, M., Ferraris, L., 2024. Winter snow deficit was a harbinger of summer 2022 socio-hydrologic drought in the Po Basin, Italy. Commun. Earth Environ. 5, 1–12. https://doi.org/10.1038/s43247-024-01222-z

Baronetti, A., González-Hidalgo, J.C., Vicente-Serrano, S.M., Acquaotta, F., Fratianni, S., 2020. A weekly spatio-temporal distribution of drought events over the Po Plain (North Italy) in the last five decades. Int. J. Climatol. 40, 4463–4476. https://doi.org/10.1002/joc.6467

Baronetti, A., Dubreuil, V., Provenzale, A., Fratianni, S., 2022. Future droughts in northern Italy: high-resolution projections using EURO-CORDEX and MED-CORDEX ensembles. Clim. Change 172, 22. https://doi.org/10.1007/s10584-022-03370-7

Bartoli, M., Racchetti, E., Delconte, C.A., Sacchi, E., Soana, E., Laini, A., Longhi, D., Viaroli, P., 2012. Nitrogen balance and fate in a heavily impacted watershed (Oglio River, Northern Italy): In quest of the missing sources and sinks. Biogeosciences 9, 361–373. https://doi.org/10.5194/bg-9-361-2012

Bhatti, M.T., Anwar, A.A., Aslam, M., 2017. Groundwater monitoring and management: Status and options in Pakistan. Comput. Electron. Agric. 135, 143–153. https://doi.org/10.1016/j.compag.2016.12.016

Bierkens, M.F.P., Wada, Y., 2019. Non-renewable groundwater use and groundwater depletion: A review. Environ. Res. Lett. 14. https://doi.org/10.1088/1748-9326/ab1a5f

Bini, A., Zuccoli, L., 2004. Anfiteatro morenico del Lago di Garda 17, 333–342.

Bloomfield, J.P., Marchant, B.P., Bricker, S.H., Morgan, R.B., 2015. Regional analysis of groundwater droughts using hydrograph classification. Hydrol. Earth Syst. Sci. 19, 4327–4344. https://doi.org/10.5194/hess-19-4327-2015

Bonaldo, D., Bellafiore, D., Ferrarin, C., Ferretti, R., Ricchi, A., Sangelantoni, L., Vitelletti, M.L., 2023. The summer 2022 drought: a taste of future climate for the Po valley (Italy)? Reg. Environ. Chang. 23, 1. https://doi.org/10.1007/s10113-022-02004-z

Bonomi, T., Canepa, P., Del Rosso, F., Rossetti, A., 2008. Relazioni temporali pluridecennali di dati pluviometrici, idrologici e piezometrici nella pianura lombarda tra Ticino e Oglio. G. di Geol. Appl. 9, 227–248. https://doi.org/https://dx.doi.org/10.1474/GGA.2008-02.2-12.0242

Cochand, M., Christe, P., Ornstein, P., Hunkeler, D., 2019. Groundwater Storage in High Alpine Catchments and Its Contribution to Streamflow. Water Resour. Res. 55, 2613–2630. https://doi.org/10.1029/2018WR022989

Colombo, N., Guyennon, N., Valt, M., Salerno, F., Godone, D., Cianfarra, P., Freppaz, M., Maugeri, M., Manara, V., Acquaotta, F., Petrangeli, A.B., Romano, E., 2023.

Unprecedented snow-drought conditions in the Italian Alps during the early 2020s. Environ. Res. Lett. 18. https://doi.org/10.1088/1748-9326/acdb88

Colyer, A., Butler, A., Peach, D., Hughes, A., 2021. How groundwater time series and aquifer property data explain heterogeneity in the Permo-Triassic sandstone aquifers of the Eden Valley, Cumbria, UK. Hydrogeol. J. 30, 445–462. https://doi.org/10.1007/s10040-021-02437-6

Crespi, A., Borghi, A., Facchi, A., Gandolfi, C., Maugeri, M., 2021. Spatio-temporal variability and trends of drought indices over Lombardy plain (northern Italy) from meteorological station records 5625, 3–18. https://doi.org/10.13128/ijam-1101

Dangar, S., Asoka, A., Mishra, V., 2021. Causes and implications of groundwater depletion in India: A review. J. Hydrol. 596, 126103. https://doi.org/10.1016/j.jhydrol.2021.126103

De Luca, D.A., Destefanis, E., Forno, M.G., Lasagna, M., Masciocco, L., 2014. The genesis and the hydrogeological features of the Turin Po Plain fontanili, typical lowland springs in Northern Italy. Bull. Eng. Geol. Environ. 73, 409–427. https://doi.org/10.1007/s10064-013-0527-y

Di Giovanni, A., Di Curzio, D., Pantanella, D., Picchi, C., Rusi, S., 2023. Estimating a Reliable Water Budget at a Basin Scale: A Comparison between the Geostatistical and Traditional Methods (Foro River Basin, Central Italy). Water 15, 4083. https://doi.org/10.3390/w15234083

Dierauer, J.R., Allen, D.M., Whitfield, P.H., 2019. Snow Drought Risk and Susceptibility in the Western United States and Southwestern Canada. Water Resour. Res. 55, 3076–3091. https://doi.org/10.1029/2018WR023229

Dierauer, J.R., Whitfield, P.H., Allen, D.M., 2018. Climate Controls on Runoff and Low Flows in Mountain Catchments of Western North America. Water Resour. Res. 54, 7495–7510. https://doi.org/10.1029/2018WR023087

Egidio, E., Lasagna, M., Mancini, S., De Luca, D.A., 2022. Climate impact assessment to the groundwater levels based on long time-series analysis in a paddy field area (Piedmont region, NW Italy): preliminary results. Acque Sotter. - Ital. J. Groundw. 11, 21–29. https://doi.org/10.7343/as-2022-576

Fabbri, P., Piccinini, L., Marcolongo, E., Pola, M., Conchetto, E., Zangheri, P., 2016. Does a change of irrigation technique impact on groundwater resources? A case study in Northeastern Italy. Environ. Sci. Policy 63, 63–75. https://doi.org/10.1016/j.envsci.2016.05.009

Faquseh, H., Grossi, G., 2023. The effect of climate change on groundwater resources availability: a case study in the city of Brescia, northern Italy. Sustain. Water Resour. Manag. 9, 1–15. https://doi.org/10.1007/s40899-023-00892-5

Faranda, D., Pascale, S., Bulut, B., 2023. Persistent anticyclonic conditions and climate change exacerbated the exceptional 2022 European-Mediterranean drought. Environ. Res. Lett. 18. https://doi.org/10.1088/1748-9326/acbc37

Fronzi, D., Narang, G., Galdelli, A., Pepi, A., Mancini, A., Tazioli, A., 2024. Towards Groundwater-Level Prediction Using Prophet Forecasting Method by Exploiting a High-Resolution Hydrogeological Monitoring System. Water (Switzerland) 16, 1–19. https://doi.org/10.3390/w16010152

Fumagalli, N., Senes, G., Ferrario, P.S., Toccolini, A., 2017. A minimum indicator set for assessing fontanili (lowland springs) of the Lombardy Region in Italy. Eur. Countrys. 9, 1–16. https://doi.org/10.1515/euco-2017-0001

Haaf, E., Giese, M., Reimann, T., Barthel, R., 2023. Data-Driven Estimation of Groundwater Level Time-Series at Unmonitored Sites Using Comparative Regional Analysis. Water Resour. Res. 59. https://doi.org/10.1029/2022WR033470

Hinegk, L., Adami, L., Zolezzi, G., Tubino, M., 2022. Implications of water resources management on the long-term regime of Lake Garda (Italy). J. Environ. Manage. 301, 113893. https://doi.org/10.1016/j.jenvman.2021.113893

Intergovernmental Panel on Climate Change (IPCC), 2023. Climate Change 2021 – The Physical Science Basis. Cambridge University Press. https://doi.org/10.1017/9781009157896

Jasechko, S., Birks, S.J., Gleeson, T., Wada, Y., Fawcett, P.J., Sharp, Z.D., McDonnell, J.J., Welker, J.M., 2014. The pronounced seasonality of global groundwater recharge. Water Resour. Res. 50, 8845–8867. https://doi.org/10.1002/2014WR015809

Jasechko, S., Seybold, H., Perrone, D., Fan, Y., Shamsudduha, M., Taylor, R.G., Fallatah, O., Kirchner, J.W., 2024. Rapid groundwater decline and some cases of recovery in aquifers globally. Nature 625, 715–721. https://doi.org/10.1038/s41586-023-06879-8

Lafare, A.E.A., Peach, D.W., Hughes, A.G., 2016. Use of seasonal trend decomposition to understand groundwater behaviour in the Permo-Triassic Sandstone aquifer, Eden Valley, UK. Hydrogeol. J. 24, 141–158. https://doi.org/10.1007/s10040-015-1309-3

Lall, U., Josset, L., Russo, T., 2020. A Snapshot of the World's Groundwater Challenges. Annu. Rev. Environ. Resour. 45, 171–194. https://doi.org/10.1146/annurev-environ-102017-025800

Lasagna, M., Mancini, S., De Luca, D.A., 2020. Groundwater hydrodynamic behaviours based on water table levels to identify natural and anthropic controlling factors in the Piedmont Plain (Italy). Sci. Total Environ. 716, 137051. https://doi.org/10.1016/j.scitotenv.2020.137051

Liu, P.-W., Famiglietti, J.S., Purdy, A.J., Adams, K.H., McEvoy, A.L., Reager, J.T., Bindlish, R., Wiese, D.N., David, C.H., Rodell, M., 2022. Groundwater depletion in California's Central Valley accelerates during megadrought. Nat. Commun. 13, 7825. https://doi.org/10.1038/s41467-022-35582-x

Liu, Y., Yuan, S., Zhu, Y., Ren, L., Chen, R., Zhu, X., Xia, R., 2023. The patterns, magnitude, and drivers of unprecedented 2022 mega-drought in the Yangtze River

Basin, China. Environ. Res. Lett. 18, 114006. https://doi.org/10.1088/1748-9326/acfe21

Marchetti, M., 2002. Environmental changes in the central Po Plain (northern Italy) due to fluvial modifications and anthropogenic activities. Geomorphology 44, 361–373. https://doi.org/10.1016/S0169-555X(01)00183-0

Masseroni, D., Gangi, F., Ghilardelli, F., Gallo, A., Kisekka, I., Gandolfi, C., 2024. Assessing the water conservation potential of optimized surface irrigation management in Northern Italy. Irrig. Sci. 42, 75–97. https://doi.org/10.1007/s00271-023-00876-5

Meggiorin, M., Passadore, G., Bertoldo, S., Sottani, A., Rinaldo, A., 2021. Assessing the long-term sustainability of the groundwater resources in the Bacchiglione basin (Veneto, Italy) with the Mann–Kendall test: suggestions for higher reliability. Acque Sotter. - Ital. J. Groundw. 10, 35–48. https://doi.org/10.7343/as-2021-499

Meixner, T., Manning, A.H., Stonestrom, D.A., Allen, D.M., Ajami, H., Blasch, K.W., Brookfield, A.E., Castro, C.L., Clark, J.F., Gochis, D.J., Flint, A.L., Neff, K.L., Niraula, R., Rodell, M., Scanlon, B.R., Singha, K., Walvoord, M.A., 2016. Implications of projected climate change for groundwater recharge in the western United States. J. Hydrol. 534, 124–138. https://doi.org/10.1016/J.JHYDROL.2015.12.027

Montanari, A., Nguyen, H., Rubinetti, S., Ceola, S., Galelli, S., Rubino, A., Zanchettin, D., 2023. Why the 2022 Po River drought is the worst in the past two centuries. Sci. Adv. 9, 1–8. https://doi.org/10.1126/sciadv.adg8304

Ndehedehe, C.E., Adeyeri, O.E., Onojeghuo, A.O., Ferreira, V.G., Kalu, I., Okwuashi, O., 2023. Understanding global groundwater-climate interactions. Sci. Total Environ. 904, 166571. https://doi.org/10.1016/j.scitotenv.2023.166571

Noori, A.R., Singh, S.K., 2021. Spatial and temporal trend analysis of groundwater levels and regional groundwater drought assessment of Kabul, Afghanistan. Environ. Earth Sci. 80, 1–16. https://doi.org/10.1007/s12665-021-10005-0

Nourani, V., Ghaneei, P., Kantoush, S.A., 2022. Robust clustering for assessing the spatiotemporal variability of groundwater quantity and quality. J. Hydrol. 604, 127272. https://doi.org/10.1016/j.jhydrol.2021.127272

Obergfell, C., Bakker, M., Maas, K., 2019. Identification and Explanation of a Change in the Groundwater Regime using Time Series Analysis. Groundwater 57, 886–894. https://doi.org/10.1111/gwat.12891

Pathak, A.A., Dodamani, B.M., 2019. Trend Analysis of Groundwater Levels and Assessment of Regional Groundwater Drought: Ghataprabha River Basin, India. Nat. Resour. Res. 28, 631–643. https://doi.org/10.1007/s11053-018-9417-0

Pool, S., Francés, F., Garcia-Prats, A., Pulido-Velazquez, M., Sanchis-Ibor, C., Schirmer, M., Yang, H., Jiménez-Martínez, J., 2021. From Flood to Drip Irrigation Under Climate Change: Impacts on Evapotranspiration and Groundwater Recharge in the Mediterranean Region of Valencia (Spain). Earth's Futur. 9, 1–20. https://doi.org/10.1029/2020EF001859

Pool, S., Francés, F., Garcia-Prats, A., Puertes, C., Pulido-Velazquez, M., Sanchis-Ibor, C., Schirmer, M., Yang, H., Jiménez-Martínez, J., 2022. Impact of a transformation from flood to drip irrigation on groundwater recharge and nitrogen leaching under variable climatic conditions. Sci. Total Environ. 825, 153805. https://doi.org/10.1016/j.scitotenv.2022.153805

R Core Team, 2021. R: A Language and Environment for Statistical Computing. Foundation for Statistical Computing, Vienna. http://www.r-project.org

Raymond, F., Ullmann, A., Tramblay, Y., Drobinski, P., Camberlin, P., 2019. Evolution of Mediterranean extreme dry spells during the wet season under climate change. Reg. Environ. Chang. 19, 2339–2351. https://doi.org/10.1007/s10113-019-01526-3

Regione Lombardia, 2007. Geoportal of the Lombardy Region, Italy. https://www.geoportale.regione.lombardia.it/en-GB/download-pacchetti?p_p_id=dwnpackageportlet_WAR_gptdownloadportlet&p_p_lifecycle

=0&p_p_state=normal&p_p_mode=view&_dwnpackageportlet_WAR_gptdownloadportlet_metadataid=r_lombar%3A2318b9c5-f8f0-421f-97c0-6e4d912e2b93&_jsfBridgeRedirect=true. (accessed 10 May 2025).

Regione Lombardia, 2023. Geoportal of the Lombardy Region, Italy. https://www.geoportale.regione.lombardia.it/en-GB/metadati?p_p_id=detailSheetMetadata_WAR_gptmetadataportlet&p_p_lifecycle=0&p_p_state=normal&p_p_mode=view&_detailSheetMetadata_WAR_gptmetadataportlet_identifier=r_lombar%3A7cd05e9f-b693-4d7e-a8de-71b40b45f54e&_jsfBridgeRedirect=true. (accessed 4 June 2025).

Regione Lombardia, 2016. Programma di tutela e uso delle acque (PTUA 2016) "Programme for the protection and use of water."

Ronchi, B., Stassen, F., Drevet, J.-P., Frippiat, C.C., Berger, J.-L., Dingelstadt, C., Veschkens, M., 2018. Long-Term Time-Series Analysis to Understand Groundwater Flow in Abandoned Subsurface Mines with Application to a Coalfield in Liège, Belgium. Mine Water Environ. 37, 470–481. https://doi.org/10.1007/s10230-018-0528-y

Rotiroti, M., Bonomi, T., Sacchi, E., McArthur, J.M., Stefania, G.A., Zanotti, C., Taviani, S., Patelli, M., Nava, V., Soler, V., Fumagalli, L., Leoni, B., 2019a. The effects of irrigation on groundwater quality and quantity in a human-modified hydro-system: The Oglio River basin, Po Plain, northern Italy. Sci. Total Environ. 672, 342–356. https://doi.org/10.1016/j.scitotenv.2019.03.427

Rotiroti, M., Zanotti, C., Fumagalli, L., Taviani, S., Stefania, G.A., Patellio, M., Soler, V., Sacchi, E., Leoni, B., 2019b. Multivariate statistical analysis supporting the hydrochemical characterization of groundwater and surface water: a case study in northern Italy. Rend. Online della Soc. Geol. Ital. 47, 90–96. https://doi.org/10.3301/ROL.2019.17

Rotiroti, M., Sacchi, E., Caschetto, M., Zanotti, C., Fumagalli, L., Biasibetti, M., Bonomi, T., Leoni, B., 2023. Groundwater and surface water nitrate pollution in

an intensively irrigated system: Sources, dynamics and adaptation to climate change. J. Hydrol. 623, 129868. https://doi.org/10.1016/j.jhydrol.2023.129868

Russo, T.A., Lall, U., 2017. Depletion and response of deep groundwater to climate-induced pumping variability. Nat. Geosci. 10, 105–108. https://doi.org/10.1038/ngeo2883

Sakizadeh, M., Mohamed, M.M.A., Klammler, H., 2019. Trend Analysis and Spatial Prediction of Groundwater Levels Using Time Series Forecasting and a Novel Spatio-Temporal Method. Water Resour. Manag. 33, 1425–1437. https://doi.org/10.1007/s11269-019-02208-9

Sartirana, D., Rotiroti, M., Bonomi, T., De Amicis, M., Nava, V., Fumagalli, L., Zanotti, C., 2022. Data-driven decision management of urban underground infrastructure through groundwater-level time-series cluster analysis: the case of Milan (Italy). Hydrogeol. J. 30, 1157–1177. https://doi.org/10.1007/s10040-022-02494-5

Scanlon, B.R., Fakhreddine, S., Rateb, A., de Graaf, I., Famiglietti, J., Gleeson, T., Grafton, R.Q., Jobbagy, E., Kebede, S., Kolusu, S.R., Konikow, L.F., Long, D., Mekonnen, M., Schmied, H.M., Mukherjee, A., MacDonald, A., Reedy, R.C., Shamsudduha, M., Simmons, C.T., Sun, A., Taylor, R.G., Villholth, K.G., Vörösmarty, C.J., Zheng, C., 2023. Global water resources and the role of groundwater in a resilient water future. Nat. Rev. Earth Environ. 4, 87–101. https://doi.org/10.1038/s43017-022-00378-6

Severi, P., Bonzi, L., Ferrari, V., Emilia-romagna, R., Rimini, P., Le, A.E., Provincia, R., 1994. Geologia e Idrogeologia della Conoide del Fiume Marecchia. Geol. dell'Emilia-Romagna 23–33.

Sofia, G., Zaccone, C., Tarolli, P., 2024. Agricultural drought severity in NE Italy: Variability, bias, and future scenarios. Int. Soil Water Conserv. Res. 12, 403–418. https://doi.org/10.1016/j.iswcr.2023.07.003

Somers, L.D., McKenzie, J.M., 2020. A review of groundwater in high mountain environments. Wiley Interdiscip. Rev. Water 7, 1–27.

https://doi.org/10.1002/wat2.1475

Stephan, R., Erfurt, M., Terzi, S., Žun, M., Kristan, B., Haslinger, K., Stahl, K., 2021. An inventory of Alpine drought impact reports to explore past droughts in a mountain region. Nat. Hazards Earth Syst. Sci. 21, 2485–2501. https://doi.org/10.5194/nhess-21-2485-2021

Stigter, T.Y., Miller, J., Chen, J., Re, V., 2023. Groundwater and climate change: threats and opportunities. Hydrogeol. J. 31, 7–10. https://doi.org/10.1007/s10040-022-02554-w

Taylor, R.G., Scanlon, B., Döll, P., Rodell, M., Van Beek, R., Wada, Y., Longuevergne, L., Leblanc, M., Famiglietti, J.S., Edmunds, M., Konikow, L., Green, T.R., Chen, J., Taniguchi, M., Bierkens, M.F.P., Macdonald, A., Fan, Y., Maxwell, R.M., Yechieli, Y., Gurdak, J.J., Allen, D.M., Shamsudduha, M., Hiscock, K., Yeh, P.J.F., Holman, I., Treidel, H., 2013. Ground water and climate change. Nat. Clim. Chang. https://doi.org/10.1038/nclimate1744

Teuling, A.J., Van Loon, A.F., Seneviratne, S.I., Lehner, I., Aubinet, M., Heinesch, B., Bernhofer, C., Grünwald, T., Prasse, H., Spank, U., 2013. Evapotranspiration amplifies European summer drought. Geophys. Res. Lett. 40, 2071–2075. https://doi.org/10.1002/grl.50495

Toreti, A., Bavera, D., Acosta Navarro, J., Cammalleri, C., de Jager, A., Di Ciollo, C.., Hrast Essenfelder, A., Maetens, W., Masante, D., Magni, D., Mazzeschi, M., Spinoni, J., 2022. Drought in Europe August 2022 24. https://doi.org/10.2760/264241

Tramblay, Y., Koutroulis, A., Samaniego, L., Vicente-Serrano, S.M., Volaire, F., Boone, A., Le Page, M., Llasat, M.C., Albergel, C., Burak, S., Cailleret, M., Kalin, K.C., Davi, H., Dupuy, J.-L., Greve, P., Grillakis, M., Hanich, L., Jarlan, L., Martin-StPaul, N., Martínez-Vilalta, J., Mouillot, F., Pulido-Velazquez, D., Quintana-Seguí, P., Renard, D., Turco, M., Türkeş, M., Trigo, R., Vidal, J.-P., Vilagrosa, A., Zribi, M., Polcher, J., 2020. Challenges for drought assessment in the

Mediterranean region under future climate scenarios. Earth-Science Rev. 210, 103348. https://doi.org/10.1016/j.earscirev.2020.103348

Treviño, J., Rodríguez-Rodríguez, M., Montes-Vega, M.J., Aguilera, H., Fernández-Ayuso, A., Fernández-Naranjo, N., 2023. Wavelet Analysis on Groundwater, Surface-Water Levels and Water Temperature in Doñana National Park (Coastal Aquifer in Southwestern Spain). Water (Switzerland) 15. https://doi.org/10.3390/w15040796

Triki, I., Trabelsi, N., Hentati, I., Zairi, M., 2014. Groundwater levels time series sensitivity to pluviometry and air temperature: A geostatistical approach to Sfax region, Tunisia. Environ. Monit. Assess. 186, 1593–1608. https://doi.org/10.1007/s10661-013-3477-8

UNESCO, 2022. The United Nations World Water Development Report 2022: groundwater: making the invisible visible.

Vercesi, P.L., 1994. Aspetti quali-quantitativi delle risorse idriche sotterranee del bresciano. Nat. Brescia. Ann. Mus. Civ. Sc. Nat. Brescia 21–52.

Vicente-Serrano, S.M., Peña-Angulo, D., Beguería, S., Domínguez-Castro, F., Tomás-Burguera, M., Noguera, I., Gimeno-Sotelo, L., El Kenawy, A., 2022. Global drought trends and future projections. Philos. Trans. R. Soc. A Math. Phys. Eng. Sci. 380. https://doi.org/10.1098/rsta.2021.0285

Ward, J.H., 1963. Hierarchical Grouping to Optimize an Objective Function. J. Am. Stat. Assoc. 58, 236. https://doi.org/10.2307/2282967

Weaver, S.M., Guinan, P.E., Semenova, I.G., Aloysius, N., Lupo, A.R., Hunt, S., 2023. A Case Study of Drought during Summer 2022: A Large-Scale Analyzed Comparison of Dry and Moist Summers in the Midwest USA. Atmosphere (Basel). 14, 1448. https://doi.org/10.3390/atmos14091448

Whittemore, D.O., Butler, J.J., Wilson, B.B., 2016. Assessing the major drivers of water-level declines: new insights into the future of heavily stressed aquifers. Hydrol. Sci.

J. 61, 134–145. https://doi.org/10.1080/02626667.2014.959958

Wu, W.Y., Lo, M.H., Wada, Y., Famiglietti, J.S., Reager, J.T., Yeh, P.J.F., Ducharne, A., Yang, Z.L., 2020. Divergent effects of climate change on future groundwater availability in key mid-latitude aquifers. Nat. Commun. 11. https://doi.org/10.1038/s41467-020-17581-y

Yin, J., Medellín-Azuara, J., Escriva-Bou, A., 2022. Groundwater levels hierarchical clustering and regional groundwater drought assessment in heavily drafted aquifers. Hydrol. Res. 53, 1031–1046. https://doi.org/10.2166/nh.2022.048

Zanotti, C., Rotiroti, M., Fumagalli, L., Stefania, G.A., Canonaco, F., Stefenelli, G., Prévôt, A.S.H., Leoni, B., Bonomi, T., 2019. Groundwater and surface water quality characterization through positive matrix factorization combined with GIS approach. Water Res. 159, 122–134. https://doi.org/10.1016/j.watres.2019.04.058

Zanotti, C., Rotiroti, M., Caschetto, M., Redaelli, A., Bozza, S., Biasibetti, M., Mostarda, L., Fumagalli, L., Bonomi, T., 2022. A cost-effective method for assessing groundwater well vulnerability to anthropogenic and natural pollution in the framework of water safety plans. J. Hydrol. 613, 128473. https://doi.org/10.1016/j.jhydrol.2022.128473

Zhang, L., Yu, X., Zhou, T., Zhang, W., Hu, S., Clark, R., 2023. Understanding and Attribution of Extreme Heat and Drought Events in 2022: Current Situation and Future Challenges. Adv. Atmos. Sci. 40, 1941–1951. https://doi.org/10.1007/s00376-023-3171-x

Zhou, F., Liu, Y., Guo, H., 2007. Application of multivariate statistical methods to water quality assessment of the watercourses in Northwestern New Territories, Hong Kong. Environ. Monit. Assess. 132, 1–13. https://doi.org/10.1007/s10661-006-9497-x

Zucaro, R., Pontrandolfi, A., Dodaro, G.M., Gallinoni, C., Pacicco, C.L., Vollaro, M., 2011. Atlante Nazionale dell'irrigazione. Roma.

Electronic Supplementary Material

The Dual Role Of Irrigation In The Groundwater Budget Under Baseline Conditions versus The 2022 Drought: Lessons For Future Climate Adaptation

Agnese Redaelli[1], Tullia Bonomi[1], Davide Sartirana[1], Gianfranco Sinatra[2], Marco Rotiroti[1] and Chiara Zanotti[1,*]

[1]Department of Earth and Environmental Sciences, University of Milano-Bicocca, Milan, Italy.

[2]Acque Bresciane S.r.l. SB, Via 25 Aprile, 18, 25038 Rovato, BS, Italy.

*corresponding author: chiara.zanotti@unimib.it

Supporting Information

Content:

Number of pages: 21

Number of sections: 8

Number of figures: 23

Number of references: 3

S.6.1 – Water level maps

In this section, the groundwater levels (Regione Lombardia, 2016) of the main aquifers in the study area are reported (Fig.S.6.1). Figure S.6.1a shows water table depth and water table contour map, while Figure S.6.1b shows the potentiometric map of the deep aquifer. Both maps are referred to September 2014.

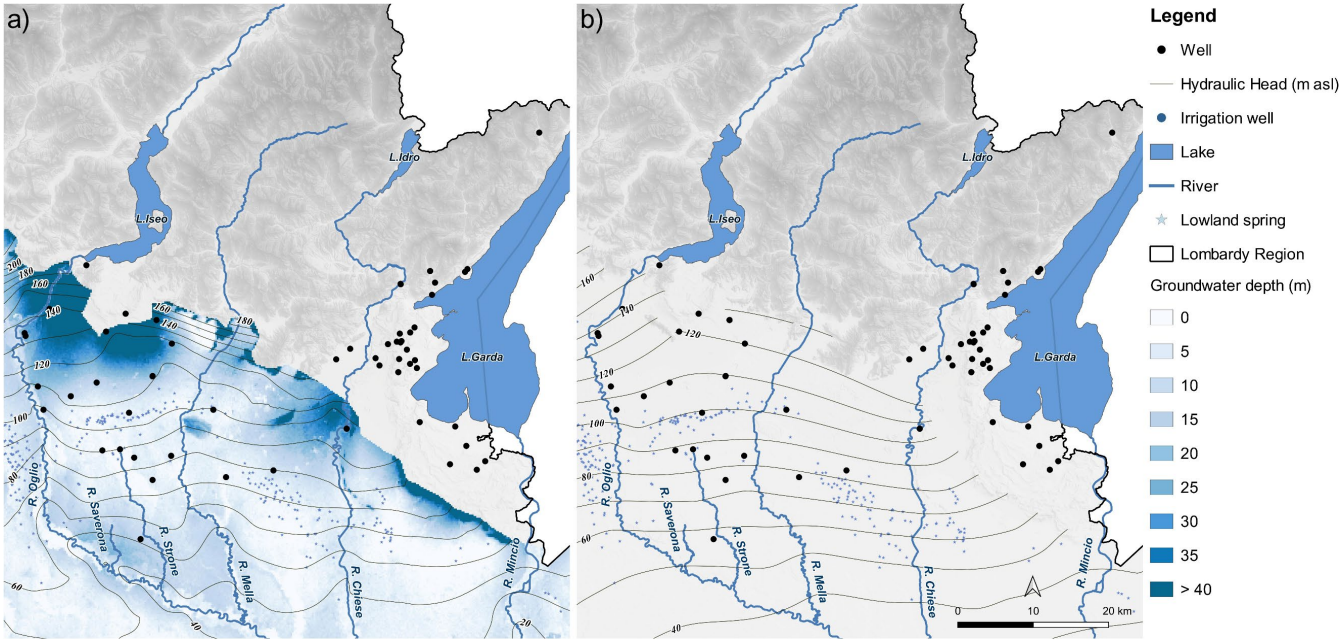

Figure S.6.1 – a) *Water table depth (color shade – m b.g.s.) and contour map (m a.s.l.) and* ***b)*** *potentiometric map (m a.s.l.) of the deep aquifer - September 2014 (Regione Lombardia, 2016).*

Reference

Regione Lombardia. (2016). Programma di tutela e uso delle acque (PTUA 2016) “Programme for the protection and use of water.”

S.6.2 – Distribution analysis of static and dynamic data

Groundwater level data in the present work were collected from wells tapping for drinking water purposes. Drinking water wells are rarely completely switched off, which means that most of the collected data are not static but associated with a specific discharge rate.

To maximize the exploitation of the available data collected from active wells, the possibility of selecting groundwater level measures associated with a minimum flow value was considered. Specifically, the static/semi-static groundwater levels trend in wells was obtained by selecting the groundwater level data associated with an abstraction rate class ≤ 5 L/s. Since the data came from operating wells, this cutoff was selected as a necessary trade-off between the requirement to maintain as many data and wells as possible, and that of obtaining time series representing the aquifer groundwater trend, avoiding the effect of data associated with higher pumping rates. Successively, to reduce the remaining noise in the data, the maximum daily values were extracted from the selected semi-static trend. To verify the significance of the selected 5 L/s cut-off value, the Wilcoxon signed-rank test at 95% significance level was conducted in the RStudio environment using the "wilcoxon.test" function from the "stats" package (R Core Team (2021) Development Core Team, 2021). The Wilcoxon test is a nonparametric statistical test that considers the differences between two paired data groups and does not require the assumption of normality of distributions. (Wilcoxon, 1945). This test was used to determine whether there were statistically significant differences in weekly aggregated groundwater level data associated with Q = 0 L/s and groundwater level data associated with Q ≤ 5 L/s. The comparison was based on weekly medians to minimize the effect of long-term changes and to obtain enough paired couples to be tested. Therefore, weekly medians were calculated using only data associated with Q = 0 L/s and including also data associated with Q ≤ 5 L/s, and the test was performed to investigate whether the two time series could be comparable. Specifically, the following null and alternative hypotheses for the statistical testing were formulated:

- H_0 = There is no statistically significant difference between time series calculated on GW level data associated with Q = 0 L/s and GW level data associated with Q ≤ 5 L/s.
- H_1 = There is a statistically significant difference between time series calculated on GW level data associated with Q = 0 L/s and GW level data associated with Q ≤ 5 L/s.

For 21 out of 61 wells, the test could not be applied as a) groundwater level data are all associated with Q = 0 L/s (3 wells), b) groundwater level data are all associated with Q ≤ 5 L/s (3 wells), c) the abstraction rate data are missing (6 wells), and d) the well has a paired data (i.e. static data and dynamic data ≤ 5 L/s in the same week) number n°< 3 (10 wells). Within the 40 tested wells, the majority of the wells (31 wells) showed no significant differences between the two time series (pvalue > 0.05). Among the remaining nine wells that showed a significant statistical difference between the two time series, it was found that 7 wells showed a difference in the total averages of the two groups lower than 0.47 m, accounting for 2% of the total groundwater level variability for each well. Only for two wells average differences of 5.6 m and 6.5 m emerged, which accounts for 14% and 15% of the two wells total variability of the semistatic data. These average differences are mostly associated with sporadic data, whose effect is canceled by the monthly median calculation in the successive step. The 5 L/s value was, therefore, selected as an advantageous trade-off between data quality and availability for the considered dataset.

References

R Core Team (2021) Development Core Team. (2021). R: A Language and Environment for Statistical Computing. In R Foundation for Statistical Computing (Vol. 3, p. https://www.R-project.org). R Foundation for Statistical Computing.

Wilcoxon, F. (1945). Individual Comparisons by Ranking Methods. Biometrics Bulletin, 1(6), 80. https://doi.org/10.2307/3001968

S.6.3 – Groundwater level data preprocessing

In this section, the preprocessing of the time series is reported for some time series examples (Figures S.6.2-S.6.14). In all figures, graph a) shows the raw data, color-coded by the associated abstraction rate; graph b) shows the daily maxima data extracted from the subset of data associated with an abstraction rate lower than 5 L/s; graph c) shows the monthly median extracted from the data selected for graph b). The graphs show how the selection of only static data would have led to an excessive loss of data and how, instead, the identification of a minimum flow threshold made it possible to obtain representative data.

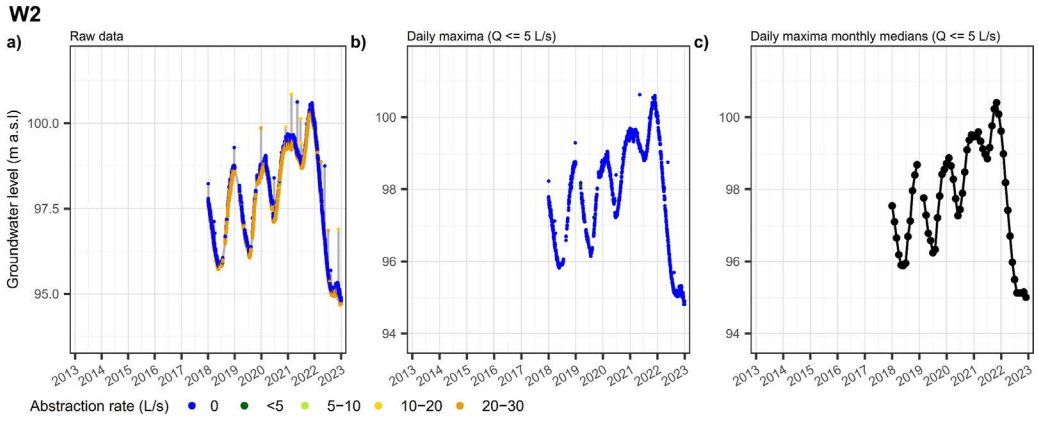

Figure S.6.2 *– Preprocessing of the W2 well time series.*

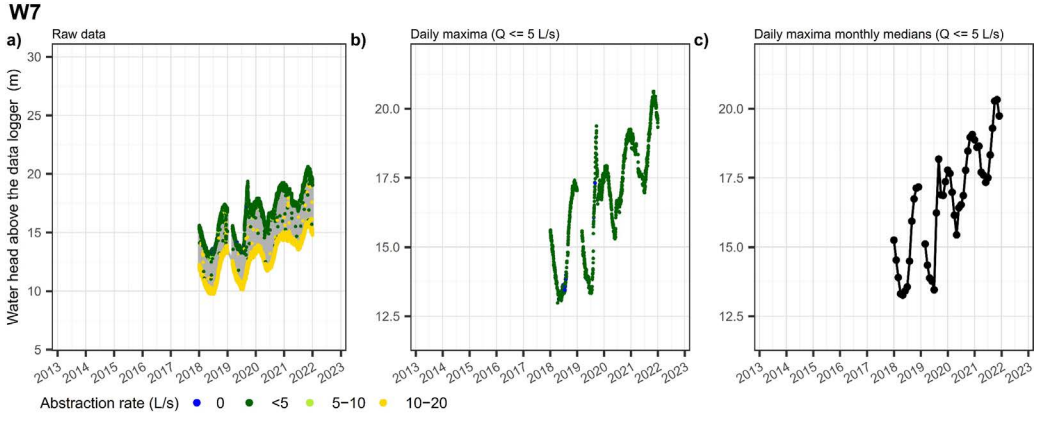

Figure S.6.3 *– Preprocessing of the W7 well time series.*

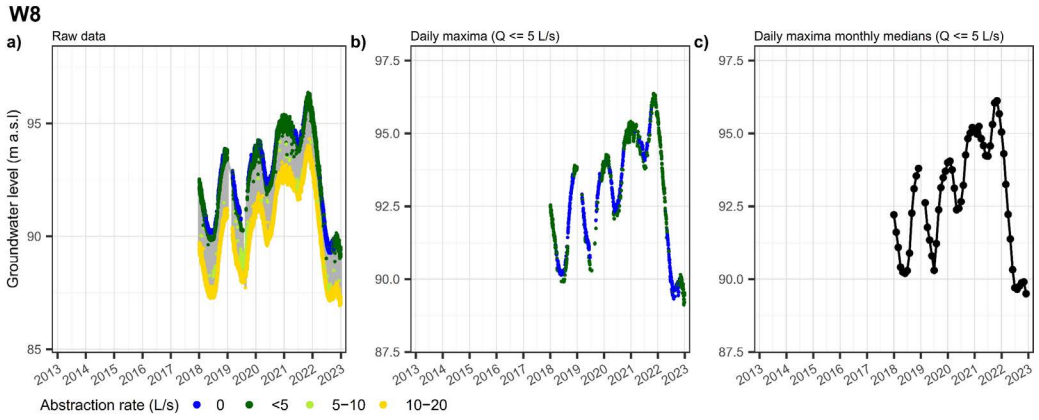

Figure S.6.4 *– Preprocessing of the W8 well time series.*

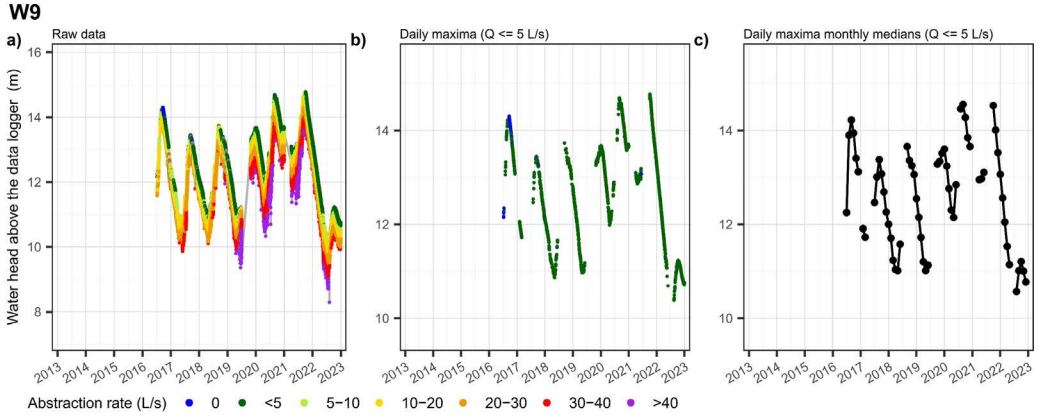

Figure S.6.5 *– Preprocessing of the W9 well time series.*

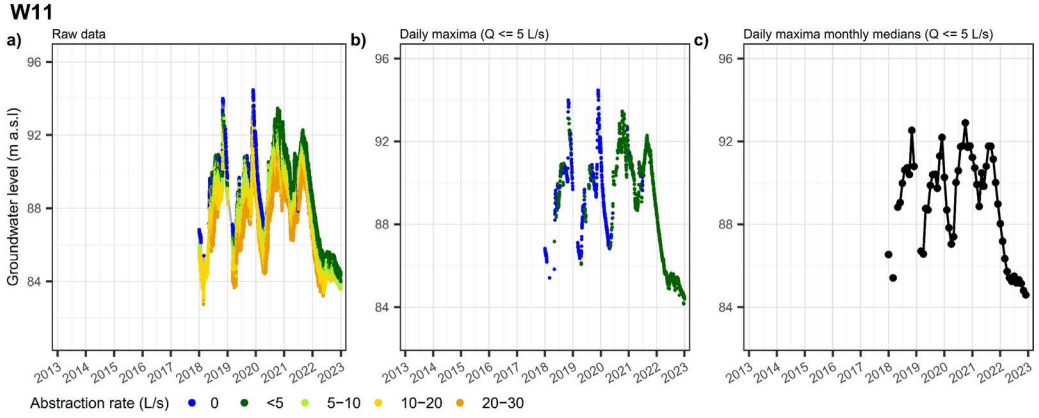

Figure S.6.6 *– Preprocessing of the W11 well time series.*

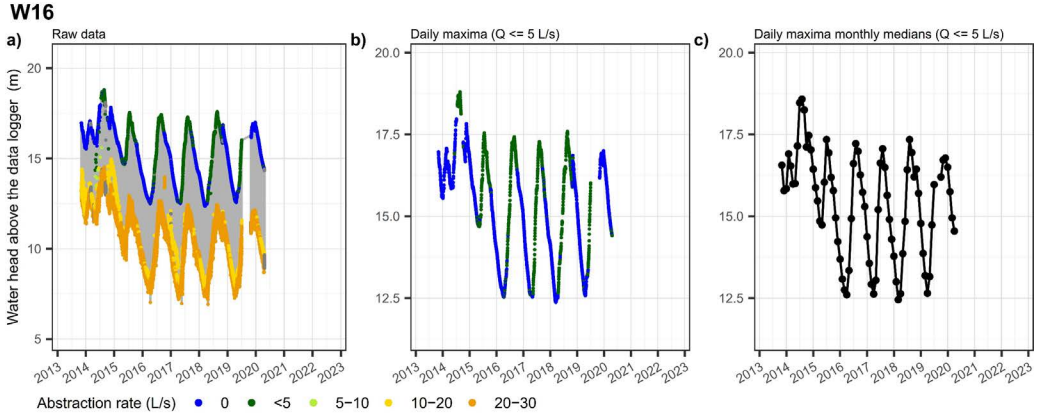

Figure S.6.7 *– Preprocessing of the W16 well time series.*

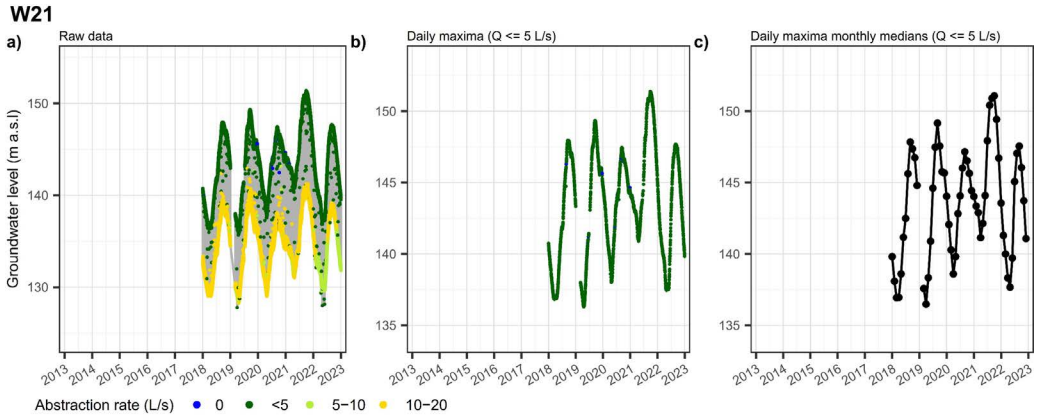

Figure S.6.8 *– Preprocessing of the W21 well time series.*

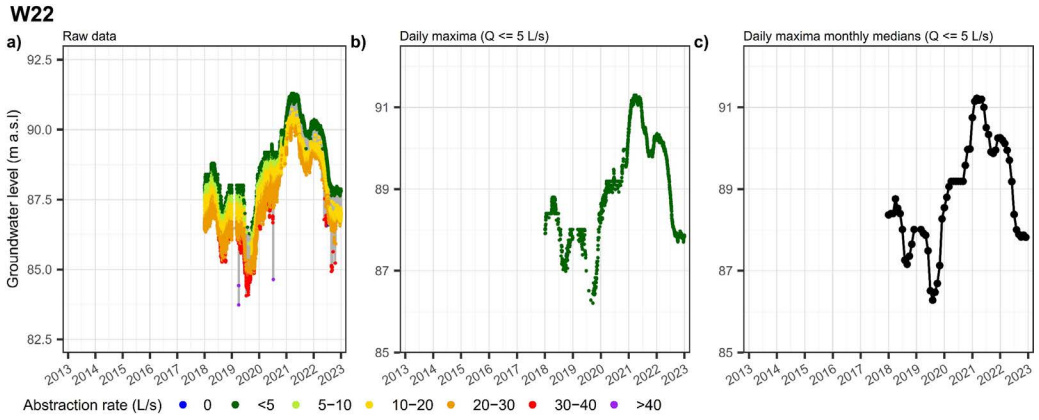

Figure S.6.9 *– Preprocessing of the W22 well time series.*

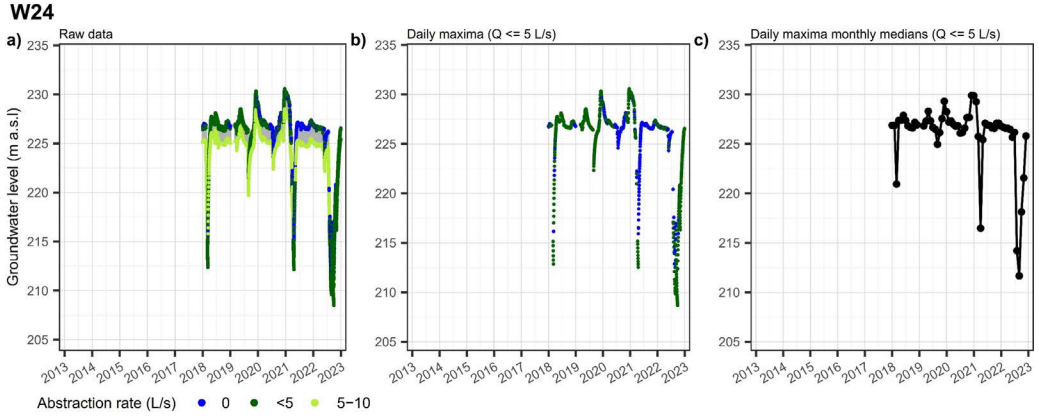

Figure S.6.10 *– Preprocessing of the W24 well time series.*

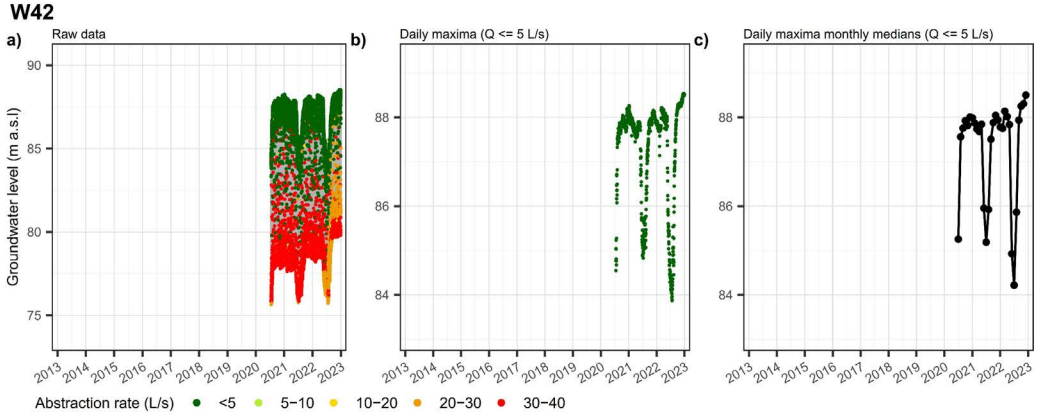

Figure S.6.11 *– Preprocessing of the W42 well time series.*

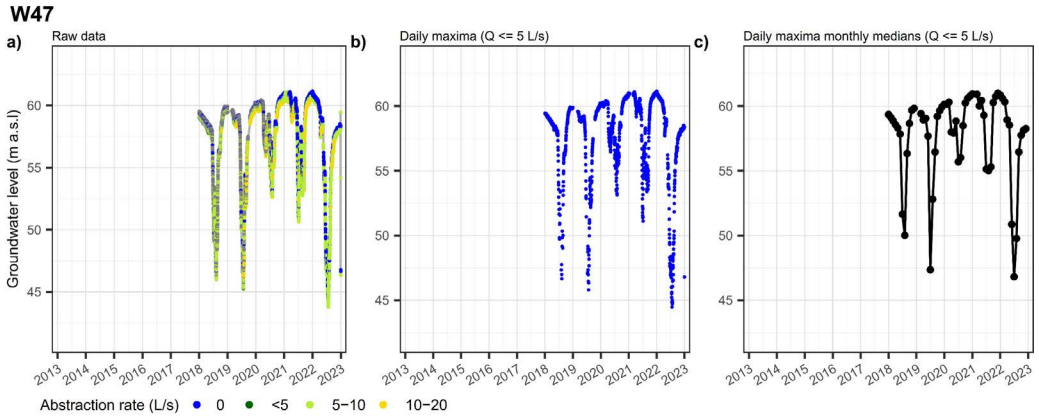

Figure S.6.12 *– Preprocessing of the W47 well time series.*

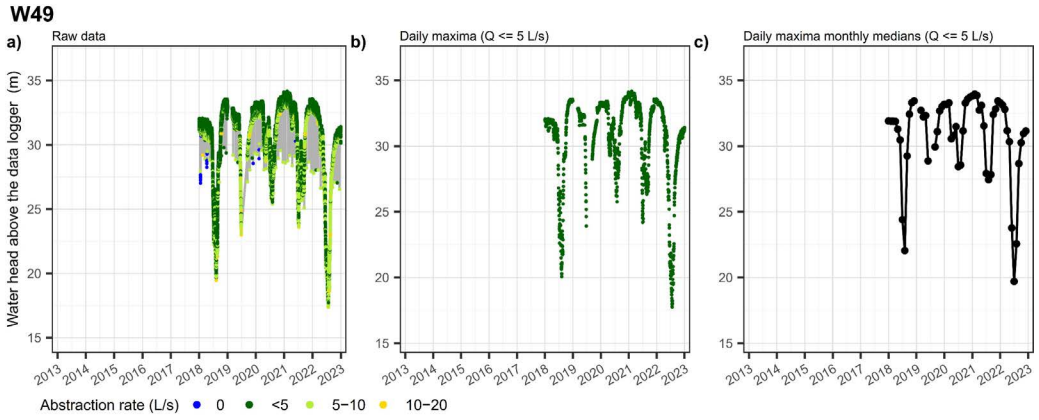

Figure S.6.13 *– Preprocessing of the W49 well time series.*

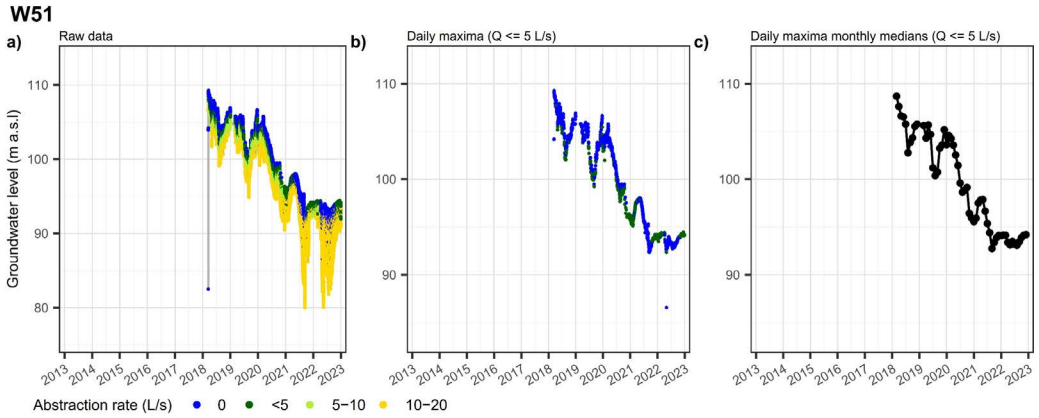

Figure S.6.14 *– Preprocessing of the W51 well time series.*

S.6.4 – Exploration of seasonal patterns

Figure S.6.15 and Figure S.6.16 show examples of how subtracting the yearly mean allows for extracting meaningful seasonal profiles for a single well while using the original data could lead to noisy information. Furthermore, the use of detrended data allows for the comparison within wells with different time spans. In both figures, graphs a) show the monthly median extracted by the daily maxima of the data associated with an abstraction rate lower than 5 L/s; graphs b) show the monthly median detrended by subtracting the yearly mean; graphs c) show the monthly boxplots of data in graphs a); graphs d) show the monthly boxplots of data in graphs b).

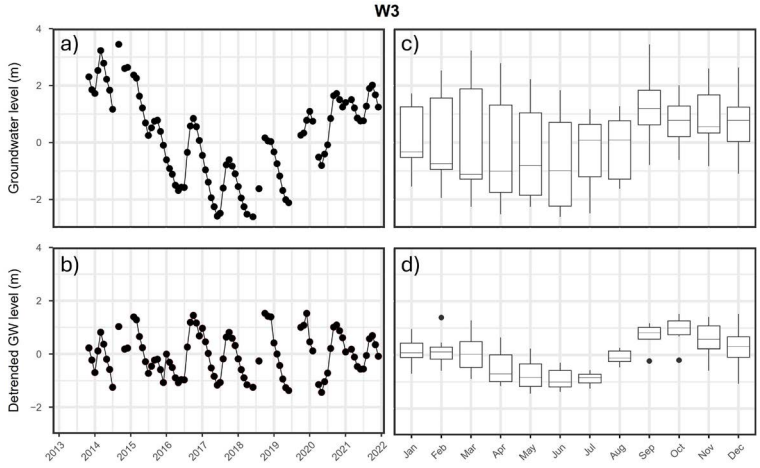

Figure S.6.15 *– Comparison of data* ***(a)*** *and monthly boxplot* ***(c)*** *over raw data versus data* ***(b)*** *and monthly boxplot* ***(d)*** *detrended by subtracting the yearly mean for well W3.*

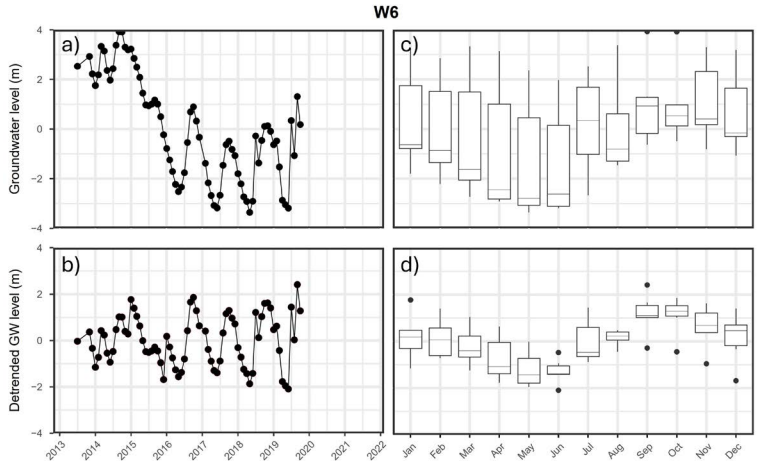

Figure S.6.16 *– Comparison of data* ***(a)*** *and monthly boxplot* ***(c)*** *over raw data versus data* ***(b)*** *and monthly boxplot* ***(d)*** *detrended by subtracting the yearly mean for well W6.*

S.6.5 – Meteorological data analysis

In this section, additional graphs underline the extreme meteorological conditions of 2022. Figure S.6.17 shows monthly temperature anomalies as percentages: the grey bars indicate maxima, minima, 25th and 75th percentile of the percentage anomalies over the reference period, while red and blue bars indicate percentage anomalies of the 2021 and 2022 data. Figure S.6.18 reports seasonal cumulative precipitation, and Figure S.6.19 reports the mean temperature.

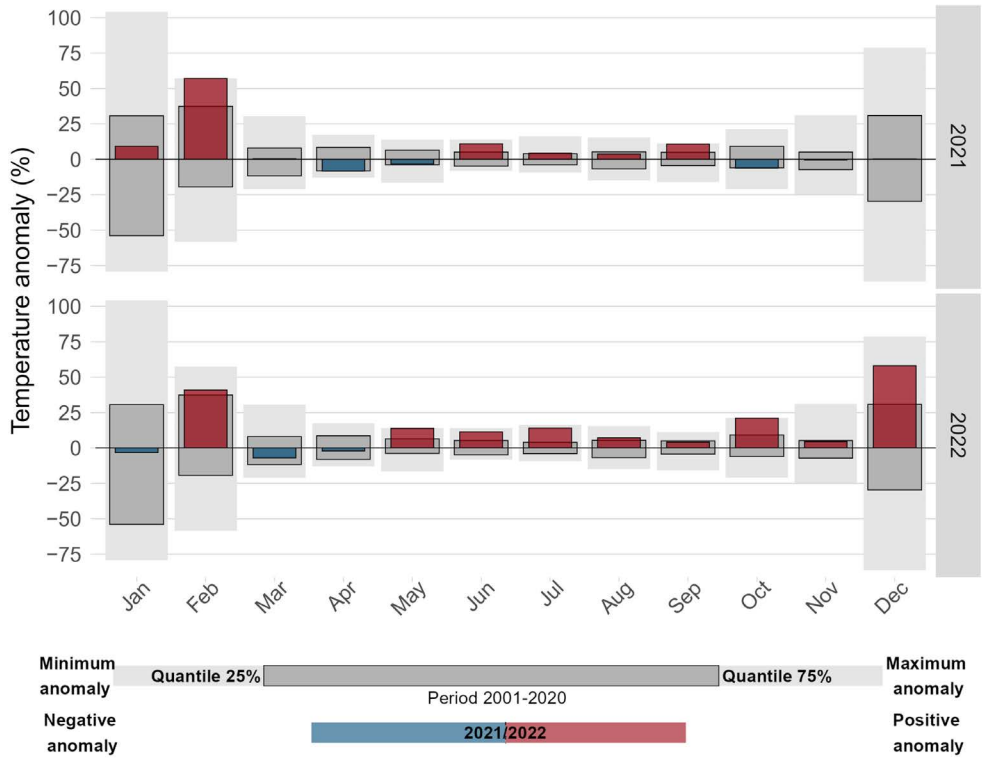

Figure S.6.17 *– Temperature anomalies (as percentages): grey bars indicate maxima and minima (light grey) and 25th and 75th percentile (dark grey) of precipitation anomalies over the reference period, while red and blue bars indicate 2021 and 2022 anomalies compared to the reference period.*

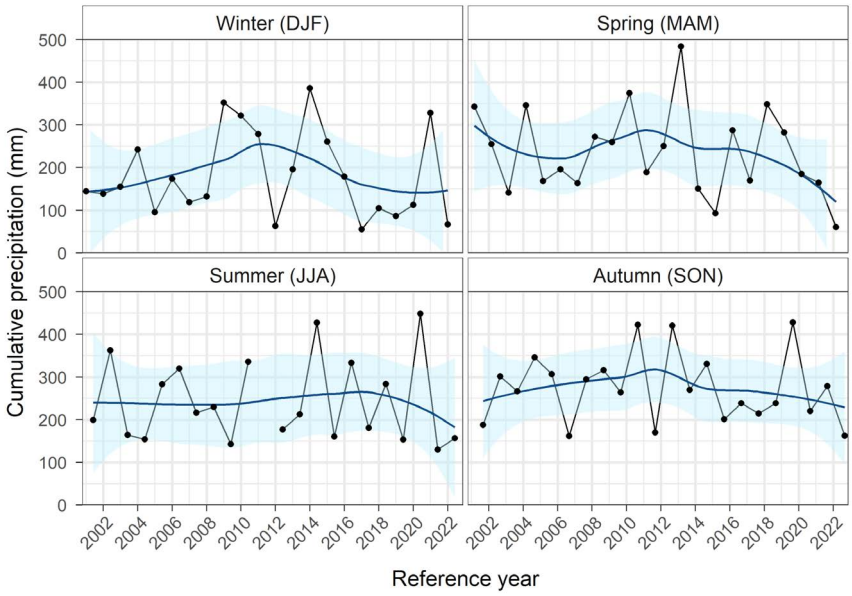

Figure S.6.18 *– Seasonal cumulative precipitation. The blue line represents the loess regression, while the light-blue area represents the confidence interval.*

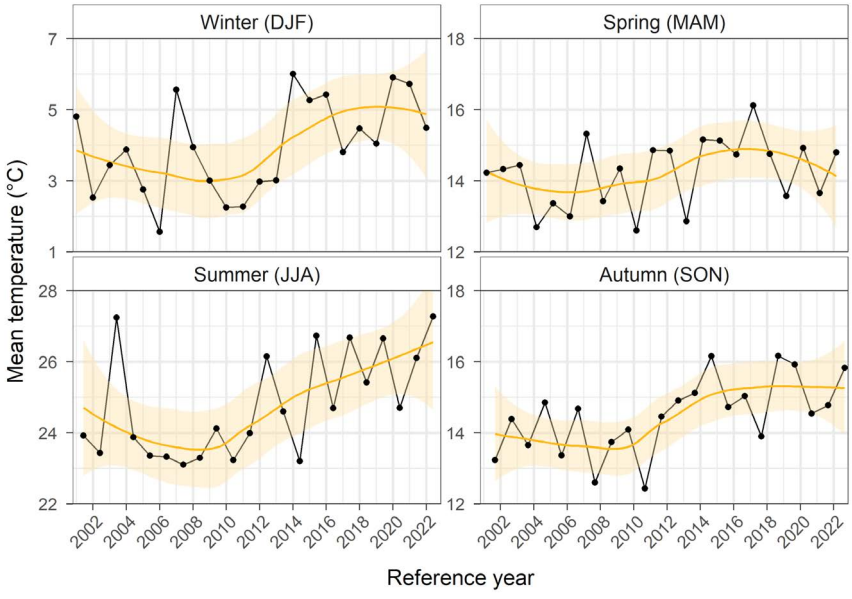

Figure S.6.19 *– Seasonal cumulative temperature. The orange line represents the loess regression, while the light-orange area represents the confidence interval.*

S.6.6 – Clusters information

In this section, additional information on the single clusters belonging to groups A, C, and D are reported, together with a focus on group B which includes only one cluster but representing three different cases with the same seasonal pattern.

Group A

Cluster A1 consists of 10 wells, each showing a seasonal groundwater head minimum in May, a maximum in September-October, and a maximum yearly oscillation of 2.6 m, which is the narrowest oscillation within group A, with a wider pluriannual variability (Fig. 6.5); the seasonal variability corresponds to 63% of the total variability (Table 6.1). Cluster A2 (8 wells) shows a minimum in April and a maximum in August-September, with a maximum yearly oscillation of 3.8 m and a narrow pluriannual variability (Fig. 6.5) and a seasonal variability accounting for ca. 85% of the total variability (Table 6.1). Similarly to cluster A1, cluster A3 (2 wells) presents the groundwater head level minimum in May while the highest level is in October with a yearly oscillation equal to 5.5 m and a wide pluriannual variability, with the seasonal variability constituting 64% of the total variability. Cluster A4 (1 well) presents the widest yearly oscillation, reaching up to 10.3 m, and a seasonal pattern comparable to cluster A2, with a minimum in April and a maximum in September; the seasonal variability constitutes 92% of the total variability. In detail, A1 includes wells located in the outer limit of the morainic aquifer systems and in the northern part of the higher plain where surface irrigation is rarer (Fig. 6.1d) and irrigation canals are sparser or correspondent to the distal portions of the irrigation canals network (Fig. 6.1c), which leads to a smaller summer rise compared to the other A clusters. Wells in cluster A1 show a wider pluriannual variability (Fig. 6.5), and the seasonal variability corresponds to 63% of the total variability (Table 6.1) Cluster A2 groups wells located in the southern sector of the higher plain where traditional surface irrigation is largely practiced (Fig. 6.1d). In this aquifer system, the rise in groundwater levels between April and October is caused by the sum of water leaking from the irrigation canals and, to a significant extent, by the return of irrigation water. The wells in cluster A2 show a narrow pluriannual variability,

with seasonal oscillations around an almost constant mean (Fig. 6.5), and the seasonal variability accounts for ca. 85% of the total variability (Table 6.1). Cluster A3 includes two columns of the same well, tapping at different depths. For this well, the seasonal variability is wider than the neighboring wells (cluster A1), but, similar to the wells in cluster A1, it presents a wide pluriannual variability, and the seasonal variability constitutes 64% of the total variability. Cluster A4 includes a single well tapping a small aquifer in the outer circle of the Garda morainic amphitheater, which is characterized by reduced lateral amplitude but is highly transmissive and has a significant thickness. The combination of these elements contributes to the definition of a sensitive system with a rapid response to the summer superficial input and underground intake from upstream basins.

Group B

Within group B, including only one cluster, different cases can be identified, characterized by specific hydrogeological determining a narrow seasonal oscillation: a) proximity to the spring belt, b) proximity to the lake shores, and c) morainic compartment and alpine valleys. The spring belt's proximity mostly affects medium plain wells W23, W25, W26, and W31. For these wells, the pluriannual variability is also extremely reduced. Wells in the eastern part of the middle plain, W23 and W25, show an extremely reduced seasonal level oscillation, while W26 and W31, located in the western part, downstream to the intensively irrigated areas, show a seasonal profile comparable to that exhibited by group A, albeit with a significantly lower amplitude. Proximity to the Lake Garda shore is the main driver of W32, W35, and W36 narrow variability, presenting a strong similarity with the Lake Garda trend. A correspondence between the two trends is the result of the pressure balance between the aquifer and the dam-regulated lake; a comparison of groundwater level and Lake Garda hydrometric level is shown in Figure S.6.20. The third case involves wells W22, W28, W29, and W30 in the Garda morainic amphitheater, W27 in the Iseo morainic amphitheater, and W33, W34, and W24 in the alpine valleys. Wells W22, W24, W27, and W30 show the highest

variability within group B, linked to a major contribution of the pluriannual trend to the total variability (Fig. 6.5), while the seasonal oscillations are narrow.

Group C

C1 (8 wells) groups all wells located in the lower plain and one well located in the morainic compartment. This cluster's seasonal pattern shows the weakest groundwater level variations range within group C (up to 2.5 m), with a minimum in July. Only W44 shows the lowest seasonal value in August. C2 (5 wells) gathers all the confined and semi-confined wells in the morainic compartment south of Lake Garda. Cluster C2's pattern presents a summer minimum that lasts in July and August and a groundwater level seasonal oscillation of approximately 7.0 m. Cluster C3, with only one well located in the morainic compartment, shows the lowest seasonal value in August but it emerges for the widest seasonal pattern magnitude within all clusters (13.6 m).

Group D

Cluster D1 (4 wells) shows a maximum in March and a minimum in August. D1's seasonal pattern highlights the lowest yearly oscillation of the group that reaches a maximum value of 5.0 m. Cluster D2 consists of 2 wells with a seasonal pattern oscillation up to 7.4 m. Both wells show a maximum in spring (March) and a minimum in autumn (October). Well W55 shows a different pattern during summer, which results from the data of a single year (Fig. 6.5). Cluster D3 (1 well) has a seasonal groundwater head maximum in February, a minimum in September, and a maximum yearly oscillation of up to 8.0 m, the highest oscillation within Group D.

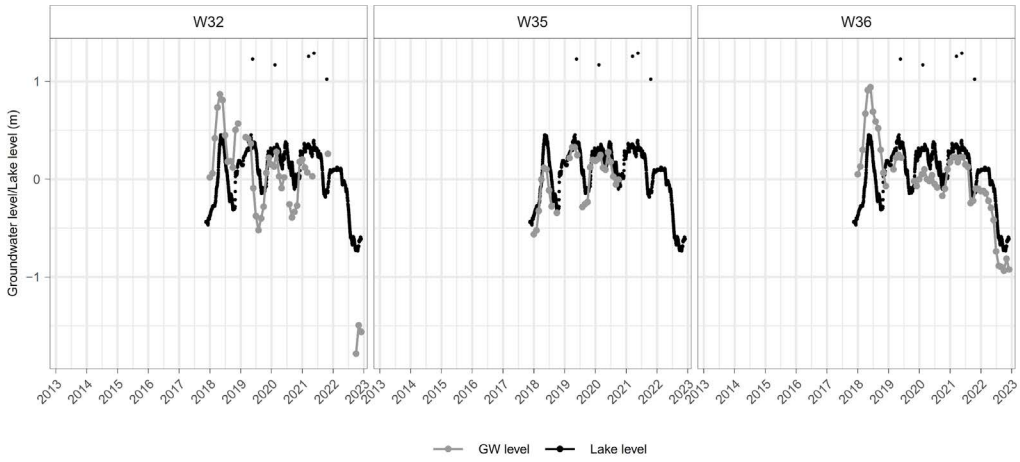

Figure S.6.20 *– Comparison of the groundwater levels at wells W32, W35, and W36 with the hydrometric level of Lake Garda. All the time series have been standardized by subtracting the mean for a quicker comparison. The black line represents the Lake level, while the grey lines represent the groundwater level for the different wells.*

S.6.7 – Focuses on groups A, and C time series

This section focuses on the monthly groundwater level for the wells in groups A (Fig. S.6.21) and C (Fig. S.6.22). Each trend is color-coded by cluster: grey dots indicate the annual maxima, black dots the annual minima, while red dots indicate maxima and minima used to calculate the 2022 decrease and increase. Each graph has its own scale to provide better visibility.

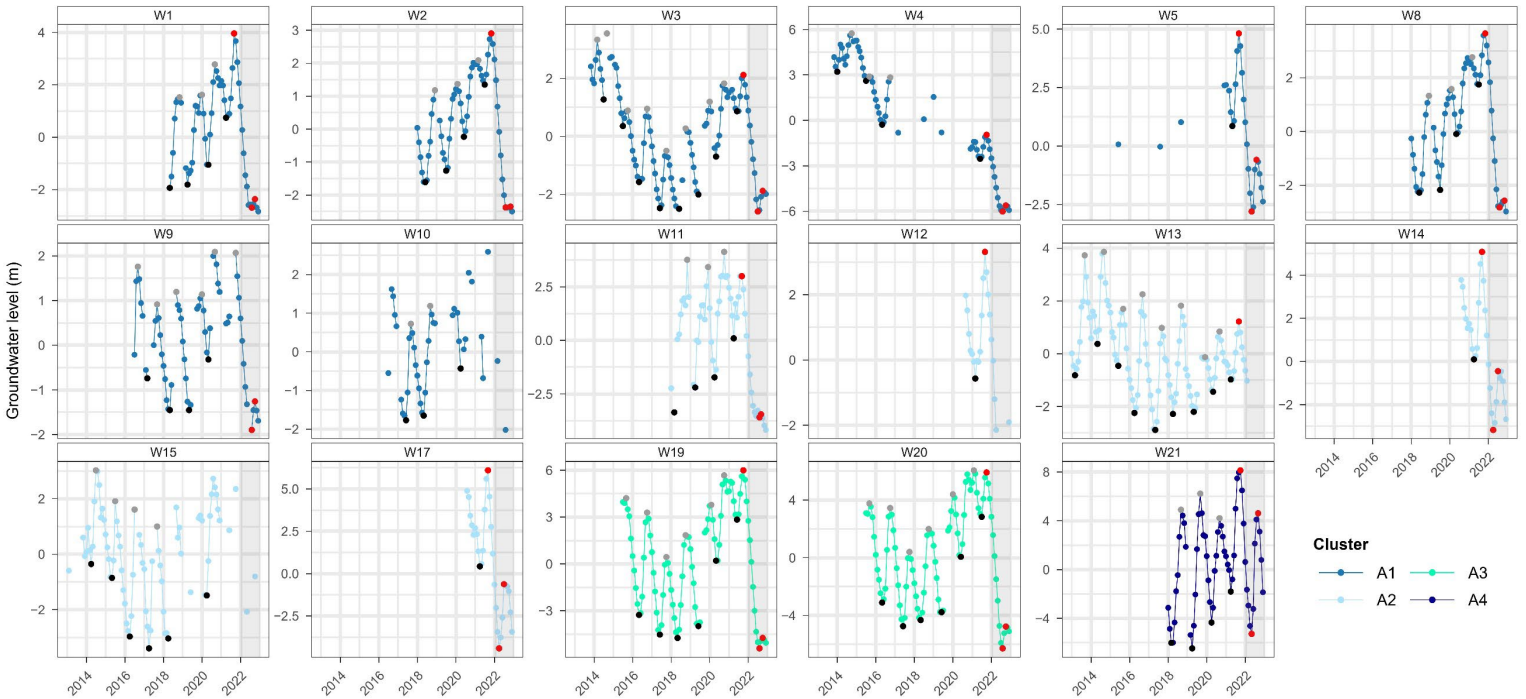

Figure S.6.21 *– Groundwater level time series of wells in group A, color-coded by cluster: grey dots indicate the annual maxima, black dots the annual minima, while red dots indicate maxima and minima used to calculate the 2022 decrease and increase.*

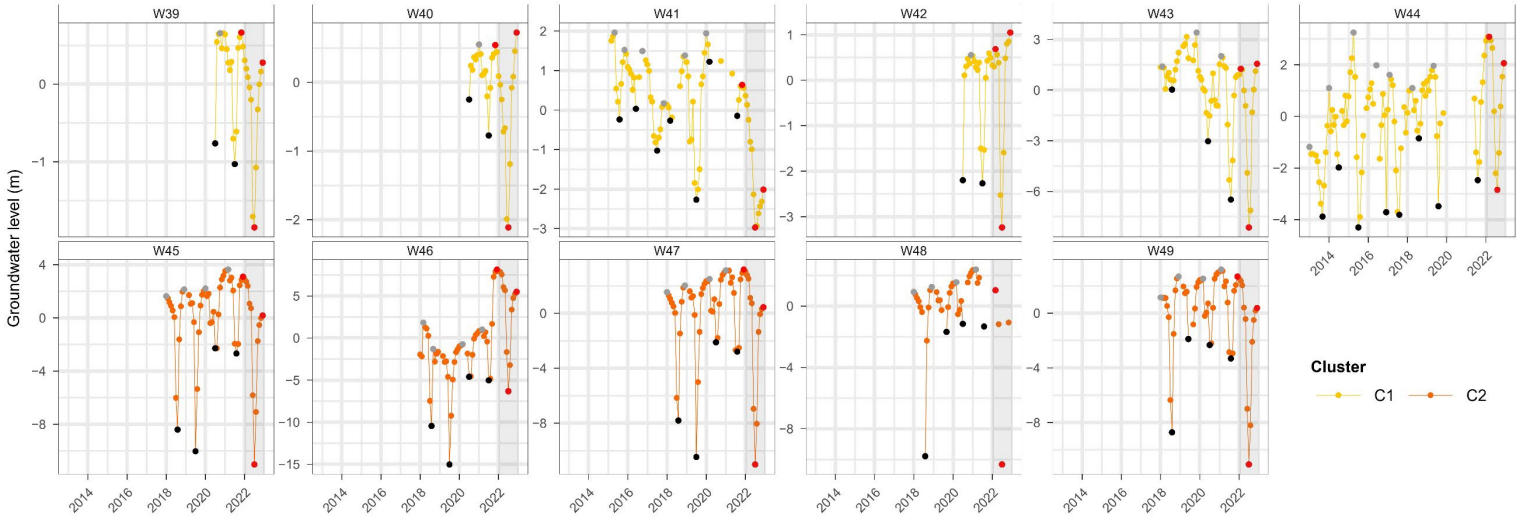

Figure S.6.22 *– Groundwater level time series of wells in group C, color-coded by cluster: grey dots indicate the annual maxima, black dots the annual minima, while red dots indicate maxima and minima used to calculate the 2022 decrease and increase.*

S.6.8 – Focuses on groups B, D, E, and F time series

This section focuses on the monthly groundwater level for the wells in groups B, D, E, and F (Fig. S.6.23). Each graph has its own scale to provide better visibility.

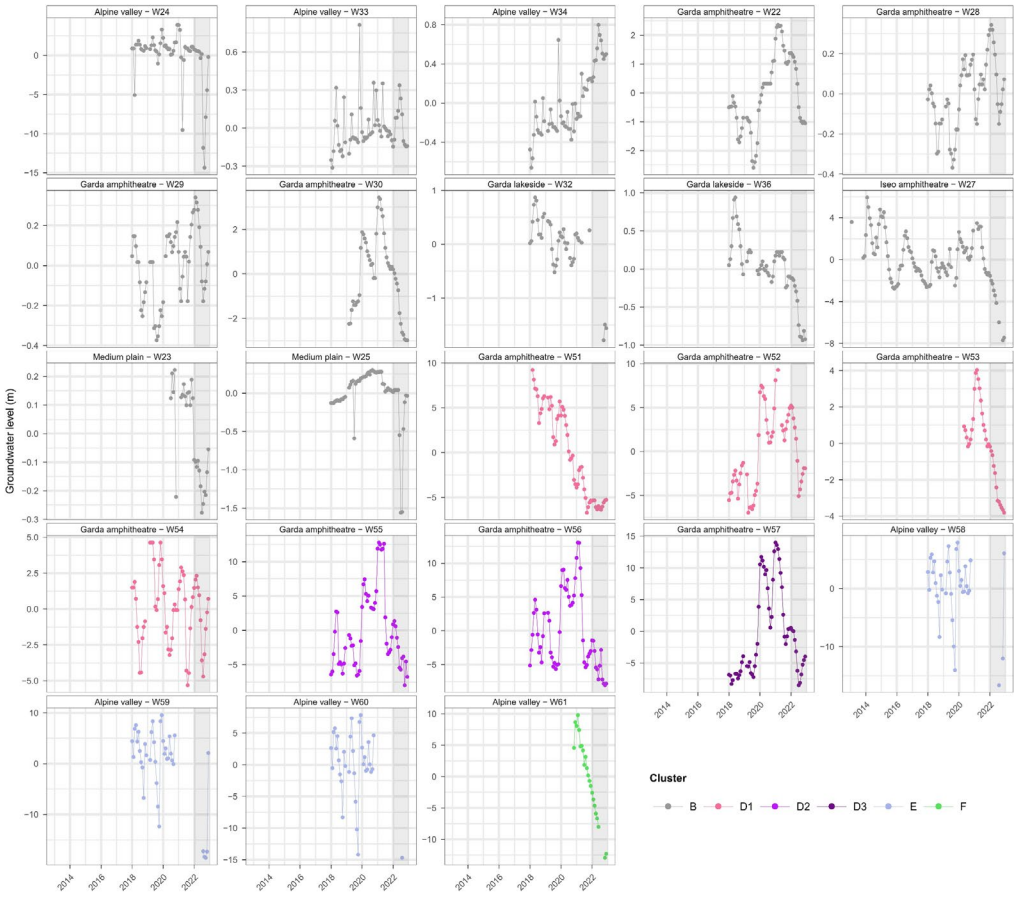

Figure S.6.23 *– Focus on the variability of groups B, D, E, and F.*

Chapter 7: Implementation of the Groundwater Numerical Model and Results from Synthetic Scenarios

Changes in irrigation practices may bankrupt aquifers faster than meteorological droughts: a numerical modeling approach

Agnese Redaelli[1,*], Tullia Bonomi[1], Davide Sartirana[1], Gianfranco Sinatra[2], Daniel T. Feinstein[3], Randall J. Hunt[4], Marco Rotiroti[1] and Chiara Zanotti[1]

[1]Department of Earth and Environmental Sciences, University of Milano-Bicocca, Milan, Italy.

[2]Acque Bresciane S.r.l. SB, Via 25 Aprile, 18, 25038 Rovato, BS, Italy.

[3]Department of Geoscience, University of Wisconsin-Milwaukee, Lapham Hall, R 3209 North Maryland Avenue, Milwaukee, WI 53211, USA.

[4]Department of Geoscience, University of Wisconsin-Madison, Lewis G. Weeks Hall, 1215 West Dayton Street, Madison, WI 53706-1692, USA.

*corresponding author: agnese.redaelli@unimib.it

This chapter is largely based on a paper submitted to the *Journal of Hydrology.*

Keywords: Groundwater Recharge; Climate Change; Water Management, Po Plain.

Highlights

- A groundwater numerical model developed for an intensively irrigated aquifer
- Two scenarios simulated: a drought and a shift to drip irrigation
- Drought reduces recharge and storage yet maintains seasonal dynamics
- Reduced irrigation return flow significantly depletes the aquifer
- Adaptation measures need to be carefully designed to avoid significant impacts on groundwater

Abstract

Groundwater availability worldwide is threatened by a changing climate. Aquifers in intensively irrigated systems may present peculiar vulnerability to climate change related to changes in irrigation practices triggered by potential surface water scarcity. This work aims to provide a quantitative assessment of the major drivers of aquifer depletion in

agricultural areas: hydrological droughts and changes to more efficient irrigation practices as a response to reduced surface availability. A three-dimensional combined steady-state and transient numerical groundwater flow model was developed for an intensively irrigated hydrogeological system where irrigation return flow constitutes a major recharge source. Two hypothetical scenarios were simulated: (1) a two-year meteorological drought and (2) a transition from surface irrigation to the more efficient drip irrigation technique, while maintaining all other conditions the same as in the reference period. The drought scenario leads to a significant reduction of the recharge processes but preserves the overall relative dynamics and seasonal patterns in groundwater storage, groundwater heads, lowland springs discharge, and surface water-groundwater interactions, with a total groundwater storage loss of -2.34×10^5 m^3/d over the two simulated years. In contrast, the scenario representing the reduction in irrigation return flow determines a disruption in the seasonal pattern over the two simulated years, leading to a loss in groundwater storage up to -2.77×10^5 m^3/d and critical impacts on lowland springs and connected surface water bodies. Therefore, the results indicate that possible adaptation measures to address surface water scarcity induced by climate change may have a more significant impact on groundwater resources than the direct effects of climate change itself, highlighting the crucial role of scientific evidence in informing and guiding policymakers.

7.1 Introduction

Groundwater provides societies with social, economic, and environmental benefits and opportunities (UNESCO, 2022). Although considered more resilient than surface water to meteorological conditions, groundwater is facing direct and indirect impacts worldwide due to a changing climate (Taylor et al., 2013).

Projections indicate that global surface temperature will increase until at least mid-century under all emissions scenarios, leading to changes in the climate system, including increases in hot extremes and droughts (IPCC, 2023; Stigter et al., 2023). Studies highlight that meteorological drought will increase in frequency and intensity (Baronetti et al., 2020; Wu et al., 2020), threatening groundwater and groundwater-

dependent ecosystems worldwide, including terrestrial vegetation, rivers, springs, wetlands, and riparian zones, which not only support biodiversity but also provide fundamental ecosystem services for human communities (Howard et al., 2023; Rohde et al., 2024; Saito et al., 2025; Stigter et al., 2023).

Groundwater recharge is a complex process controlled by a combination of natural (e.g., precipitation, geology, or vegetation characteristics) and anthropogenic (e.g., land use and irrigation return flows) drivers (Atawneh et al., 2021; Jasechko et al., 2014). Moreover, aquifer systems are subject to specific combinations of recharge mechanisms, each of which responds differently to the direct and indirect effects of climate change, defining a region's peculiar sensitivity to climate change (Amanambu et al., 2020; Meixner et al., 2016).

In this context, groundwater systems in agricultural areas characterized by intense irrigation are extremely vulnerable, as they are currently threatened by the direct effects of a changing climate, as well as by human-driven impacts related to changes in irrigation practices (e.g., increased abstraction and reduced recharge due to the loss of irrigation return flows) (Van der Gun, 2022, Wu et al., 2020). Most of the world’s large aquifer systems are located in regions characterized by extensive agricultural and irrigation activity, making them essential not only for local agricultural needs but also for global food security, and the sustainability of related ecosystems (Ndehedehe et al., 2023). Examples include the Ogallala Aquifer and the California’s Central Valley Aquifer in North America (Davis and Putnam, 2013; Faunt, 2009), Indo-Gangetic Basin and the North China Plain systems in Asia (Du et al., 2024; MacDonald et al., 2016; Yang et al., 2015), and the Po Plain aquifer in Europe (Carlson et al., 2025; Masseroni et al., 2024; Van der Gun, 2022).

Agriculture can have a dual effect on many of these systems, either depleting them through withdrawals or contributing to the system’s recharge through irrigation return flow, especially when surface water is used as the source of irrigation (Redaelli et al., 2025; Scanlon et al., 2023; Taylor et al., 2013; Van der Gun, 2022). However, surface water is highly vulnerable to meteorological droughts. Consequently, there is a growing

global attention toward efficient irrigation methods such as drip or subsurface irrigation to conserve surface water and reduce the risk of water shortages (Guo and Li, 2024; Masseroni et al., 2024; Nikolaou et al., 2020). These methods can achieve high efficiency levels (up to 90%) by delivering water directly to the plant's roots, significantly reducing the amount of water that percolates through the soil toward the aquifer (Munir et al., 2018; Nikolaou et al., 2020). However, while these strategies can be beneficial in terms of reducing surface water consumption, the subsequent decrease in irrigation return flow percolating toward the aquifer may lead to a reduction in aquifer recharge. Therefore, aquifers in agricultural and heavily irrigated areas present a peculiar vulnerability to climate change, being exposed not only to its direct effects, such as reduced precipitation, but also to indirect impacts related to changes in water management as a response to surface water scarcity.

To date, only a few studies have directly investigated the effects of a reduction in irrigation return flow on groundwater systems and groundwater-dependent ecosystems (e.g., Jin et al., 2018; Pool et al., 2021), but no quantitative estimates of the resulting loss in recharge volumes are currently available. Understanding and quantifying the influence of irrigation management combined with future climatic changes and other drivers is crucial for developing sustainable strategies and long-term water resources management, considering not only groundwater but also its interconnection with the surface water system (Meixner et al., 2016; Scanlon et al., 2023).

The aim of this work is to perform a quantitative assessment of the effects of meteorological droughts and changes in irrigation practices on groundwater and groundwater-dependent ecosystems (e.g., rivers and springs) in order to favor evidence-based decisions for stakeholders and water managers. For this reason, a transient groundwater flow model was developed to simulate groundwater dynamics in a complex, highly human-modified system where land use is primarily agricultural, and to investigate how it may be affected by potential changes in climate and water use.

To quantify and compare the effects of meteorological conditions and irrigation management changes on the system, two hypothetical scenarios were run: a) a two-year

meteorological drought and b) a change in irrigation practices, from surface irrigation to a more efficient drip irrigation method. The effects of the two scenarios are evaluated by comparing the impacts on multiple system's components: (1) the aquifer storage, as one of the most susceptible components to climate change (Ndehedehe et al., 2023; Wu et al., 2020), (2) the lowland spring discharge, fundamental from a hydrogeological, agricultural, and ecosystem perspective (De Luca et al., 2014), and (3) the groundwater-surface water relation (expressed as flow exchanges), one of the most important indicators of change in an aquifer system (Stefania et al., 2018; Stigter et al., 2023).

7.2 Materials and Methods

7.2.1 Study Area

This study focuses on a ~2000 km² area within the Oglio River basin (N Italy), between the outflow of Lake Iseo and the river's confluence with the Mella River (Fig. 7.1). Along the ~95 km stretch considered in this study, the Oglio River receives water from five tributaries: the Cherio River, the Scolmatore di Genivolta Channel, the Saverona Stream, the Strone River, and the Mella River (Fig. 7.1).

The study area has a temperate continental climate, characterized by cold winters and humid, hot summers. The average temperature is 12.5 °C, and the mean annual precipitation is ≈ 900 mm (Faquseh and Grossi, 2023). The rainfall regime is denoted by a bimodal trend with two maxima, with moderate prevalence of the autumn maximum over the spring maximum. Spatially, precipitation intensity shows a north-south decreasing trend due to orographic effects in the northern piedmont areas (Faquseh and Grossi, 2023; Rotiroti et al., 2019a).

Land use in the study area is mostly agricultural (Fig. 7.1c), with extensive cultivation of corn primarily used for livestock feeding (cattle and swine). Agricultural irrigation is practiced through the surface irrigation technique, that is, flooding of farm fields (Caschetto et al., 2025). In the northern part of the plain, surface water is used for irrigation, which is diverted from the Oglio River and distributed to the fields through an extensive network of century-old irrigation canals. In contrast, groundwater-fed

irrigation is mainly used in the southern part of the plain, supported by hundreds of irrigation wells (Rotiroti et al., 2019a; Zanotti et al., 2022). Surface water diversions from the Oglio River occur within 35 km from the Lake Iseo outlet, whose flow regime is dam-regulated for hydropower and agricultural purposes (Hinegk et al., 2022). During the irrigation period, from May to September, the water discharged from Lake Iseo to the Oglio River increases up to 67±19 m^3/s compared to the average of 48±20 m^3/s during the non-irrigation period (Consorzio dell'Oglio, 2019).

7.2.2 Hydrogeological Conceptual Model

A concise summary of the hydrogeological conceptual model for the study area is reported here; extensive descriptions are available in previous studies (Redaelli et al., 2025; Rotiroti et al., 2019b, 2019a).

7.2.2.1 Geological and Hydrogeological System

The Oglio-Mella River basin is located within the Po Plain alluvial basin, which is composed of an alternating sequence of sediments belonging to the continental depositional system of Plio-Pleistocene age (Garzanti et al., 2011). The plain area exhibits a gentle north–south elevation gradient, and its morphology is interrupted by isolated hills, resulting from Quaternary uplift of the rocky substrate that crosses the Brescia plain with an ENE-WSW direction (Denti et al., 1988; Rotiroti et al., 2019a; Vercesi, 1994).

From a hydrogeological perspective, the plain area can be subdivided into higher and lower plains by the so-called "spring belt" (Fig. 7.1b), a narrow area characterized by numerous (semi)natural lowland springs, often engineered to increase flow, which cross the entire plain in a transverse direction (Bartoli et al., 2012). The higher plain hosts an unconfined, monolayer aquifer primarily composed of coarse sediments such as gravel and sand, with a cumulative thickness reaching up to 100-150 m (Fig. 7.2). The lower plain is characterized by a multilayer aquifer system consisting of vertically alternating sandy aquifers and silty-clay aquitards (Fig. 7.2). Previous works (Regione Lombardia & ENI Divisione AGIP, 2002) classified these overlapping aquifers into 4 Aquifer

Groups (A-D) based on the glacial deposition cycles that shaped the plain, from the shallowest (Aquifer Group A) to the deepest (Aquifer Group D). The present work only focuses on Aquifer Groups A and B. Although the Aquifer Group A in the lower plain is mainly confined, in some cases, the shallow confining layer thins locally, creating semi-confined or unconfined conditions. As a result of these lithological differences, the permeability of the aquifer on the higher plain is significantly greater than that of the lower plain (Perego et al., 2014; Rotiroti et al., 2019a).

As the study focuses on the Oglio-Mella River basin, the model domain was extended north-south, from the Alpine area limits to the Po River, and east-west, including the portion of the Po Plain between the Serio and the Chiese Rivers, to set boundary conditions far from the study area.

Groundwater heads range from ~160 m a.s.l. in the northwest to ~35 m a.s.l. in the southeast. In the shallow aquifer, groundwater flows from NW to SE, with surface water bodies causing local deviations, especially in the lower plain, where the Oglio, Saverona, Strone, and Mella rivers are gaining (Bartoli et al., 2012; Delconte et al., 2014). In the northernmost part of the higher plain, the water table is around 50 m below ground level (b.g.l.) and progressively approaches the land surface toward the spring belt (<5 m b.g.l.). Groundwater levels in the surface-water-fed irrigated plain exhibit a seasonal trend, with the lowest levels occurring in April-May, following the reduced winter precipitation, and the maximum in August-September, after the irrigation season. In the lower groundwater-fed irrigated plain, the typical seasonal trend shows a steady summer decline due to increased withdrawals and a rebound in fall (Redaelli et al., 2025; Rotiroti et al., 2019a).

7.2.2.2 Groundwater Recharge and Discharge

The higher surface-water-fed irrigated plain aquifer is recharged by (1) irrigation return flow from surface-water-fed irrigation, (2) local precipitation, (3) surface mountain-front recharge (Markovich et al., 2019) in the northernmost sector, and (4) losing river reaches, and discharges through (1) gaining rivers, (2) the spring belt, (3) the downstream lower plain aquifer, and (4) groundwater abstraction (Rotiroti et al., 2019a, 2023). In contrast,

the lower groundwater-fed irrigated plain aquifer receives almost all its recharge water by lateral recharge from the upstream higher plain aquifer, as extensive shallow low-permeability layers reduce vertical recharge from the surface. However, vertical recharge may also occur due to local discontinuities or incomplete confinement. Discharges mainly occur through gaining rivers and well abstraction (Rotiroti et al., 2019a, 2023).

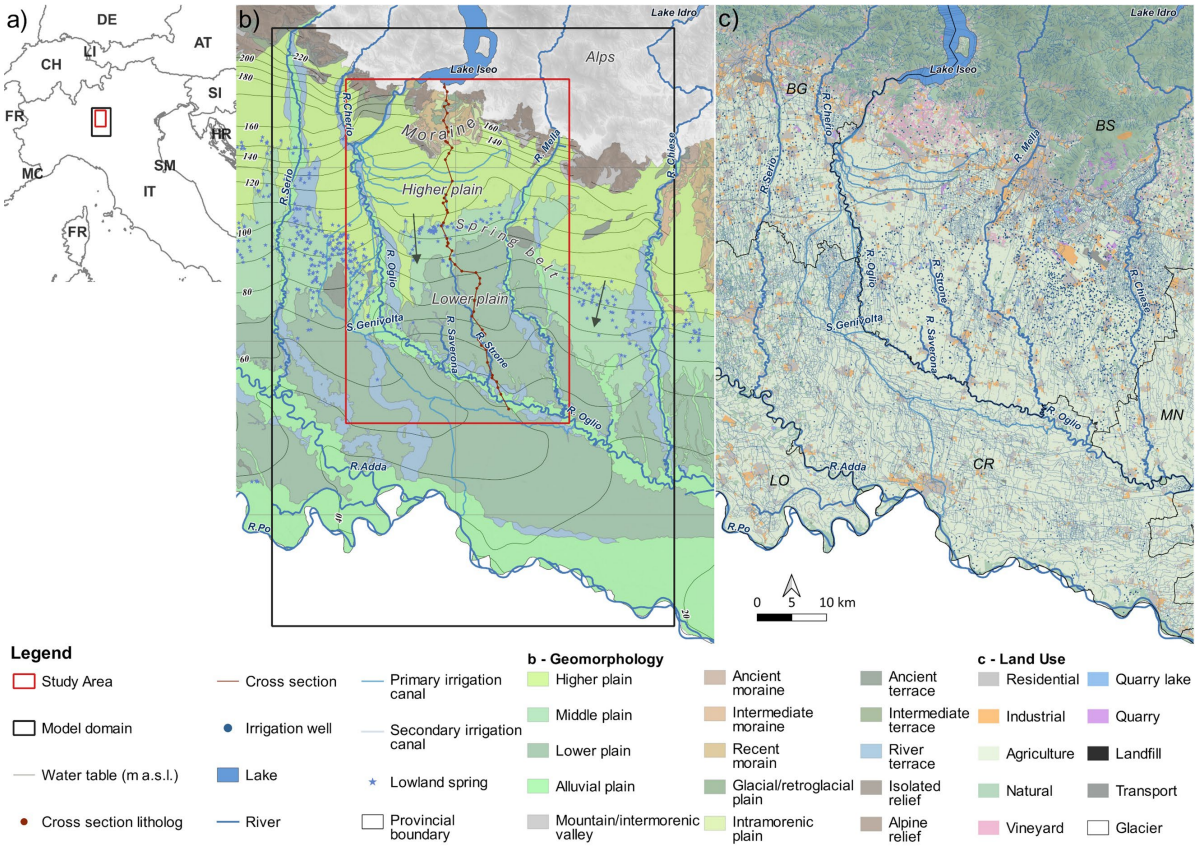

***Figure 7.1** – **a)** Geographical setting; **b)** Study area, model domain, geomorphology (Regione Lombardia, 2007), water table contour map (September 2014 (Regione Lombardia, 2016)) with groundwater flow direction, and cross-section trace. The cross-section is visible in Fig. 7.2;*

c) *Land use (land use classes have been represented from the geographic database Dusaf 7.0 (Regione Lombardia 2023)), and Lombardy provinces (BG = Bergamo, BS = Brescia, LO = Lodi, CR = Cremona, MN = Mantova).*

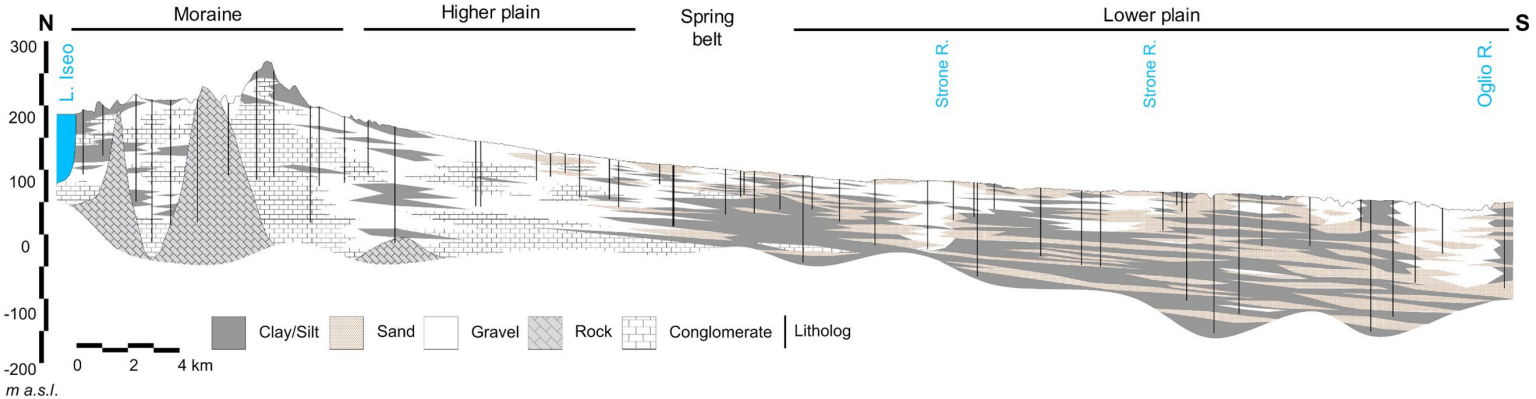

Figure 7.2 *– Cross-section (modified from Zanotti et al., 2022). The cross-section trace is visible in Fig. 7.1.*

7.2.3 Available data

Eight field measurement campaigns were conducted between October 2015 and October 2017 to monitor the following parameters: river stage at 21 sites, river discharge at 17 sites, and groundwater head in 46 wells (see Sup. Info. Sect. S.7.1 for details). Additional groundwater level data for the same period from 12 wells were provided by Acque Bresciane S.r.l. SB, a local water supplier (Fig. S.7.1).

Monthly data from 2015 to 2017 of the Oglio River stages and discharges, and irrigation canal discharges, with the corresponding distribution areas, were acquired from the Consorzio dell'Oglio, the authority responsible for controlling Lake Iseo levels and downstream flows to the Oglio River (Consorzio dell'Oglio, 2019). The discharges of the other main rivers in the model domain, lowland springs' location and elevation, and daily precipitation from 2015 to 2017 were acquired from the Regional Agency for Environmental Protection of Lombardy (ARPA Lombardia, 2019).

Furthermore, 32 estimates of groundwater-river flow exchange were calculated for 9 river stretches (Tab. S.7.1) between 2015 and 2017 (7 stretches of the Oglio River, 1 of the Strone River, and 1 of the Mella River). These values were obtained by measuring the difference in river discharge on the same day at two consecutive locations along the river, while taking into account all known tributary or effluent discharges. Except for the upgradient stretch of the Oglio River, which alternates between losing and gaining behavior throughout the year, the remaining stretches are permanently gaining (Rotiroti et al., 2019a), so their groundwater-river flow exchanges can be considered baseflow values.

7.2.4 Numerical Model

A three-dimensional combined steady-state and transient numerical groundwater flow model was developed using MODFLOW-NWT, the Newton-Raphson formulation of MODFLOW-2005 (Niswonger et al., 2011). The MODFLOW-NWT was selected to address problems caused by the drying and rewetting nonlinearities of the unconfined groundwater-flow equation (Hunt and Feinstein, 2012). The model grid covers an area

of ~ 5000 km^2 (active cell ~ 3400 km^2) and consists of 7,990,080 cells with a uniform cell size of 100 m x 100 m arranged into 861 rows (NS direction) and 580 columns (EW direction) (Fig. 7.4). The model domain is divided into a near-field, including the area between the Oglio and Mella Rivers (~ 780 km^2), and a far-field, including surrounding areas for a total of ~ 4220 km^2. Vertically, the model is discretized into 16 layers of variable thickness (Fig. 7.3). The model simulates the Aquifer Groups A and B (Sect. 7.2.1). These are reconstructed through 11 and 5 layers, respectively, modeling a total depth of 625 m, which is reached in the south-eastern part of the model. Details on grid construction are reported in Sup. Info. Sect. S.7.2.1.

The groundwater model is temporally discretized into 109 stress periods, consisting of one initial steady-state period, referring to the average conditions of the period 2015-2017, and 108 monthly transient stress periods, including an initial 6-year spin-up (for a total of 72 stress periods), consisting of two repetitions of the three-year period 2015-2017 selected to reach the system equilibrium and to establish the initial condition for the simulation of the 3 years of interest (2015-2017, the last 36 stress periods) (Ajami et al., 2014; Seck et al., 2015). The spin-up period was defined due to a lack of sufficient data prior to 2015, which did not allow for the reconstruction of the previous groundwater levels and flow conditions. A monthly stress period was selected to capture seasonally variable processes (i.e., recharge, groundwater use).

A first hydrogeological parametrization was performed before calibration, as described below. A total of 4686 stratigraphic logs, extracted from the TANGRAM database (Bonomi et al., 2014), were used to reconstruct the spatial distribution of hydraulic conductivity (K) following the coding method proposed by Bonomi (2009). This coding assigns hydraulic conductivity values to each lithological unit based on its textural composition, using reference K values for selected lithologies (Freeze and Cherry, 1979; Fetter, 1994). The hydraulic conductivity values were then interpolated using GOCAD (Paradigm, 2009) by ordinary kriging through a quasi-3D stratified approach (Fabbri and Trevisani, 2005). Further details are reported in Sup. Info. Sect. S.7.2.2. The continuous distribution of hydraulic conductivity (K) was then discretized into 20 zones through the

analysis of the frequency distribution of the obtained hydraulic conductivity, with values of horizontal K ranging from 2.4×10^{-2} m/d to 2.0×10^{2} m/d (Fig. 7.3). This conversion from continuous to (several) discrete K values is justified by a trade-off between the number of variables to be calibrated (thousands of pilot points needed to maintain a continuous K distribution) and the level of detail with which heterogeneity is represented. For each K zone, the vertical K value was calculated by multiplying the vertical anisotropy factor of 0.1 to the horizontal K value. Regarding specific yield (Sy), 3 zones (0.07, 0.14, and 0.20) were set, with a spatial distribution derived from the aggregation of the hydraulic conductivity zonation. The specific storage (Ss) follows the same zonation used for Sy (3 zones); however, a single value for the entire system, equal to $1\times10^{-5}\,m^{-1}$, was initially set.

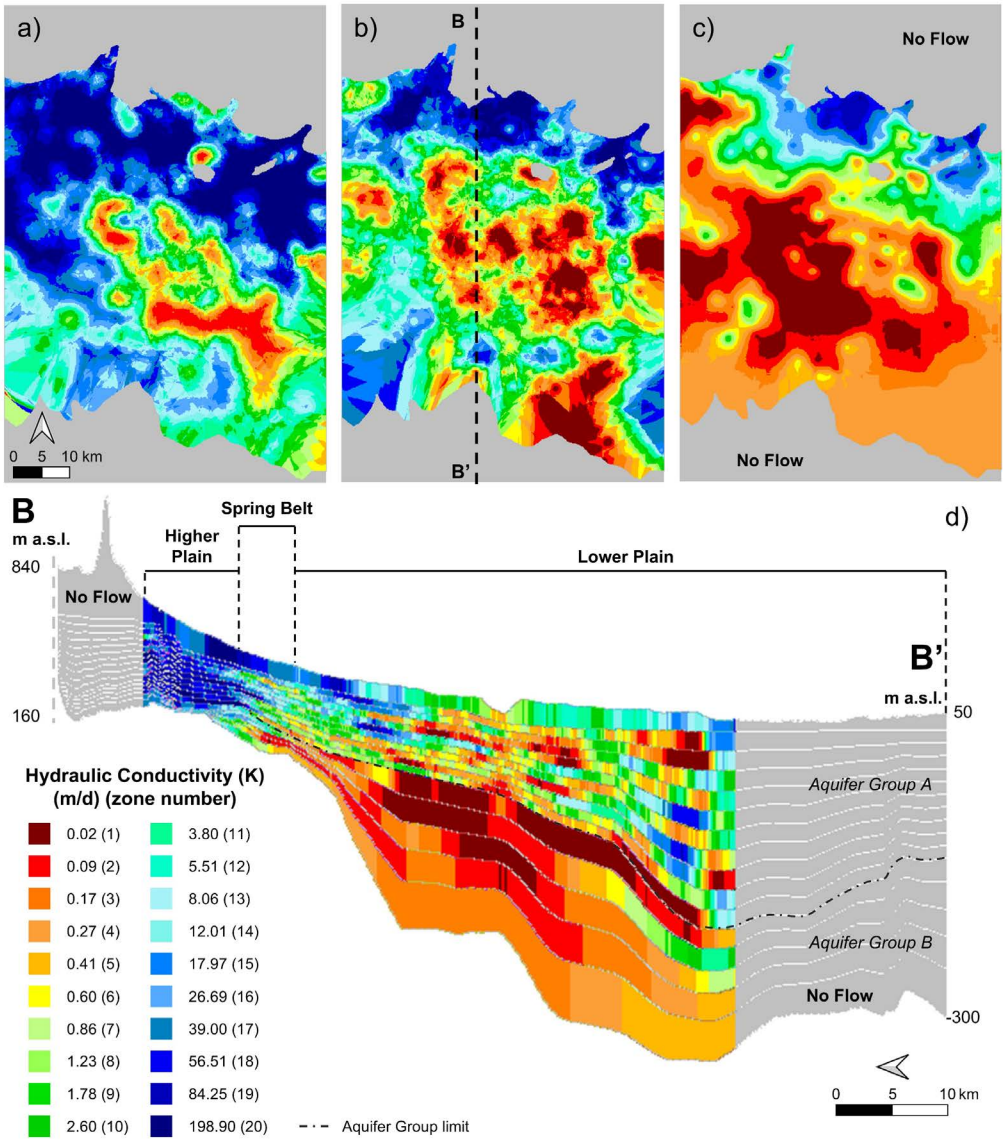

Figure 7.3 – *Spatial distribution of the initial values of the hydraulic conductivity in a) layer 1, b) layer 8, c) layer 12, and d) within a cross-section (N-S). The dotted line refers to the limit between Aquifer Groups A and B, as defined by the model vertical discretization.*

Vertical recharge was simulated using 21 zones, with monthly-variable values. In 17 of these 21 zones, vertical recharge was simulated considering both effective precipitation and irrigation return flow (zones 1-17, Fig. 7.4b); the latter was applied only during the irrigation season (May-September). These 17 zones represent the irrigation management areas used by the local irrigation authority. In the remaining 4 zones, the sole effective precipitation was simulated (zones 18-21, Fig. 7.4b). The detailed recharge values are reported in Sup. Info. Sect. S.7.2.3.

Other internal conditions were implemented according to the conceptual model, including the complex hydrographic network of rivers and primary irrigation canals (simulated with SFR2 Package) and secondary irrigation canals (simulated with RIV Package), 385 lowland springs (simulated with the DRN Package), 7426 pumping wells (simulated with WEL Package), recharge contribution from the Alpine area (simulated with GHB Package), and southern groundwater outflow from the plain (simulated with CHD Package). No flow boundaries were placed in the northern part of the model, corresponding to the southernmost outcrop of the Alpine area, and in the area south of the Po River, corresponding to a separate aquifer system. In addition, no flow boundaries were used to represent isolated bedrock reliefs with the plain (Fig. 7.4a). Details on boundary conditions are reported in Sup. Info. Sect. S.7.2.4

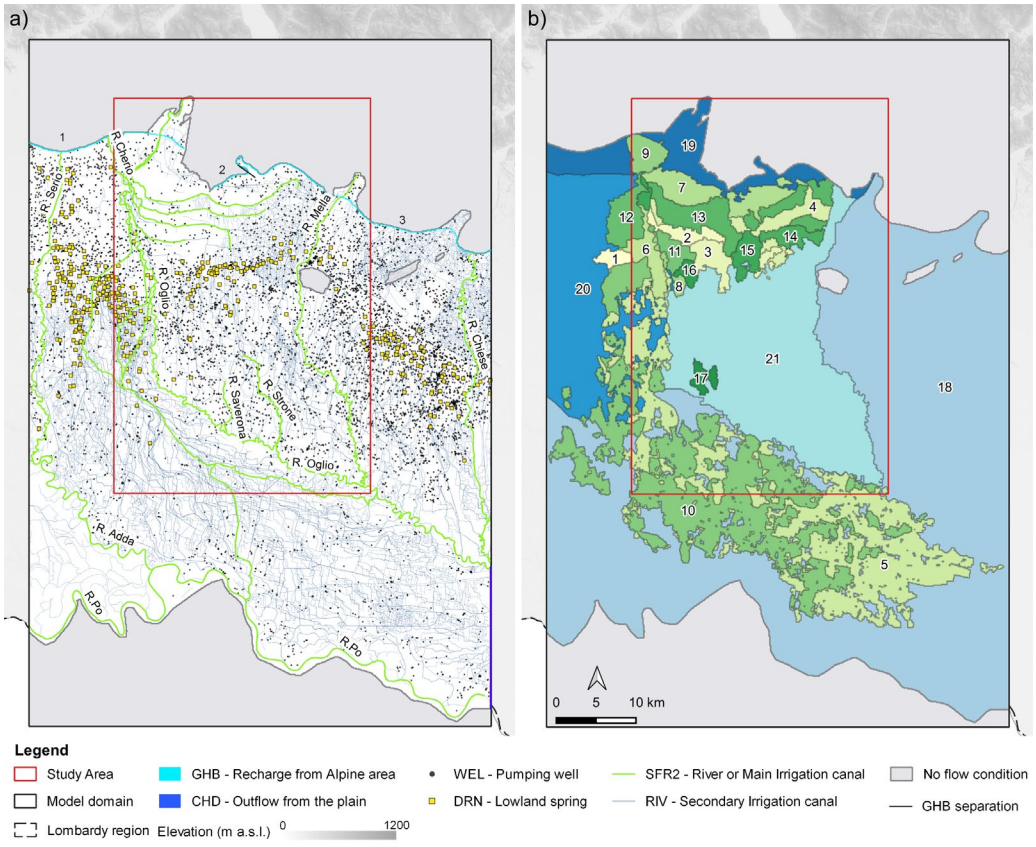

Figure 7.4 – a) *Boundary conditions of the model (Numbers 1-3 refer to the three General Head Boundaries);* ***b)*** *Spatial distribution of the 21 recharge zones. Each color corresponds to a specific zone (recharge values are reported in Tab. S.7.3).*

7.2.5 Model Calibration

The calibration process included two steps: (1) a preliminary manual trial and error calibration, adjusting hydraulic conductivity, vertical recharge (RCH), abstraction rate, riverbed (SFR2) and drain (DRN, lowland springs) K, pumping rate of wells (WEL), groundwater head of General Head Boundaries (GHB) and Constant Head Boundary (CHB), followed by (2) a parameter estimation calibration, performed on the last 36 stress periods (corresponding to the January 2015-December 2017 period), through the Parameter Estimation (PEST) software suite, through formal mathematical regression techniques (Doherty, 2025). Subspace regularization techniques were applied using

singular value decomposition (SVD) in conjunction with Tikhonov regularization (Doherty and Hunt, 2010).

A total of 8 parameter groups (474 parameters) were calibrated. These groups include: 1) hydraulic conductivity multiplier for the secondary canals (RIV) bed, 2) streambeds (SFR2) and lowland springs (DRN) hydraulic conductivity, 3) stream inflow from unmodeled upstream surface water features added in the first cell of the Oglio and Cherio rivers (SFR2), 4) recharge rate (RCH) multiplier, 5) horizontal hydraulic conductivity, 6) vertical anisotropy, 7) specific yield (Sy) and specific storage (Ss), and 8) abstraction rate multipliers for the irrigation wells (WEL). To constrain the minimum and maximum values each parameter could assume during calibration, specific upper and lower bounds were set for each parameter. For groups 1, 4, and 8, calibration was performed by applying a multiplier to each parameter whose value was set during manual trial-and-error calibration, whereas for the other groups, the values set during manual trial-and-error were calibrated directly. Further information on the upper and lower bounds are reported in Table S.7.5. Specifically, for group 1, the K values of the secondary canal beds were adjusted by a single multiplier. For group 2, the streambed K value of each SFR2 segment was calibrated individually (to achieve finer resolution, the first segments of the Serio and Chiese rivers were further subdivided into two sub-segments each), whereas a unique value was adjusted for the K of the lowland springs, for a total of 80 parameters calibrated. For group 3, the discharge value was calibrated individually for each river, using different multipliers for each of the 36 stress periods, for a total of 72 parameters calibrated. For group 4, to preserve spatial heterogeneity while managing parameter dimensionality, recharge zones were aggregated into three wider homogeneous recharge areas: the higher surface-water-fed irrigated plain (zones 1–4, 6–9, and 11–16); the lower groundwater-fed plain (zone 21); and the remaining portion of the plain (zones 5, 10, and 17–20). A multiplier was defined for each of the 36 stress periods for the three defined areas, resulting in a total of 108 parameters calibrated. Concerning Group 5, the horizontal hydraulic conductivity values were calibrated by dividing the 20 zones originally defined for the entire model (Sect. 2.4) according to Aquifer Group classification. The 20 zones of K pertaining to the Aquifer Group A

(layers 1-11) were calibrated separately from those pertaining to the Aquifer Group B (layers 12-16), thus effectively creating 40 zones of horizontal K (40 calibrated parameters). For group 6, the 20 zones of vertical anisotropy were singularly calibrated. For group 7, each Sy zone was calibrated individually (3 parameters), whereas Ss zones were divided following the same vertical discretization used for hydraulic conductivity (6 parameters), resulting in a total of 9 parameters calibrated. Finally, irrigation wells were subdivided into 4 different groups: (1) wells located upstream of the main irrigation canals, (2) wells in the higher surface-water-fed irrigated plain, (3) wells in the medium-lower groundwater-fed plain, and (4) wells in the lower groundwater-fed plain. For each group, irrigation well abstraction rates were parameterized with one multiplier per stress period, with variations allowed only during the irrigation season (May–September) for a total of 144 parameters calibrated.

Two types of calibration targets were used: 571 head targets from the 58 monitored wells and the 32 groundwater-river exchange flow difference targets, 31 of which are baseflow targets (Sec. 7.2.3). Prior to automated calibration, the calibration targets were weighted to account for the different availability of target types and the error in each observation (Anderson et al., 2015). Specifically, smaller weights were assigned to the baseflow targets due to the high uncertainty in river discharge measurements and consequent exchange flow calculation. Indeed, due to the high complexity of the heavily anthropized system under investigation, it was not possible to exclude the presence of unknown inflows or outflows (e.g., industrial waste, tailwater contribution, and controlled movement of water flows for irrigation purposes) along the considered sections. The head targets were divided into four groups, following the same spatial subdivision adopted for the irrigation wells, to ensure consistency in the representation of different parts of the study area. The baseflow targets were instead divided into three groups: 1) the calculated values from the northernmost portion of the Oglio River, corresponding to the stretch where the river behavior shifts from gaining to losing, 2) the calculated values from the remaining segments of the Oglio River, and 3) the calculated values from the Mella and Strone river stretches.

To address the large computational effort associated with the calibration process, model runs were performed in parallel on a high-performance computing cluster by using the HTCondor run management software (HTCondor Team, 2021).

7.2.6 Hypothetical scenarios

To better understand the effects of climate change on the groundwater budget, two scenarios were simulated, including: (1) prolonged drought conditions, and (2) changes in irrigation practices. To minimize computational time and optimize the model's use as a practical, management-oriented, and operational tool, the parameters of two out of the three simulated years were selectively modified. This approach was designed to reconstruct the conditions of the two scenarios, avoiding the need for additional stress periods in the simulations. The two simulated scenarios were then compared with the baseline condition.

In the first scenario (Scenario 1 (S1) - Prolonged Drought Simulation), a synthetic drought parameter setting was developed to represent prolonged drought conditions. Recent studies have demonstrated that climate change is expected to cause frequent and severe impacts on groundwater, with drought episodes that in Northern Italy have become stronger in both frequency and duration since 2001 (Baronetti et al., 2020; Montanari et al., 2023). In this trend, 2022 emerged as one of the most critical years, with record-low rainfall and high temperatures, causing a 1-year severe hydrological drought that impacted surface water availability and the agricultural systems (Montanari et al., 2023). The S1 scenario was defined by modifying the parameters of the final 24 simulated stress periods with respect to baseline conditions to reproduce the meteorological conditions observed during the 2022 drought, considered as an example of effective drought in the study area. Specifically, the inflow to the Oglio River, the abstraction rate of irrigation wells in the higher surface-water-fed irrigated plain, and the two main components of recharge (precipitation and irrigation return flow) have been modified accordingly to reflect the observed 2022 data, which are extended over 2 years. Details on parameter setting for defining S1 Scenario are reported in Sup. Info. Sect. S.7.3.

In the second scenario (Scenario 2 (S2) – Change in Irrigation Practices), all the areas subjected to surface-water irrigation were assumed to change to drip irrigation, to simulate the potential impacts of adopting more efficient irrigation techniques, in accordance with recommendations from the European Union (e.g., "The European Water Resilience Strategy (2024/2104(INI)" (European Parliament, 2025), and "Regulation (EU) No 1305/2013 – Support to rural development" (European Parliament & Council of the European Union, 2013)). This change in irrigation methods was simulated by reducing (with respect to baseline conditions) vertical recharge by irrigation return flow in the corresponding 17 recharge zones during the last 24 stress periods, while keeping all other model parameters and boundary conditions identical to those of the baseline simulation. Specifically, the return flow of drip irrigation was calculated by changing the infiltration coefficient (Sect. S.7.2.3) from 20–40% (used in the simulation of baseline conditions) to 10% (Munir et al., 2018; Nikolaou et al., 2020).

These scenarios were used to (1) quantify the effects on groundwater storage, (2) estimate the effects on lowland spring outflow, and (3) evaluate the possible change in the relation between the Oglio River and groundwater.

7.2.7 Groundwater budget calculation

To quantitatively evaluate the water exchanges among the different components involved in the model water budget, the MODFLOW's Hydrostratigraphic Unit (HSU) option was employed, as in other recent studies (Alberti et al., 2025; Sartirana et al., 2022). This feature allows for the calculation of the water budget within a specified area and time span. Particularly, a sub-accounting of annual and monthly inflows and outflows was computed separately for the higher surface-water-fed irrigated plain and the lower groundwater-fed irrigated plain. Therefore, the analysis of the water budget focuses on the two near field compartments and the exchange between them, with a comparative analysis of the baseline simulation and the two scenarios.

The results of the water budget are expressed as exchange flows between the system components (e.g., rivers, drains, and upstream and downstream areas' flows) and the aquifer, as well as changes in water storage in the study area. Following MODFLOW

convention, positive values indicate discharges toward the aquifer (i.e., inflow) while negative values represent discharges from the aquifer to a system's components (i.e., outflow). Change in storage occurs when inflows are not balanced with outflows, leading to a loss or gain of groundwater storage in the aquifer and consequently a change in groundwater head (Anderson et al., 2015)

It is noted that, in the water budget calculated by MODFLOW, positive groundwater storage variations indicate aquifer gain from storage (that is, storage loss) in response to declining groundwater heads, whereas negative groundwater storage variations indicate aquifer loss to storage (that is, storage gain) in response to rising groundwater heads. In general, the magnitude of storage loss or gain balances the gains to groundwater from sources and the losses from groundwater to sinks. Falling water levels prompt a release from storage to the aquifer system, which, even though represented by a positive number in groundwater budget terms, represents a storage deficit. Conversely, rising water levels prompt a gain in storage, which, however, is represented by a negative number in groundwater budget terms. Hereafter, the following notation will be used: positive storage variation will be noted as storage loss (i.e., declining groundwater levels), while negative storage variations will be noted as storage increase (i.e., rising groundwater levels).

7.3 Results

7.3.1 Baseline Model Calibration and Statistics

An acceptable agreement between the observed and simulated groundwater heads was obtained after parameter estimation, as supported by the statistical parameters reported in Table 7.1 and Figure 7.5. Specifically, the groundwater-level residuals ranged from −7.87 to +3.79 m, with a mean residual of 0.16 m and an absolute residual mean of 1.31 m. The simulated groundwater-level range was 106.04 m, and the root mean square error (RMSE) was 1.66 m, with 79 % of residuals being within ±2 m (Fig. 7.5f and Fig. 7.5g). As shown in Figure 7.5a, the distribution of groundwater-level residuals was overall random, with wells showing both positive and negative biases across different parts of

the model domain. The largest misfits were mainly located outside the main area of interest, across the Oglio River, and in the southernmost portion of it. The local deviations are attributable to site-specific behaviors of the system, which cannot be represented by a basin-scale model; however, the scaled RMSE (1.6%) falls within the accepted threshold of 10% used to evaluate a good model fit (Anderson et al., 2015; Feinstein et al., 2010). The simulated baseflow targets were lower than the estimated values used for calibration in 84% of cases, with an average of percent discrepancies of 53% between the estimated and the simulated values. This is mainly due to the higher uncertainty in the estimated values of the baseflow flow targets, given the system's high complexity, compared to the head targets, which are based on direct measurements.

The reconstructed water level surfaces of both shallow and deep aquifers (Fig. 7.5a) indicate a dominant NW-SE flow direction, consistent with previous regional and local reconstructions (Regione Lombardia & ENI Divisione AGIP, 2002; Rotiroti et al., 2019a). A local deviation to the regional flow direction is observed in the southern sector for the shallower aquifer (Group A) due to the gaining behavior of the rivers. In the higher plain, simulated groundwater levels exhibited strong seasonal variability, characterized by spring minima and summer or late-summer maxima (see Fig. 7.5b and Fig. 7.5c). In the lower plain, groundwater levels showed an increase in 2016, followed by a progressive decline that reached their minimum during the summer of 2017 (see Fig. 7.5d and Fig. 7.5e). Details on calibrated parameter values are reported in Sup. Info. Sect. S.7.4.

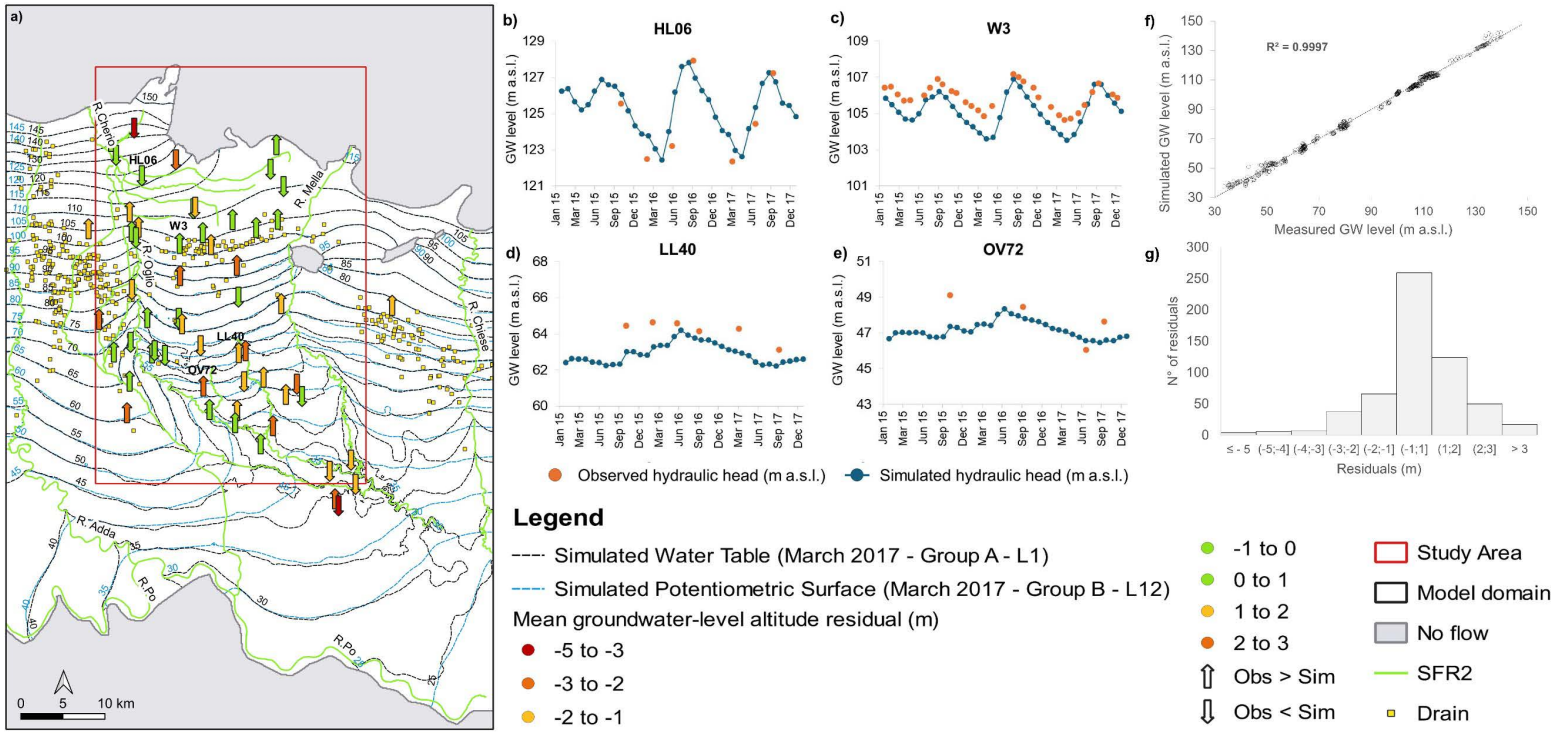

Figure 7.5 – a) *Groundwater potentiometric map at model scale, head target mean groundwater-level residuals (L = Layer);* ***b-e)*** *Observed (m a.s.l.) vs simulated (m a.s.l.) values for some selected targets;* ***f)*** *Linear regression of observed and simulated hydraulic heads;* ***g)*** *Frequency of hydraulic-head residuals.*

Table 7.1 *– Statistical analysis of head targets.*

Statistical parameter	Target Value
Minimum residual	-7.87
Maximum residual	3.79
Residuals Mean (ME)	0.16
Absolute residual mean (MAE)	1.31
RMSE	1.66
Range of observation	106.04
Scaled RMSE	1.6%
Number of Observations	571

In the higher surface-water-fed irrigated plain (~ 320 km^2), vertical recharge represented the larger component of the total inflow (36%), with a marked seasonal pattern characterized by summer peaks, with maxima occurring in July (2015 and 2016) or August (2017) (Fig. 7.6). As shown in Figure 7.6a and Figure 7.6c, the decomposition of vertical recharge into its two main components showed that irrigation return flow constituted the main component over effective precipitation during the summer months, ranging between 2.91×10^5 m^3/d in September 2016 to 2.37×10^6 m^3/d in July 2016. On an annual basis, irrigation return flow contributed to an average of 83% of the total recharge (ranging from 81% in 2016 (4.87×10^5 m^3/d) to 85% in 2017(5.54×10^5 m^3/d)); the remaining 17% corresponds to effective precipitation with 9.72×10^4 m^3/d. The monthly contribution of irrigation to total recharge exhibited a marked variability, ranging from 64% in May 2016 to 99% in July 2015 (Fig. 7.6a). These results agree with the analysis by Redaelli et al. (2025), which suggested that seasonal variability associated with surface-water-fed irrigation accounts for most of the total variability, with an average contribution of 84.7%, comparable to the average irrigation return flow contribution simulated in this work. These results are further supported by the isotopic analysis by Rotiroti et al. (2023). Specifically, the analysis of the monitoring points located in the higher surface-water-fed irrigated plain (i.e., HL11, HL13, and OV62, see Fig. S.7.1) closely matches the return flow contribution simulated by the calibrated model for the corresponding zones (i.e., zones 13 and 8), with an average of differences

equal to 8%. Outflow was mainly generated by discharge to the lower plain aquifer (31%) (Fig. 7.6c).

In the lower groundwater-fed plain (~ 460 km^2), the main inflow was the outflow from the higher plain, which accounted for 31% (Fig. 7.6d), with annual cumulative values equal to 4.95×10^5 m^3/d in 2015, 4.63×10^5 m^3/d in 2016, and 4.96×10^5 m^3/d in 2017. These results highlighted the role of the higher surface-water-fed irrigated plain as the major recharge source for the entire aquifer system, as also validated by previous studies (Éupolis Lombardia, 2015; Rotiroti et al., 2023).

Vertical recharge from effective precipitation represented the second most significant component of the total inflows (28%). The highest monthly recharge was recorded in May 2016 (2.18×10^6 m^3/d) (Fig. 7.6b). On an annual basis, the cumulative recharge in 2016 (6.45×10^5 m^3/d) was 36% higher than in 2015 and 63% higher than in 2017, as 2016 was a wetter year with above-mean precipitation. The main outflow was generated by gaining rivers (39%) (Fig. 7.6d).

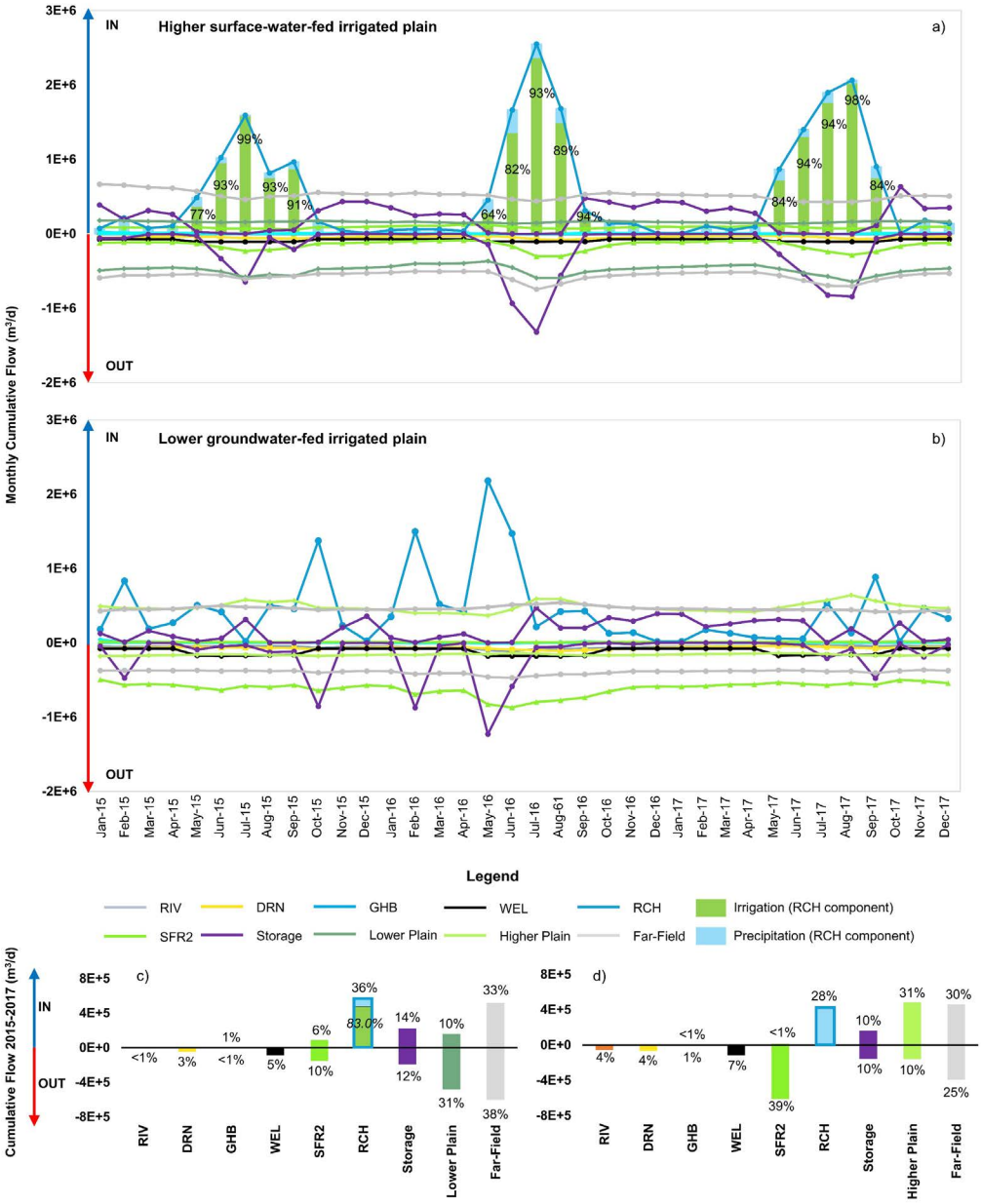

Figure 7.6 *– **(a-b)** Monthly and **(c-d)** annual cumulative model mass balance. **a)** and **c)** refer to the higher surface-water-fed irrigated plain, **b)** and **d)** refer to the lower groundwater-fed irrigated plain. The color coding for the boundary conditions is the same as in Fig. 7.4. Positive and negative values indicate, respectively, inflows (blue arrow) and outflows (red arrow) from*

the considered element to the groundwater. For instance, a positive net storage variation indicates a loss of storage, corresponding to a decrease in groundwater level.

The monthly storage variation of the higher surface-water-fed irrigated plain followed the seasonal recharge dynamics with increased storage during the irrigation periods, reflecting the summer increase in groundwater levels (Fig. 7.7a). On an annual basis, a storage loss occurred in 2015 (8.94×10^4 m^3/d) and in 2017 (1.85×10^4 m^3/d), indicative of overall falling water levels, whereas in 2016 the storage increased (-1.36×10^4 m^3/d) (see Fig. S.7.4 in Sup. Info. Sect. S.7.5). The annual storage loss in 2015 and 2017 reflects the reduced precipitation and the low surface water availability that characterized those years. However, the increased irrigation inputs in 2017 partly compensated for this deficit. On the contrary, in the lower groundwater-fed irrigated plain, no evident seasonal trend was identified. Here, the storage volume increased in 2015 (-3.46×10^4 m^3/d) and in 2016 (-5.62×10^4 m^3/d), indicative of net rising level, whereas 2017 led to a storage loss (1.06×10^5 m^3/d) (Fig. S.7.4b).

Simulated discharges of the lowland springs exhibited a marked seasonal variability, with maximum values during the periods of highest irrigation return flow (Fig. 7.8). Specifically, monthly discharge peaks were observed in October 2015 (-1.39×10^5 m^3/d), in August 2016 (-1.89×10^5 m^3/d), and in September 2017 (-1.42×10^5 m^3/d) (Fig. 7.8b). In contrast, the minimum discharges were consistently observed in spring with values of -9.55×10^4 m^3/d in May 2015, -8.88×10^4 m^3/d in April 2016, and -7.12×10^4 m^3/d in May 2017, reflecting the reduced recharge during winter. On an annual scale, the maximum cumulative outflow occurred in 2016 (-1.28×10^5 m^3/d), which was 9% higher than in 2015 and 22% higher than in 2017 (Fig. 7.8b).

The net monthly groundwater/Oglio River flow exchanges showed distinct patterns along the river course. In the northernmost stretch (segments 1–10), the model indicated a fully losing behavior of the river, with an inflow to the aquifer ranging between 6.89×10^3 m^3/d in March 2017 and 9.48×10^3 m^3/d in June 2016, and a three-year mean of 8.01×10^3 m^3/d (Fig. 7.8c). In the central stretch (segments 11–21), a seasonal variability was observed: the river shifted to gaining conditions in all three simulated years between

June and September/October, with outflow from the aquifer ranging between -9.04×10^3 in June 2016 and -1.17×10^5 m³/d in July and August 2016 (Fig. 7.8d). During the remaining months, the river was predominantly losing, with a maximum inflow into the aquifer of 6.28×10^4 m³/d in April 2016. In the southern stretch (segments 22–29), the Oglio River consistently behaved as gaining during all stress periods, with fluxes ranging from -6.50×10^5 m³/d in January 2015 to -1.08×10^6 m³/d in July 2016 (Fig. 7.8e). The simulated groundwater/surface-water exchanges along the Oglio River are in line with previous studies (Bartoli et al., 2012; Delconte et al., 2014; Rotiroti et al., 2019a).

7.3.2 Scenarios

7.3.2.1 Scenario S1 – Prolonged Drought

Results of the synthetic 2-year drought S1 scenario, based on 2022 data, showed that in the higher surface-water-fed irrigated plain, the storage increase of the baseline simulation turned into a storage loss in the first year of drought (Y1) (9.32×10^4 m^3/d), with a relative change of –784% (Fig S.7.4). The second year of drought (Y2) yielded to a further storage loss, equivalent to a 78% increment compared to the baseline simulation (3.29×10^4 m^3/d) (Fig. S.7.4a). On a monthly scale, during the irrigation period storage decreased by 58% in Y1 and by 50% in Y2, with the most significant changes occurring in May, when storage variation switched from negative to positive values in both simulated drought years (Fig. 7.7a). In the lower groundwater-fed irrigated plain, in Y1, the storage increase of the baseline simulation turned into a storage loss (8.40×10^4 m^3/d) with a relative change of –249%, while in Y2, the storage loss (7.89×10^4 m^3/d) was 26% lower compared to the baseline simulation (Fig. S.7.4b).

In the higher plain, simulated groundwater levels exhibited slight seasonal variability, with consistently reduced summer peaks (Fig. 7.7a), while in the lower plain, Y1 showed the absence of the late-spring rise (May–June) evident in 2016 under baseline conditions (Fig. 7.7b).

Simulated lowland spring discharge showed a slight dampened seasonal variability, with a maximum during the irrigation season. During simulated drought years, the maxima

occurred in August of Y1 (-9.71×10^4 m^3/d) and in September of Y2 (-5.58×10^4 m^3/d), representing respectively a 49% and a 61% reduction compared to the same months in the baseline simulation. Seasonal minima occurred in December of Y1 (-6.36×10^4 m^3/d) and in June of Y2 (-4.10×10^4 m^3/d). Overall, lowland spring discharge decreased by 36% in Y1 (-8.12×10^4 m^3/d) and by 51% in Y2 relative to the baseline (-4.91×10^4 m^3/d) (Fig. 7.8b).

The groundwater-Oglio River exchanges showed spatial patterns comparable to the baseline but with notable changes in flux magnitude. In the northernmost stretch (segments 1–10), the river was losing, with an inflow to the aquifer ranging from 5.53×10^3 m^3/d in August of Y1 (-36% relative to the same month of the baseline simulation), and 8.20×10^3 m^3/d in June of the same year (-14% relative to the same month of the baseline simulation) (Fig. 7.8c). The annual inflows to the aquifer decreased by 18% and 15% in Y1 and Y2, respectively. In the central stretch (segments 11–21), a seasonal pattern was evident with gaining behavior simulated in the summer months (July-September of Y1, and June-September of Y2). The outflow from the aquifer ranged from -5.56×10^2 m^3/d (June of Y2) to -4.05×10^4 m^3/d (August of Y1) (Fig. 7.8d). In the remaining months, losing conditions prevailed, with a maximum inflow to the aquifer of 7.45×10^4 m^3/d simulated in March of Y2. On an annual scale, cumulative exchanges shift from gaining to losing, with relative changes of -477% and -450% over the baseline simulation in Y1 and Y2, respectively. In the southern stretch (segments 22–29), the Oglio river consistently showed a gaining behavior, with outflows from the aquifer ranging from -5.83×10^5 m^3/d (October of Y2) to -8.54×10^5 m^3/d (August of Y1) (Fig. 7.8e). The annual simulated outflow from the aquifer decreased by 14% and 16% in Y1 and Y2, respectively, compared to baseline conditions.

Figure 7.7 *– Monthly storage variations and groundwater level trend for the* ***a)*** *higher surface-water-fed irrigated plain, and the* ***b)*** *lower groundwater-fed irrigated plain into the 36 monthly stress periods. Y1 and Y2 refer to the first and the second year of the two scenarios, S1 (yellow) and S2 (orange). Baseline (green) refers to the 2015-2017 simulation. Positive storage variation indicates a loss of storage, corresponding to a decrease in groundwater levels.*

7.3.2.2 Scenario S2 – Changes in irrigation practices

Results of scenario S2, with a change from surface to drip irrigation, showed that in the higher surface-water-fed irrigated plain, the annual storage increase of the baseline simulation turned into a storage loss (1.33×10^5 m^3/d) in the first year of using drip irrigation (Y1) correlated to falling water levels, with a relative change of -1080% compared to the baseline simulation. In the second year of using drip irrigation (Y2), the storage loss (7.81×10^4 m^3/d) increased by 323% compared to the baseline simulation (Fig. S.7.4a). On a monthly basis, only June of Y1, and September and November of Y2 showed a slight increase in storage (Fig. 7.7a). Overall, storage increase observed in the baseline simulation during the irrigation period, turned into a storage loss with a relative change of -109% in Y1 and of -112% in Y2. In the lower groundwater-fed irrigated plain,

Y1 led to a storage increase (-2.18×10^4 m^3/d), but a reduction of 61% relative to the baseline simulation was registered. In Y2, the storage decreases (1.42×10^5 m^3/d) by 34% compared to the baseline simulation (Fig. S.7.4b). In the higher plain, simulated groundwater levels showed the absence of the summer rise observed under baseline conditions, instead exhibiting a progressively declining trend starting from Y1 (Fig. 7.7a). In contrast, the simulated groundwater levels in the lower plain showed no significant deviations from the baseline trend (Fig. 7.7b).

Simulated lowland spring discharge showed a maximum value occurring in June of Y1 (-1.12×10^5 m^3/d), representing a 41% reduction compared to the baseline maximum of August, followed by a decreasing trend that lasted until September of Y2. During this month, a slight increase was registered, reaching the maximum of Y2 (-4.24×10^4 m^3/d), corresponding to a 70% reduction compared to the baseline simulation maximum. Overall, total lowland spring discharge decreased by 29% in Y1 (-9.08×10^4 m^3/d) and by 54% in Y2 (-4.60×10^4 m^3/d) relative to the baseline simulation (Fig. 7.8b).

The groundwater-Oglio River exchanges were further evaluated under the change in irrigation practice scenario. Specifically, in the northern stretch (segments 1–10), the river showed a trend identical to the baseline simulation during both simulated years, showing a consistently losing behavior in the higher plain (Fig. 7.8c). In the central stretch (segments 11–21), seasonal shifts from losing to gaining behavior occurred only during Y1, with gaining conditions between July and August. The outflow from the aquifer ranged from -5.87×10^3 m^3/d to -1.73×10^4 m^3/d during these months, while in all the other months of scenario S2, the river was constantly losing (Fig. 7.8d). Annual cumulative exchanges shifted from negative to positive in both S2 scenario years, with relative changes of -1125% and -896% in Y1 and Y2, respectively, compared to the baseline simulation. In the southern stretch (segments 22–29), the river behaved as gaining throughout the simulation, with outflows from the aquifer ranging between -5.79×10^5 m^3/d (October of Y2) and -1.00×10^6 m^3/d (June of Y1) (Fig. 7.8e). The cumulative annual outflows from the aquifer decreased by 6% and 12% in the two years of scenario S2 compared to the baseline.

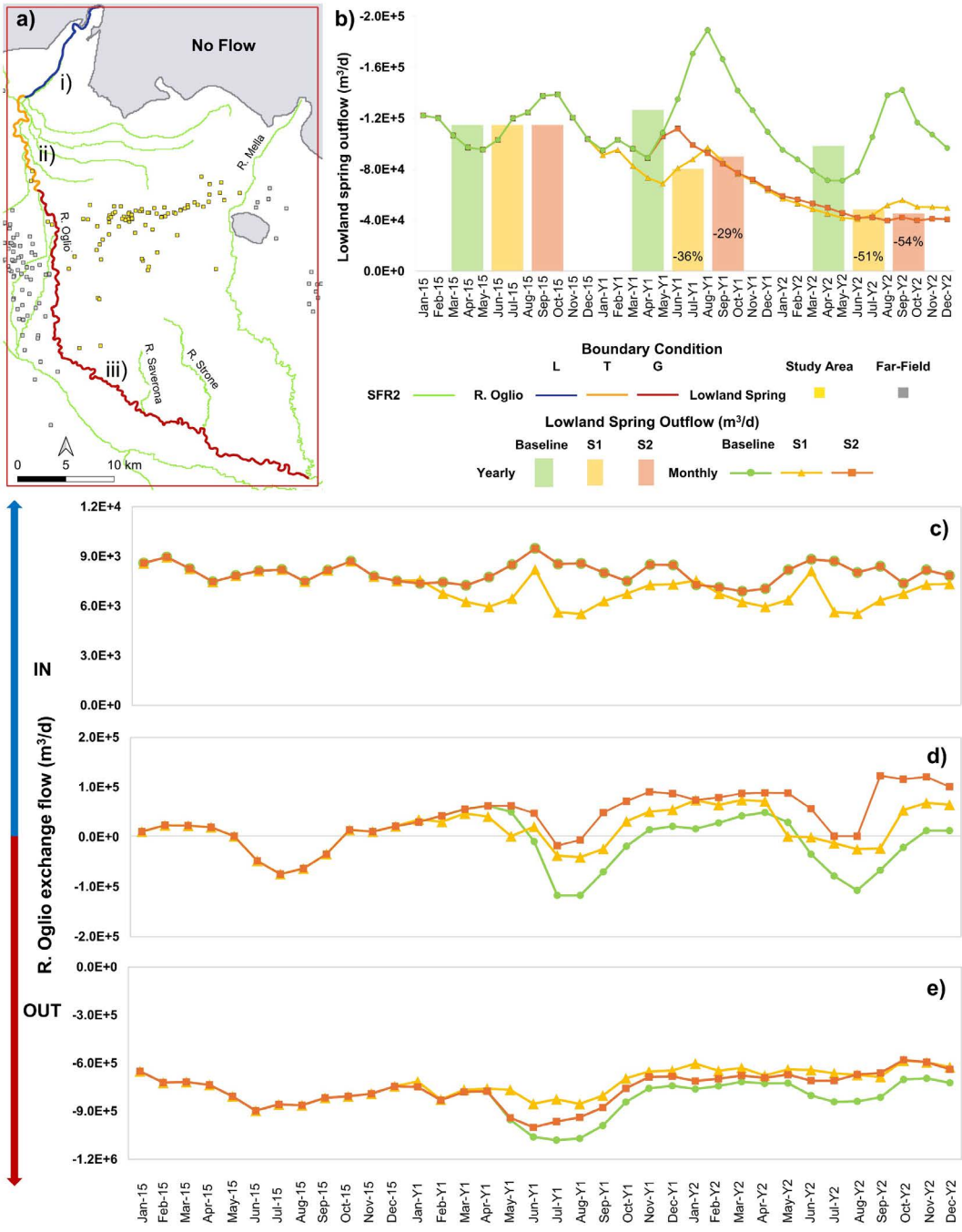

Figure 7.8 – a) *Map with the Oglio River divided into i) northern (blue), ii) central (orange), and iii) southern (red) stretches. L stands for Losing, T stands for Transition, and G stands for*

Gaining stretch; ***b)*** *Monthly (lines) and annual (bars) lowland spring discharge. The percentages refer to the annual outflow reduction in Y1 and Y2 of the two simulations S1 (yellow) and S2(orange) compared to the baseline simulation (green, 2015-2017). Y1 and Y2 refer to the first and the second year of the S1 and S2 scenarios;* ***c)****,* ***d)****, and* ***e)*** *net flow exchanges between the three Oglio river stretches (respectively stretches i, ii, and iii) and the aquifer system. IN refers to the inflow into the aquifer (blue arrow), whereas OUT refers to the outflow from the aquifer (red arrow).*

7.4 Discussion

7.4.1 A prolonged drought can dramatically reduce both groundwater storage and springs discharge

The S1 Scenario, based on conditions observed in 2022 but extended over a two-year period, revealed a strong sensitivity of the aquifer system to changes in climatic conditions combined with a decreased surface-water availability for irrigation, as evidenced by a pronounced attenuation of the typical seasonal patterns of the main water budget components observed under baseline conditions. The results highlight that prolonged drought conditions not only reduce groundwater availability but also alter the temporal dynamics of recharge, storage, and discharge processes.

On an annual scale, the cumulative storage variation dynamics exhibited similar patterns in both the higher surface-water-fed irrigated plain and the lower groundwater-fed irrigated plain (Fig. S.7.4). In the higher plain, the simulated loss in groundwater storage recorded during the first year, Y1, is primarily due to the reduction in summer irrigation return flow, which, when summed with the change in total precipitation, resulted in a strong reduction of the recharge and, consequently, in a reduction in groundwater accumulation during this season. Although 2017 had already been a critical year with below-average precipitation, the drought scenario conditions, which extended 2022 1-year drought conditions, led to a higher annual storage loss in the second year, Y2, compared to the baseline simulation, highlighting the greater stress on the system under a two-year drought scenario. On a monthly scale, the effect of the summer storage

reduction is even more evident, reflecting the system's inability to sustain the seasonal groundwater rise observed in the baseline simulation (Fig. 7.7a).

In the lower plain, Y1 resulted in a significant storage loss and decreased groundwater heads, highlighting the effect of the reduced precipitation, the reduced inflow from the higher surface-water-fed irrigated plain, and effects of increased pumping. Consequently, groundwater level trends showed an evident reduction in the 2016 groundwater level rise detected in the baseline simulation (Fig. 7.7b).

The two-year drought led to a significant reduction in lowland spring discharge, resulting in an annual discharge loss of 4.65×10^4 m^3/d (-36%) in Y1 and 5.01×10^4 m^3/d (-51%) in Y2, compared to the baseline simulation. The less pronounced seasonal trend, marked by reduced summer peaks, highlights their sensitivity and strong connection to the recharge from the higher surface-water irrigated plain and the specific irrigation methods used in the study area.

The groundwater-Oglio River exchanges maintained the same spatial pattern as in the baseline simulation, but the flow magnitudes changed considerably. In the northern stretch (segments 1-10), the inflow to the aquifer during the two drought years decreased by 2.62×10^3 m^3/d (-16%) compared to the baseline (Fig. 7.8c), while in the southern stretch (segments 22-29), the outflows from the aquifer to the river decreased by 2.42×10^5 m^3/d (-15%) compared to the total drained water in the baseline simulation (Fig. 7.8e). The most evident change was detected in the central stretch of the Oglio River (segments 11-21), where the magnitude of the outflow from the aquifer during the irrigation period decreased drastically (Fig. 7.8d). This decrease indicates that the transition zone between losing and gaining behavior shifted towards the south, as a consequence of the lowering of the piezometric levels that moved the boundary between these behaviors further downstream.

7.4.2 A change to drip irrigation can disrupt the typical aquifer dynamics

The S2 Scenario has further elucidated a central role of surface-water irrigation techniques. In the second scenario, the simulated transition to drip irrigation led to a

dramatic change in system dynamics, which was particularly evident in the higher surface water-fed irrigated plain. In contrast to the S1 scenario, the impacts are entirely controlled by the severe reduction in recharge derived from irrigation return flow.

In the higher surface-water-fed irrigated plain, the simulated dynamics further highlight the sensitivity of storage in highly managed basin to irrigation return flows. Although, as for the S1 scenario, a loss in groundwater storage was evident in both simulated years (Fig. S.7.4). The monthly analysis highlighted the complete loss of the characteristic seasonal dynamic observed in the baseline simulation. On a monthly scale, indeed, almost all months showed a persistent storage loss even during the irrigation season. This drastic trend change was confirmed by the simulated groundwater heads, which showed a complete absence of summer rises during both S2 years scenarios, replaced by a continuous decreasing trend (Fig. 7.7a).

In the lower groundwater-fed plain, the annual storage variation exhibited a general behavior comparable to that observed in the baseline simulation (Fig. S.7.4). Despite the observed changes, the simulated groundwater heads in this area did not show significant deviation from the baseline simulated trend (Fig. 7.7b). This suggests that in the lower plain, the effect of changed irrigation practices, and the consequent reduction of the total inflow from the higher plain of about -14% in the two simulated years, is not detectable within a two-year time frame, indicating a higher resilience of this compartment compared to the higher plain, if the precipitation patterns and the other components of the groundwater budget (e.g., groundwater abstraction) remain unchanged. However, it is unlikely a technology shift to more efficient irrigation would be reversed after two years, thus our results are best thought of as a reflection of the transition of the system more than the final endpoint.

The reduction of lowland spring discharge became even more pronounced under the S2 drip irrigation scenario, compared to the S1 scenario, further highlighting the critical dependence of the spring system on the irrigation return flow. The typical seasonal trend observed in the baseline simulation disappeared completely, substituted by a steady, progressive decrease throughout the two simulated years, resulting in an annual

discharge loss of 3.68×10^4 m^3/d (-29%) in the Y1 scenario and 5.32×10^4 m^3/d (-54%) in the Y2 scenario, compared to the baseline simulation (Fig. 7.8b).

The groundwater-Oglio River exchanges further emphasized the impacts of reduced return flow irrigation recharge. The S2 simulation indicated that the Oglio River maintained a predominantly losing behavior in the northern stretch (segments 1–10), without deviations from the baseline simulation (Fig. 7.8c), and a consistently gaining behavior in the southern stretch (segments 22–29), where the outflows from the aquifer decreased by 1.44×10^5 m^3/d (-9%) in the two simulated years compared to the total drained water in the baseline simulation (Fig. 7.8e). In the central stretch (segments 11–21), the S2 scenario induced an almost complete suppression of the seasonal alternation between gaining and losing behavior (Fig. 7.8d), indicating an even more marked shift towards the south of the transition zone compared to the S1 scenario, driven by the lowering of the groundwater levels. Such results are expected in systems where irrigation return flow constitutes a large source of aquifer recharge.

7.4.3 Meteorological droughts vs. irrigation management: which drives greater disruption to the aquifer system?

The comparison of the baseline conditions with the results of the two modeled scenarios identifies the drip irrigation Scenario S2 as the worst-case condition for the study area in the two simulated years, with major effects on the higher plain aquifer system, lowland springs, and rivers. Under 2-year drought conditions (S1), the primary effect is the attenuation of the typical seasonal dynamics that emerged in the simulated trend of all the main water budget components, which is still preserved thanks to the irrigation return flow. On the contrary, the second scenario (S2) induced a systematic disruption of typical temporal and spatial dynamics, especially in the higher surface-water-fed irrigated plain. Quantitatively, these results are even more pronounced when examining the storage variation across the entire study area. The first scenario, in fact, induced a storage loss with a relative change of -354% in Y1 and storage loss reduction of 10% in Y2, for a total loss in groundwater storage of 2.34×10^5 m^3/d during the two years, whereas the second scenario induced a storage loss with a relative change of -260% in Y1 and an

increased storage loss of 70% in Y2, with a larger total loss in groundwater storage of 2.77×10^5 m^3/d during the two years. Groundwater is the primary source of drinking water in several countries worldwide, including Italy. Therefore, assuming an average per-capita drinking water use of 0.272 m^3/person*d (in Lombardy region, (Polis Lombardia, 2020)), the storage deficit induced in the two simulations corresponds to the annual water demand of approximately 864,107 people, considering the S1 scenario, and of approximately 1,023,314 people, considering the S2 scenario. The European Union and local authorities strongly support a change in agricultural practices aimed at reducing the impact on surface-water resources, particularly during the summer months when the surface-water system is under increasing stress (Fabbri et al., 2016; Nikolaou et al., 2020). These policies promote surface water conservation and the resilience of agricultural systems to climate change. However, results clearly highlight that in a context where irrigation return flow constitutes a significant percentage of recharge, a large-scale shift in irrigation methods towards more efficient practices may disrupt the system's equilibrium. Furthermore, results show that such changes affect not only groundwater availability with direct socioeconomic implications but also have broader impacts on interconnected surface water bodies and springs, which provide valuable ecosystem services.

These results apply to our highly irrigation-dominated area (e.g., here, irrigation return flow is over 80% of aquifer recharge), and suggest that, in similar settings, climate change adaptation measures can have stronger effects on groundwater availability than the direct impacts of climate change itself, with crucial implications also for surface water bodies and groundwater-dependent ecosystems. Even widely implemented and popular options (e.g., drip irrigation) may be ineffective if they are not tailored to the specific hydrological and hydrogeological context. This highlights the importance of carefully selecting context-specific adaptation measures, which require targeted research and improved communication between academia and policymakers to ensure sustainable water resource management.

Therefore, if such changes were to be introduced, a holistic view of the hydrologic system is needed. Sustainable groundwater management strategies that encompass the full range of groundwater inflows and outflows will be essential to maintain the system's dynamics and protect groundwater-dependent ecosystems such as rivers and lowland springs. In particular, managed aquifer recharge (MAR) techniques (e.g., surface spreading, subsurface techniques, induced recharge and aquifer modification techniques)), if defined explicitly on the hydrogeological condition of the area, could play a crucial role in restoring natural replenishment processes and ensuring the long-term availability of water resources (Hiscock et al., 2024; Sufyan et al., 2024). These findings further highlight the need for integrated surface water and groundwater management to address the combined direct and indirect effects of climate and human stressors on these complex systems.

7.4.4 Limitations and future improvements

Groundwater is a key part of the climate system, but many potential impacts of climate change are still largely unknown due to the complexity of the systems involved, characterized by multiple interactions and different feedback loops (Amanambu et al., 2020; Davamani et al., 2024). The future impact of climate change on the groundwater system is commonly assessed using General Circulation Models (GCMs) (Zabihi et al., 2025). However, GCMs are the largest sources of uncertainty in hydrological predictions, followed by the downscaling method, the selection of the emission scenario, and the choice of the hydrological model structure or parameterization (Mustafa et al., 2019; Raju and Kumar, 2020; Zabihi et al., 2025). Moreover, irrigation practices and water management in regions characterized by extensive agricultural activity, such as the Oglio river basin, can represent a major driver in the dynamics of aquifers (Van der Gun, 2022). The aim of this work was primarily to assess which factor, meteorological variables or water management practices, is the major driver of possible future aquifer depletion in cases where human-derived mechanisms primarily control the system process, while the two scenarios are not meant to be actual predictions. In this context, working with short-term synthetic scenarios can provide a quick and effective way to

assess the main processes governing the water balance and to identify the system's vulnerabilities.

This approach helped capture the processes driving large-scale system behavior and can be of great practical value. The proposed methodologies led to an in-depth understanding of the system and its interconnections, highlighting the system's responses to changes in its main drivers. The application of two hypothetical scenarios (meteorological drought and changes in irrigation practices) enabled linking the system's great vulnerability to a probable change in irrigation practices and its impact on the surface water bodies connected to the aquifer system. Based on this new knowledge, future developments will integrate scenario analyses by coupling the groundwater numerical model with data derived from GCMs nested with dynamically downscaled and bias-corrected Regional Climate Models (RCMs) driven by different carbon dioxide emission scenarios (e.g., Representative Concentration Pathways 4.5 and 8.5). This approach will allow a better assessment of system responses to both direct and indirect climatic and socio-economic drivers as a direct human response to change in climatic conditions, providing policy-relevant insights for water-resources management.

The two scenarios analyzed in this study are not intended to represent a realistic forecast of future system evolution, but rather conceptual experiments designed to test the system sensitivity and to explore the effects of specific stresses on groundwater dynamics in a complex environment. Specifically, the 2-year drought scenario (S1), based on the repetition of a single extreme, does not represent a physically realistic multi-year drought with persistence and recovery dynamics; rather, it represents a synthetic-stress case. In this scenario, inflows from the Alpine area were kept unchanged. The water exchanges between the Alpine sector and the aquifer system in the plain area are still poorly constrained, and no quantitative estimates of these inflows are currently available, either under baseline conditions or during drought periods. Modifying these boundary conditions without a quantitative basis would have introduced additional uncertainty into the simulations, altering the interpretation of scenario results. For this reason, the scenario design focuses on changes in vertical recharge (including both precipitation and

irrigation return flow), variations in irrigation well abstraction rates, and changes in inflow to the Oglio River. Although this scenario is not intended to reproduce the 2022 conditions, focusing on parameter changes relative to realistic values enabled assessment of the simulated system's response to the combined effects of these variations. Specifically, the choice of the 2022 drought as a reference reflects the use of an observed and well-documented event to evaluate the system’s response to conditions that actually occurred and are widely recognized, thereby providing policy-relevant insights for water-resources management

Changes in irrigation practices scenario (S2) assumes an instantaneous and complete shift from surface to drip irrigation over the entire irrigated area, which is not intended as a plausible management or policy pathway but represents a theoretical stress test (a worst-case sensitivity analysis) aimed at isolating the system response to the loss of irrigation return flow contribution. In this scenario, in fact, several physical and socio-hydrological processes are simplified or not included in the model, such as detailed vadose zone processes, changes in evapotranspiration associated with irrigation methods, and adaptive farmer behavior.

Future development will aim to extend the simulation timeframe beyond the two-year period (5-10 years) to characterize the long-term trajectory of the aquifer system under persistent stressors, considering both changes in irrigation practices and multi-decadal climate shifts. This would allow for a better evaluation of the cumulative stress effect on storage, lowland spring discharge, and groundwater surface water relation future dynamics, and to better assess the role of the contribution from the higher surface-water-fed irrigated plain in controlling groundwater dynamics in the lower plain. Long-term simulations would help to distinguish transient responses from persistent trends, as well as assess potential lagged effects that cannot be entirely captured in short-term analyses. These developments would provide a more comprehensive basis for evaluating the long-term vulnerability of groundwater under the combined pressures of climate change and management.

7.5 Conclusion

This work provides a quantitative assessment of the main components of the system's mass balance in a highly irrigation-dominated area, as well as of their potential variations associated with climate variability and changes in irrigation practices. Particularly, two scenarios were compared with the baseline modeled conditions to investigate the effects of prolonged droughts (S1 scenario) and of a shift from traditional irrigation methods toward more efficient techniques aimed at reducing irrigation return flow (S2 scenario). The modeling approach allowed for the quantification not only of changes in groundwater availability but also in the discharges of interconnected rivers and springs, allowing for a comprehensive assessment of the direct and human-mediated impacts of climate change on the whole system.

Our main findings are:

- the comparison between baseline conditions and the two scenarios highlights the central role of surface-water-irrigation return flow in maintaining the groundwater balance and the ecological functions of the groundwater-dependent system (e.g., lowland springs, baseflow to rivers) in intensively cultivated areas;
- a 2-year drought mainly leads to an attenuation of the recharge processes while preserving the overall dynamics and seasonal patterns.
- in contrast, the reduction in irrigation return flow induced by a shift toward more efficient irrigation techniques induces a drastic change in the system, especially in the higher surface-water-fed irrigated plain, resulting in the disappearance of the typical summer rise in groundwater, persistent loss in groundwater storage during the irrigation season, and a sharp decrease in spring outflows;
- reducing irrigation without alternative recharge mechanisms (e.g., managed aquifer recharge) could compromise the resilience of the aquifer system and lead to long-term alterations of groundwater–surface water interactions, particularly in the higher surface-water-irrigated plain, with stronger effects than a prolonged drought.

These results offer a practical decision-support framework for managers and stakeholders responsible for water resources, highlighting the importance of carefully assessing the effects of irrigation modernization on groundwater recharge. These findings also highlight the necessity of integrating irrigation practices into hydrological models for other agricultural intensive areas to better define future scenarios and provide decision makers with a methodology to design water management policy adequately.

CRediT authorship contribution statement: Agnese Redaelli: Data Curation, Formal analysis, Visualization, Investigation, Writing - Original Draft. **Tullia Bonomi**: Conceptualization, Supervision, Validation, Resources, Funding acquisition, Project administration, Writing - Review & Editing. **Davide Sartirana**: Conceptualization, Visualization, Writing - Review & Editing. **Gianfranco Sinatra**: Resources. **Daniel T. Feinstein**: Methodology, Formal Analysis, Writing - Review & Editing. **Randall J. Hunt**: Methodology, Formal Analysis, Writing - Review & Editing. **Marco Rotiroti**: Conceptualization, Supervision, Validation, Funding acquisition, Project administration, Writing - Review & Editing. **Chiara Zanotti**: Data Curation, Formal analysis, Visualization, Investigation, Methodology, Conceptualization, Supervision, Validation, Funding acquisition, Project administration, Writing - Original Draft.

Funding: This research was financially supported by Acque Bresciane S.r.l. SB, water supplier, through the research contract no. 2021-ECO-0019, and Fondazione Cariplo, grant 2014–1282.

Declaration of competing interest: The authors declare the following financial interests/personal relationships which may be considered as potential competing interests: Marco Rotiroti is Associate Editor of the Journal of Hydrology. If there are other authors, they declare that they have no known competing financial interests or personal relationships that could have appeared to influence the work reported in this paper.

Acknowledgments: We thank Sara Taviani, Gennaro Alberto Stefania, and Luca Toscani for their essential contributions to building the numerical model, and Dr. Letizia Fumagalli of the University of Milano-Bicocca for her valuable insights and scientific support. We also thank Prof. Barbara Leoni of the University of Milano-Bicocca for managing the project funded by Fondazione Cariplo, whose results supported the development of this work. We are grateful to Marco Faggioli (freelance researcher) for carrying out river discharge measurements, and to Eng. Massimo Buizza of the Consorzio dell'Oglio for supporting the study and providing valuable data and information. Finally, we thank all private owners for granting access to their wells.

References

Ajami, H., Evans, J.P., McCabe, M.F., Stisen, S., 2014. Technical note: Reducing the spin-up time of integrated surface water-groundwater models. Hydrol. Earth Syst. Sci. 18, 5169–5179. https://doi.org/10.5194/hess-18-5169-2014

Alberti, L., Mazzon, P., Colombo, L., Cantone, M., Antelmi, M., Marelli, F., Gattinoni, P., 2025. Enhancing Groundwater Resource Management in the Milan Urban Area Through a Robust Stratigraphic Framework and Numerical Modeling. Water (Switzerland) 17. https://doi.org/10.3390/w17020165

Amanambu, A.C., Obarein, O.A., Mossa, J., Li, L., Ayeni, S.S., Balogun, O., Oyebamiji, A., Ochege, F.U., 2020. Groundwater system and climate change: Present status and future considerations. J. Hydrol. 589, 125163. https://doi.org/10.1016/j.jhydrol.2020.125163

Anderson, M.P., Woessner, W.W., Hunt, R.J., 2015. Applied Groundwater Modeling. Elsevier. https://doi.org/10.1016/C2009-0-21563-7

ARPA Lombardia, 2019. Meteoclimatic Data Request Form. https://www.arpalombardia.it/temi-ambientali/meteo-e-clima/form-richiesta-dati/ (accessed 24 July 2025).

Atawneh, D. Al, Cartwright, N., Bertone, E., 2021. Climate change and its impact on the projected values of groundwater recharge: A review. J. Hydrol. 601, 126602. https://doi.org/10.1016/j.jhydrol.2021.126602

Baronetti, A., González-Hidalgo, J.C., Vicente-Serrano, S.M., Acquaotta, F., Fratianni, S., 2020. A weekly spatio-temporal distribution of drought events over the Po Plain (North Italy) in the last five decades. Int. J. Climatol. 40, 4463–4476. https://doi.org/10.1002/joc.6467

Bartoli, M., Racchetti, E., Delconte, C.A., Sacchi, E., Soana, E., Laini, A., Longhi, D., Viaroli, P., 2012. Nitrogen balance and fate in a heavily impacted watershed

(Oglio River, Northern Italy): In quest of the missing sources and sinks. Biogeosciences 9, 361–373. https://doi.org/10.5194/bg-9-361-2012

Bonomi, T., 2009. Database development and 3D modeling of textural variations in heterogeneous, unconsolidated aquifer media: Application to the Milan plain. Comput. Geosci. 35, 134–145. https://doi.org/10.1016/j.cageo.2007.09.006

Bonomi, T., Fumagalli, L., Rotiroti, M., Bellani, A., Cavallin, A., 2014. The hydrogeological well database TANGRAM©: a tool for data processing to support groundwater assessment. Acque Sotter. - Ital. J. Groundw. 3, 35–45. https://doi.org/10.7343/AS-072-14-0098

Carlson, G., Massari, C., Rotiroti, M., Bonomi, T., Preziosi, E., Wilder, A., Whitaker, D., Girotto, M., 2025. Intensive irrigation buffers groundwater declines in key European breadbasket. Nat. Water 3, 683–692. https://doi.org/10.1038/s44221-025-00445-4

Caschetto, M., Sacchi, E., Pinti, D.L., Riparbelli, C., Bruno, S., Zanotti, C., Bonomi, T., Rotiroti, M., 2025. Surface-water-irrigation return flow dominates groundwater recharge , groundwater age and nitrate dynamics in an alluvial basin aquifer. Water Res. 285, 124040. https://doi.org/10.1016/j.watres.2025.124040

Consorzio dell'Oglio, 2019. Daily Discharge Data. https://oglioconsorzio.it/dati-idrologici/dati-della-regolazione-del-lago-d-iseo/deflussi-giornalieri/ (accessed 10 July 2025).

Davamani, V., John, J.E., Poornachandhra, C., Gopalakrishnan, B., Arulmani, S., Parameswari, E., Santhosh, A., Srinivasulu, A., Lal, A., Naidu, R., 2024. A Critical Review of Climate Change Impacts on Groundwater Resources: A Focus on the Current Status, Future Possibilities, and Role of Simulation Models. Atmosphere (Basel). 15. https://doi.org/10.3390/atmos15010122

Davis, K.W., Putnam, L.D., 2013. Conceptual and Numerical Models of Groundwater Flow in the Ogallala Aquifer in Gregory and Tripp Counties, South Dakota, Water Years 1985–2009. U.S. Geol. Surv. 82. https://doi.org/10.3133/sir20135069

De Luca, D.A., Destefanis, E., Forno, M.G., Lasagna, M., Masciocco, L., 2014. The genesis and the hydrogeological features of the Turin Po Plain fontanili, typical lowland springs in Northern Italy. Bull. Eng. Geol. Environ. 73, 409–427. https://doi.org/10.1007/s10064-013-0527-y

Delconte, C.A., Sacchi, E., Racchetti, E., Bartoli, M., Mas-Pla, J., Re, V., 2014. Nitrogen inputs to a river course in a heavily impacted watershed: A combined hydrochemical and isotopic evaluation (Oglio River Basin, N Italy). Sci. Total Environ. 466–467, 924–938. https://doi.org/10.1016/j.scitotenv.2013.07.092

Denti, E., Lauzi, S., Sala, P., Scesi, L., 1988. Studio idrogeologico della pianura bresciana compresa tra i fiumi Oglio e Chiese.

Doherty, J., 2025. Calibration and Uncertainty Analysis for Complex Environmental Models. Second Edition, Watermark Numerical Computing. Brisbane, Australia.

Doherty, J., Hunt, R., 2010. Approaches to highly parameterized inversion: a guide to using PEST for groundwater-model calibration. U. S. Geol. Surv. Sci. Investig. Rep. 2010-5169 70.

Du, J., Laghari, Y., Wei, Y.C., Wu, L., He, A.L., Liu, G.Y., Yang, H.H., Guo, Z.Y., Leghari, S.J., 2024. Groundwater Depletion and Degradation in the North China Plain: Challenges and Mitigation Options. Water (Switzerland) 16. https://doi.org/10.3390/w16020354

Éupolis Lombardia, 2015. Progetto di accompagnamento a supporto del processo di revisione del Piano di Tutela delle Acque - Attività di progettazione, monitoraggio e studio relative ai corpi idrici sotterranei della Lombadia - Relazione di Sintesi "Accompanying project supporting the revision of the Water Protection Plan - Planning, monitoring and studying activities related to groundwater bodies in Lombardy Region - Summary Report". Milan.

European Parliament, 2025. Report on the European Water Resilience Strategy 2024/2104(INI), A10-0073/2025. European Parliament. https://www.europarl.europa.eu/doceo/document/TA-10-2025-0091_EN.html

(accessed 10 November 2025).

European Parliament and Council of the European Union, 2013. Regulation (EU) No 1305/2013 of 17 December 2013 on support for rural development by the European Agricultural Fund for Rural Development (EAFRD) and repealing Council Regulation (EC) No 1698/2005. Official Journal of the European Union, L 347 (20 December): 487–548. https://eur-lex.europa.eu/eli/reg/2013/1305/oj/eng (accessed 11 November 2025).

Fabbri, P., Piccinini, L., Marcolongo, E., Pola, M., Conchetto, E., Zangheri, P., 2016. Does a change of irrigation technique impact on groundwater resources? A case study in Northeastern Italy. Environ. Sci. Policy 63, 63–75. https://doi.org/10.1016/j.envsci.2016.05.009

Fabbri, P., Trevisani, S., 2005. A geostatistical simulation approach to a pollution case in Northeastern Italy. Math. Geol. 37, 569–586. https://doi.org/10.1007/s11004-005-7307-6

Faquseh, H., Grossi, G., 2023. The effect of climate change on groundwater resources availability: a case study in the city of Brescia, northern Italy. Sustain. Water Resour. Manag. 9, 1–15. https://doi.org/10.1007/s40899-023-00892-5

Faunt, C.C., 2009. Groundwater Availability of the Central Valley Aquifer, California: U.S. Geological Survey Professional paper 1766, 225 p. https://doi.org/10.3133/pp1766

Feinstein, D.T., Hunt, R.J., Reeves, H.W., 2010. Regional groundwater-flow model of the Lake Michigan Basin in support of Great Lakes Basin water availability and use studies, Scientific Investigations Report. https://doi.org/10.3133/sir20105109

Fetter, C.W., 1994. Applied Hydrogeology. Prentice-Hall, New York, 691pp.

Freeze, R.A., Cherry, J.A., 1979. Groundwater. Prentice-Hall, Englewood Cliffs, NJ, 604pp.

Garzanti, E., Vezzoli, G., Andò, S., 2011. Paleogeographic and paleodrainage changes

during Pleistocene glaciations (Po Plain, Northern Italy). Earth-Science Rev. 105, 25–48. https://doi.org/10.1016/j.earscirev.2010.11.004

Guo, H., Li, S., 2024. A Review of Drip Irrigation's Effect on Water, Carbon Fluxes, and Crop Growth in Farmland. Water (Switzerland) 16. https://doi.org/10.3390/w16152206

Hinegk, L., Adami, L., Zolezzi, G., Tubino, M., 2022. Implications of water resources management on the long-term regime of Lake Garda (Italy). J. Environ. Manage. 301, 113893. https://doi.org/10.1016/j.jenvman.2021.113893

Hiscock, K.M., Balashova, N., Cooper, R.J., Bradford, P., Patrick, J., Hullis, M., 2024. Developing managed aquifer recharge (MAR) to augment irrigation water resources in the sand and gravel (Crag) aquifer of coastal Suffolk, UK. J. Environ. Manage. 351, 119639. https://doi.org/10.1016/j.jenvman.2023.119639

Howard, J.K., Dooley, K., Brauman, K.A., Klausmeyer, K.R., Rohde, M.M., 2023. Ecosystem services produced by groundwater dependent ecosystems: a framework and case study in California. Front. Water 5. https://doi.org/10.3389/frwa.2023.1115416

HTCondor Team, 2021. HTCondor version 9.0 manual. Technical report. University of Wisconsin-Madison.

Hunt, R.J., Feinstein, D.T., 2012. MODFLOW-NWT: Robust Handling of Dry Cells Using a Newton Formulation of MODFLOW-2005. Ground Water 50, 659–663. https://doi.org/10.1111/j.1745-6584.2012.00976.x

Intergovernmental Panel on Climate Change (IPCC), 2023. Climate Change 2021 – The Physical Science Basis. Cambridge University Press. https://doi.org/10.1017/9781009157896

Jasechko, S., Birks, S.J., Gleeson, T., Wada, Y., Fawcett, P.J., Sharp, Z.D., McDonnell, J.J., Welker, J.M., 2014. The pronounced seasonality of global groundwater recharge. Water Resour. Res. 50, 8845–8867.

https://doi.org/10.1002/2014WR015809

Jin, X., Chen, M., Fan, Y., Yan, L., Wang, F., 2018. Effects of mulched drip irrigation on soil moisture and groundwater recharge in the Xiliao River Plain, China. Water (Switzerland) 10. https://doi.org/10.3390/w10121755

MacDonald, A.M., Bonsor, H.C., Ahmed, K.M., Burgess, W.G., Basharat, M., Calow, R.C., Dixit, A., Foster, S.S.D., Gopal, K., Lapworth, D.J., Lark, R.M., Moench, M., Mukherjee, A., Rao, M.S., Shamsudduha, M., Smith, L., Taylor, R.G., Tucker, J., Van Steenbergen, F., Yadav, S.K., 2016. Groundwater quality and depletion in the Indo-Gangetic Basin mapped from in situ observations. Nat. Geosci. 9, 762–766. https://doi.org/10.1038/ngeo2791

Markovich, K.H., Manning, A.H., Condon, L.E., McIntosh, J.C., 2019. Mountain-Block Recharge: A Review of Current Understanding. Water Resour. Res. https://doi.org/10.1029/2019WR025676

Masseroni, D., Gangi, F., Ghilardelli, F., Gallo, A., Kisekka, I., Gandolfi, C., 2024. Assessing the water conservation potential of optimized surface irrigation management in Northern Italy. Irrig. Sci. 42, 75–97. https://doi.org/10.1007/s00271-023-00876-5

Meixner, T., Manning, A.H., Stonestrom, D.A., Allen, D.M., Ajami, H., Blasch, K.W., Brookfield, A.E., Castro, C.L., Clark, J.F., Gochis, D.J., Flint, A.L., Neff, K.L., Niraula, R., Rodell, M., Scanlon, B.R., Singha, K., Walvoord, M.A., 2016. Implications of projected climate change for groundwater recharge in the western United States. J. Hydrol. 534, 124–138. https://doi.org/10.1016/J.JHYDROL.2015.12.027

Montanari, A., Nguyen, H., Rubinetti, S., Ceola, S., Galelli, S., Rubino, A., Zanchettin, D., 2023. Why the 2022 Po River drought is the worst in the past two centuries. Sci. Adv. 9, 1–8. https://doi.org/10.1126/sciadv.adg8304

Munir, M.S., Bajwa, I.S., Naeem, M.A., Ramzan, B., 2018. Design and implementation of an IoT system for smart energy consumption and smart irrigation in tunnel

farming. Energies 11. https://doi.org/10.3390/en11123427

Mustafa, S.M.T., Hasan, M.M., Saha, A.K., Rannu, R.P., Van Uytven, E., Willems, P., Huysmans, M., 2019. Multi-model approach to quantify groundwater-level prediction uncertainty using an ensemble of global climate models and multiple abstraction scenarios. Hydrol. Earth Syst. Sci. 23, 2279–2303. https://doi.org/10.5194/hess-23-2279-2019

Ndehedehe, C.E., Adeyeri, O.E., Onojeghuo, A.O., Ferreira, V.G., Kalu, I., Okwuashi, O., 2023. Understanding global groundwater-climate interactions. Sci. Total Environ. 904, 166571. https://doi.org/10.1016/j.scitotenv.2023.166571

Nikolaou, G., Neocleous, D., Christou, A., Kitta, E., Katsoulas, N., 2020. Implementing sustainable irrigation in water-scarce regions under the impact of climate change. Agronomy 10, 1–33. https://doi.org/10.3390/agronomy10081120

Niswonger, R.G., Panday, S., Ibaraki, M., 2011. MODFLOW-NWT, a Newton formulation for MODFLOW-2005. US Geological Survey Techniques and Methods, 6(A37), 44. https://doi.org/10.3133/tm6A37

Paradigm, 2009. Paradigm GOCAD 2009.1 User Guide. Houston, TX.

Perego, R., Bonomi, T., Fumagalli, M.L., Benastini, V., Aghi, F., Rotiroti, M., Cavallin, A., 2014. 3D reconstruction of the multi-layer aquifer in a Po Plain area. Rend. online della Soc. Geol. Ital. 30, 41–44. https://doi.org/10.3301/ROL.2014.09

Pool, S., Francés, F., Garcia-Prats, A., Pulido-Velazquez, M., Sanchis-Ibor, C., Schirmer, M., Yang, H., Jiménez-Martínez, J., 2021. From Flood to Drip Irrigation Under Climate Change: Impacts on Evapotranspiration and Groundwater Recharge in the Mediterranean Region of Valencia (Spain). Earth's Futur. 9, 1–20. https://doi.org/10.1029/2020EF001859

Polis Lombardia, 2020. Rapporto Lombardia 2019, I. ed. Angelo Guerini e Associati, Milano.

Raju, K.S., Kumar, D.N., 2020. Review of approaches for selection and ensembling of

GCMS. J. Water Clim. Chang. https://doi.org/10.2166/wcc.2020.128

Redaelli, A., Bonomi, T., Sartirana, D., Sinatra, G., Rotiroti, M., Zanotti, C., 2025. The dual role of irrigation in the groundwater budget under baseline conditions versus the 2022 drought: Lessons for future climate adaptation. J. Hydrol. 658, 133211. https://doi.org/10.1016/j.jhydrol.2025.133211

Regione Lombardia, 2007. Geoportal of the Lombardy Region, Italy. https://www.geoportale.regione.lombardia.it/en-GB/download-pacchetti?p_p_id=dwnpackageportlet_WAR_gptdownloadportlet&p_p_lifecycle=0&p_p_state=normal&p_p_mode=view&_dwnpackageportlet_WAR_gptdownloadportlet_metadataid=r_lombar%3A2318b9c5-f8f0-421f-97c0-6e4d912e2b93&_jsfBridgeRedirect=true. (accessed 10 May 2025).

Regione Lombardia, 2023. Geoportal of the Lombardy Region, Italy. https://www.geoportale.regione.lombardia.it/en-GB/metadati?p_p_id=detailSheetMetadata_WAR_gptmetadataportlet&p_p_lifecycle=0&p_p_state=normal&p_p_mode=view&_detailSheetMetadata_WAR_gptmetadataportlet_identifier=r_lombar%3A7cd05e9f-b693-4d7e-a8de-71b40b45f54e&_jsfBridgeRedirect=true. (accessed 4 June 2025).

Regione Lombardia, 2016. Programma di tutela e uso delle acque (PTUA 2016) “Programme for the protection and use of water.”

Regione Lombardia & ENI Divisione AGIP, 2002. Geologia Degli Acquiferi Padani Della Regione Lombardia. Cipriano Carcano e Andrea Piccin. S.EL.CA, Florence, Italy.

Rohde, M.M., Albano, C.M., Huggins, X., Klausmeyer, K.R., Morton, C., Sharman, A., Zaveri, E., Saito, L., Freed, Z., Howard, J.K., Job, N., Richter, H., Toderich, K., Rodella, A.S., Gleeson, T., Huntington, J., Chandanpurkar, H.A., Purdy, A.J., Famiglietti, J.S., Singer, M.B., Roberts, D.A., Caylor, K., Stella, J.C., 2024. Groundwater-dependent ecosystem map exposes global dryland protection needs. Nature 632, 101–107. https://doi.org/10.1038/s41586-024-07702-8

Rotiroti, M., Bonomi, T., Sacchi, E., McArthur, J.M., Stefania, G.A., Zanotti, C., Taviani, S., Patelli, M., Nava, V., Soler, V., Fumagalli, L., Leoni, B., 2019a. The effects of irrigation on groundwater quality and quantity in a human-modified hydro-system: The Oglio River basin, Po Plain, northern Italy. Sci. Total Environ. 672, 342–356. https://doi.org/10.1016/j.scitotenv.2019.03.427

Rotiroti, M., Sacchi, E., Caschetto, M., Zanotti, C., Fumagalli, L., Biasibetti, M., Bonomi, T., Leoni, B., 2023. Groundwater and surface water nitrate pollution in an intensively irrigated system: Sources, dynamics and adaptation to climate change. J. Hydrol. 623, 129868. https://doi.org/10.1016/j.jhydrol.2023.129868

Rotiroti, M., Zanotti, C., Fumagalli, L., Taviani, S., Stefania, G.A., Patellio, M., Soler, V., Sacchi, E., Leoni, B., 2019b. Multivariate statistical analysis supporting the hydrochemical characterization of groundwater and surface water: a case study in northern Italy. Rend. Online della Soc. Geol. Ital. 47, 90–96. https://doi.org/10.3301/ROL.2019.17

Saito, L., Byer, S., Munn, L., Badik, K., Provencher, L., McEvoy, D.J., Rohde, M.M., 2025. Strategies to Address Risks to Groundwater Dependent Ecosystems. Hydrol. Process. 39. https://doi.org/10.1002/hyp.70229

Sartirana, D., Zanotti, C., Rotiroti, M., De Amicis, M., Caschetto, M., Redaelli, A., Fumagalli, L., Bonomi, T., 2022. Quantifying Groundwater Infiltrations into Subway Lines and Underground Car Parks Using MODFLOW-USG. Water (Switzerland) 14. https://doi.org/10.3390/w14244130

Scanlon, B.R., Fakhreddine, S., Rateb, A., de Graaf, I., Famiglietti, J., Gleeson, T., Grafton, R.Q., Jobbagy, E., Kebede, S., Kolusu, S.R., Konikow, L.F., Long, D., Mekonnen, M., Schmied, H.M., Mukherjee, A., MacDonald, A., Reedy, R.C., Shamsudduha, M., Simmons, C.T., Sun, A., Taylor, R.G., Villholth, K.G., Vörösmarty, C.J., Zheng, C., 2023. Global water resources and the role of groundwater in a resilient water future. Nat. Rev. Earth Environ. 4, 87–101. https://doi.org/10.1038/s43017-022-00378-6

Seck, A., Welty, C., Maxwell, R.M., 2015. Spin-up behavior and effects of initial conditions for an integrated hydrologic model. Water Resour. Res. 51, 2188–2210. https://doi.org/10.1002/2014WR016371

Stefania, G.A., Rotiroti, M., Fumagalli, L., Simonetto, F., Capodaglio, P., Zanotti, C., Bonomi, T., 2018. Modeling groundwater/surface-water interactions in an Alpine valley (the Aosta Plain, NW Italy): the effect of groundwater abstraction on surface-water resources. Hydrogeol. J. 26, 147–162. https://doi.org/10.1007/s10040-017-1633-x

Stigter, T.Y., Miller, J., Chen, J., Re, V., 2023. Groundwater and climate change: threats and opportunities. Hydrogeol. J. 31, 7–10. https://doi.org/10.1007/s10040-022-02554-w

Sufyan, M., Martelli, G., Teatini, P., Cherubini, C., Goi, D., 2024. Managed Aquifer Recharge for Sustainable Groundwater Management: New Developments, Challenges, and Future Prospects. Water (Switzerland) 16, 1–28. https://doi.org/10.3390/w16223216

Taylor, R.G., Scanlon, B., Döll, P., Rodell, M., Van Beek, R., Wada, Y., Longuevergne, L., Leblanc, M., Famiglietti, J.S., Edmunds, M., Konikow, L., Green, T.R., Chen, J., Taniguchi, M., Bierkens, M.F.P., Macdonald, A., Fan, Y., Maxwell, R.M., Yechieli, Y., Gurdak, J.J., Allen, D.M., Shamsudduha, M., Hiscock, K., Yeh, P.J.F., Holman, I., Treidel, H., 2013. Ground water and climate change. Nat. Clim. Chang. https://doi.org/10.1038/nclimate1744

UNESCO, 2022. The United Nations World Water Development Report 2022: groundwater: making the invisible visible.

Van der Gun, J., 2022. Large Aquifer Systems Around the World, Large Aquifer Systems Around the World. https://doi.org/10.21083/978-1-77470-020-4

Vercesi, P.L., 1994. Aspetti quali-quantitativi delle risorse idriche sotterranee del bresciano. Nat. Brescia. Ann. Mus. Civ. Sc. Nat. Brescia 21–52.

Wu, W.Y., Lo, M.H., Wada, Y., Famiglietti, J.S., Reager, J.T., Yeh, P.J.F., Ducharne, A., Yang, Z.L., 2020. Divergent effects of climate change on future groundwater availability in key mid-latitude aquifers. Nat. Commun. 11. https://doi.org/10.1038/s41467-020-17581-y

Yang, X., Chen, Y., Pacenka, S., Gao, W., Zhang, M., Sui, P., Steenhuis, T.S., 2015. Recharge and groundwater use in the north china plain for six irrigated crops for an eleven year period. PLoS One 10, 1–17. https://doi.org/10.1371/journal.pone.0115269

Zabihi, O., Ahmadi, A., Haghighi, A.T., 2025. A framework for assessing uncertainties in drought projections under climate change: Insights from CMIP6 models. Sci. Total Environ. 982, 179679. https://doi.org/10.1016/j.scitotenv.2025.179679

Zanotti, C., Rotiroti, M., Caschetto, M., Redaelli, A., Bozza, S., Biasibetti, M., Mostarda, L., Fumagalli, L., Bonomi, T., 2022. A cost-effective method for assessing groundwater well vulnerability to anthropogenic and natural pollution in the framework of water safety plans. J. Hydrol. 613, 128473. https://doi.org/10.1016/j.jhydrol.2022.128473

Electronic Supplementary Material

Changes in irrigation practices may bankrupt aquifers faster than meteorological droughts: a numerical modeling approach

Agnese Redaelli[1,*], Tullia Bonomi[1], Davide Sartirana[1], Gianfranco Sinatra[2], Daniel T. Feinstein[3], Randall J. Hunt[4], Marco Rotiroti[1] and Chiara Zanotti[1]

[1]Department of Earth and Environmental Sciences, University of Milano-Bicocca, Piazza della Scienza 1, 20126, Milan, Italy.

[2]Acque Bresciane S.r.l. SB, Via 25 Aprile, 18, 25038 Rovato, BS, Italy.

[3]Department of Geoscience, University of Wisconsin-Milwaukee, Lapham Hall, R 3209 North Maryland Avenue, Milwaukee, WI 53211, USA.

[4]Department of Geoscience, University of Wisconsin-Madison, Lewis G. Weeks Hall, 1215 West Dayton Street, Madison, WI 53706-1692, USA.

*corresponding author: agnese.redaelli@unimib.it

Supporting Information

Content:

Number of pages: 18

Number of sections: 5

Number of figures: 4

Number of tables: 5

Number of references: 19

S.7.1 – Spatial distribution of measurement points

In this section, the spatial distribution of measurement points of groundwater heads (from 58 wells), river stages (from 21 sites), and river and irrigation canal discharges (from 17 locations) is reported in Figure S.7.1. Following the classification performed by Rotiroti et al. (2019) and Zanotti et al. (2022), all the wells are color-coded based on the type of tapped aquifer: Confined (red), Semiconfined (yellow), and Unconfined (cyan). For one well, this categorization was not available (grey). The list of stretches for which groundwater-river flow exchanges were calculated is provided in Table S.7.1.

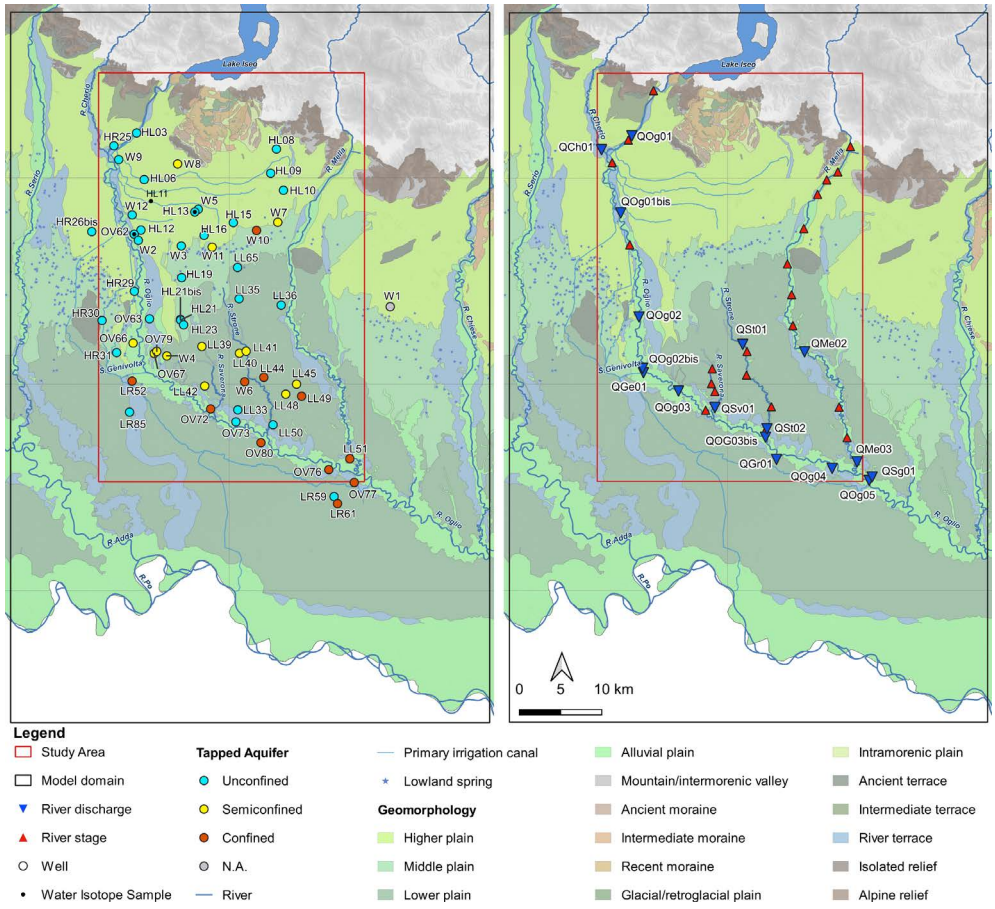

Figure S.7.1 *– Locations of measurement points for groundwater heads, river stages, and river discharges over the geomorphological map (Regione Lombardia, 2007).*

***Table S.7.1** – List of stretches for which groundwater-river flow exchanges were calculated.*

River	Stretch	Upstream site	Downstream site
Oglio	O1	QOg01	QOg02
	O2	QOg02	QOg02bis
	O3	QOg02	QOg03
	O4	QOg03	QOg03bis
	O5	QOg03	QOg04
	O6	QOg03bis	QOg04
Strone	S1	QSt01	QSt02
Mella	M1	QMe02	QMe03

References

Regione Lombardia, 2007. Geoportal of the Lombardy Region, Italy. https://www.geoportale.regione.lombardia.it/en-GB/download-pacchetti?p_p_id=dwnpackageportlet_WAR_gptdownloadportlet&p_p_lifecycle=0&p_p_state=normal&p_p_mode=view&_dwnpackageportlet_WAR_gptdownloadportlet_metadataid=r_lombar%3A2318b9c5-f8f0-421f-97c0-6e4d912e2b93&_jsfBridgeRedirect=true. (accessed 10 May 2025).

Rotiroti, M., Bonomi, T., Sacchi, E., McArthur, J.M., Stefania, G.A., Zanotti, C., Taviani, S., Patelli, M., Nava, V., Soler, V., Fumagalli, L., Leoni, B., 2019. The effects of irrigation on groundwater quality and quantity in a human-modified hydro-system: The Oglio River basin, Po Plain, northern Italy. Sci. Total Environ. 672, 342–356. https://doi.org/10.1016/j.scitotenv.2019.03.427

Zanotti, C., Rotiroti, M., Caschetto, M., Redaelli, A., Bozza, S., Biasibetti, M., Mostarda, L., Fumagalli, L., Bonomi, T., 2022. A cost-effective method for assessing groundwater well vulnerability to anthropogenic and natural pollution in the framework of water safety plans. J. Hydrol. 613, 128473. https://doi.org/10.1016/j.jhydrol.2022.128473

S.7.2 – Numerical Model

In this section, a detailed description of the numerical model's construction and characteristics is provided.

S.7.2.1 Model grid

The three-dimensional grid was developed using the GOCAD software (Geological Object Computer Aided Design, Paradigm, 2009). A vertical deformation of the grid between two bounding surfaces was applied (Paradigm, 2009). First of all, a first shallower layer (Layer 1) was defined using the Digital Terrain Model (DTM, with spatial resolution of 100 m (Regione Lombardia, 2024)) as top and an interpolated surface located 2–3 meters below the riverbed elevation as bottom. This bottom surface was defined to enable accurate positioning of riverbeds, thus improving the simulation of groundwater-river interactions. Beneath Layer 1, the geometry and thickness of the 10 layers corresponding to the Aquifer Group A were reconstructed by applying the vertical deformation between the bottom of Layer 1 and the bottom of Aquifer Group A, which was derived from Regione Lombardia & ENI AGIP (2002). Finally, the 5 layers representing the Aquifer Group B were deformed using the bottom surfaces of Aquifer Groups A and B. Layers with uniform thickness were set in the vertical deformation for Aquifer Group A, whereas layers with progressively increasing thickness toward the bottom were obtained for Aquifer Group B.

S.7.2.2 Hydraulic conductivity interpolation

The K values used in the interpolation were extracted from the 4686 available stratigraphic logs using TANGRAM (Bonomi et al., 2014), applying a vertical range of extraction of 1 m for each log. A natural log transformation was applied in order to obtain normally distributed data, which are better suited to kriging interpolation, as shown by previous studies (Martin and Frind, 1998). Three datasets were constructed following the log coding: 1) for Layer 1, 2) for Layers 2-11 (Aquifer A), and 3) for Layer 12-16 (Aquifer B). Specifically, omnidirectional experimental variograms were considered in the variogram modeling. To represent both local and regional structures, the variogram

models were nested, combining two spherical functions with different range values (Table S.7.2). Figure S.7.2 shows the experimental variogram with the respective model for ln(k) as an example. The obtained K values were then imported into the 3D grid (Sect. S.7.2.1) and interpolated using a 2D approach for each layer of the grid. This 2D method can be considered faster and more accurate than a full 3D analysis when simulating stratified sedimentary systems (Paradigm 2009).

Table S.7.2 *– Properties of variogram models.*

Layer	Model Variogram Type	Model Name	Variogram Type	Range	Cumulative Sill	Nugget effect
1	Nested (Models 1 and 2)	Model 1	Spherical	4850	10.7	8.05
		Model 2	Spherical	22170	11.9	
2-11	Nested (Models 1 and 2)	Model 1	Spherical	1938	13.4	10.5
		Model 2	Spherical	25000	17.3	
12-16	Nested (Models 1 and 2)	Model 1	Spherical	2997	14.6	11.7
		Model 2	Spherical	24000	17	

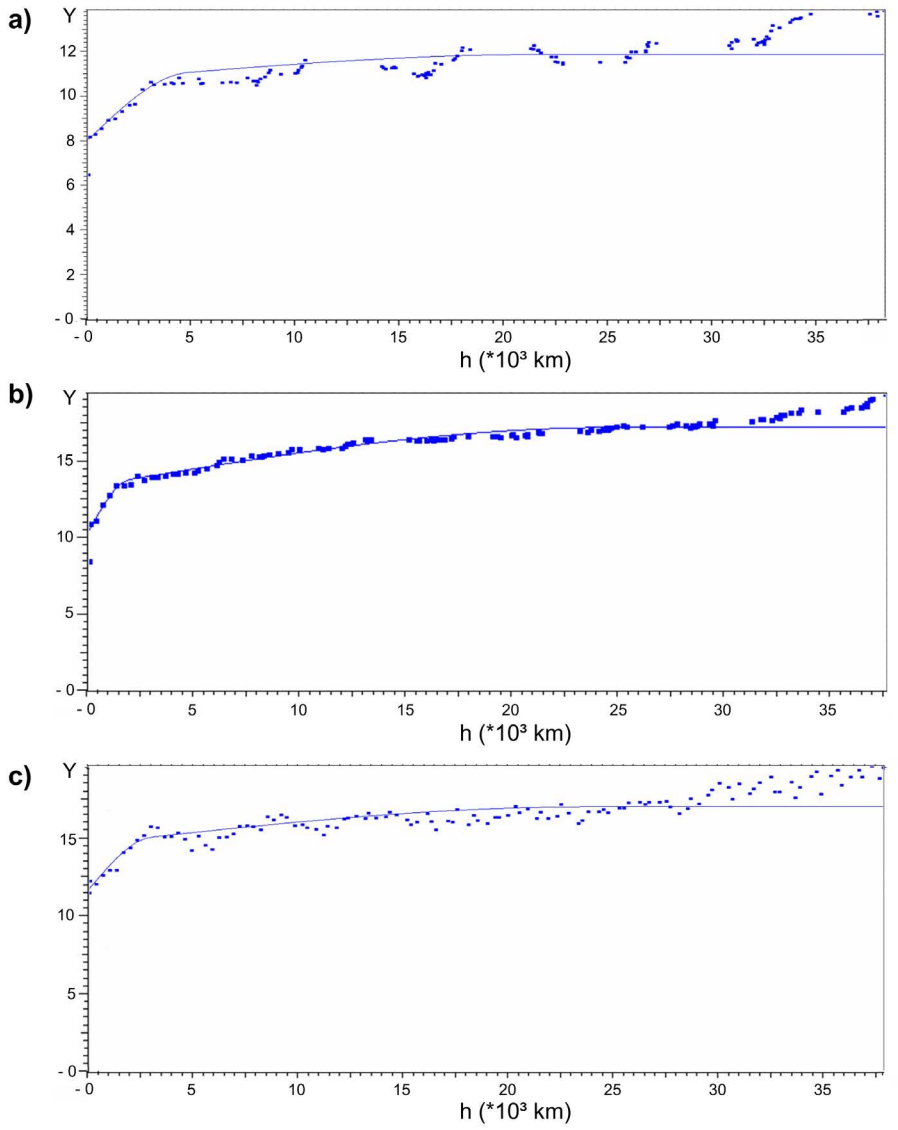

Figure S.7.2 *– Experimental variograms (blue square) and variogram models (blue line) of ln(k) for a) Layer 1, b) Layers 2-11 (Aquifer Group A), and c) Layers 12-16 (Aquifer Group B).*

S.7.2.3 Vertical Recharge zones

The monthly-variable values of effective precipitation and irrigation return flow for the different recharge zones were calculated by applying an infiltration coefficient to (a)

measured cumulative monthly precipitation and (b) estimated monthly irrigation volumes from irrigation water permits. A single infiltration coefficient of 20% was used to calculate effective precipitation, whereas two coefficient values were used for irrigation return flow: (a) 40% for the zones located in the highly permeable higher plain (zones 1-4, 6-9, and 11-15) and (b) 20% for the zones in the low-permeable lower plain (zones 5, 10, 16, and 17). A sensitivity analysis was conducted on the recharge zone values, leading to the definition of a multiplier for each zone (ranging from 0.4 to 1.6) that was applied to adjust the recharge values accordingly. Table S.7.2 reports the minimum and maximum values of vertical recharge in the 36 monthly stress periods for each zone.

Table S.7.3 *– Minimum and maximum values of vertical recharge in the 36 monthly stress periods for each zone.*

Zone Number	Min Recharge Value (m/d)	Max Recharge Value (m/d)
1	1.57E-05	4.05E-03
2	1.57E-05	4.10E-03
3	1.57E-05	8.79E-03
4	1.57E-05	3.37E-03
5	1.77E-05	1.20E-03
6	1.57E-05	6.20E-03
7	1.57E-05	3.68E-03
8	1.57E-05	1.51E-03
9	1.57E-05	3.14E-03
10	1.77E-05	1.18E-03
11	1.57E-05	1.30E-02
12	1.57E-05	8.72E-03
13	1.57E-05	3.22E-03
14	1.57E-05	8.40E-03
15	1.57E-05	6.96E-03
16	1.57E-05	2.18E-02
17	2.35E-05	2.59E-03
18	1.77E-05	1.02E-03
19	1.18E-05	6.78E-04

Zone Number	Min Recharge Value (m/d)	Max Recharge Value (m/d)
20	1.57E-05	9.04E-04
21	2.35E-05	1.36E-03

S.7.2.4 Boundary conditions

Three General Head Boundaries (GHB, a Cauchy-type boundary condition) have been imposed along the northern border of the model, with the aim of simulating the recharge contribution through the Alpine area into the plain sector (Redaelli et al., 2025; Vassena et al., 2012). GHB's position is derived from the piezometric maps reported in Rotiroti et al. (2019a) and Vassena et al. (2008). The assigned head values, reconstructed for each time step, were derived from the piezometric data of the nearest wells, measured from 2015 to 2017, to reproduce the typical seasonal groundwater level profile of this area. Along the south-eastern edge of the model domain, between the Oglio River and the southern no-flow area, a Constant Head Boundary (CHD, Dirichlet boundary condition), ranging from 23.5 m to 23.15 m a.s.l. (from N to S) was used to simulate the southern groundwater outflow from the plain. This boundary condition was selected because there are no physical limits capable of controlling the groundwater level, and because the boundary is located a great distance from the near-field area.

To simulate well withdrawals during the model simulation, the MODFLOW WEL package (a Neuman boundary condition) was used. A total of 7,426 pumping wells has been inserted into the numerical model (Fig. S.7.3), allocating pumping rates based on screen elevation. For 7408, pumping well information is derived from the TANGRAM database (Bonomi et al., 2014). Since direct measurement of pumping rate is unavailable, a discharge value equal to the daily water-use permit was initially attributed to these wells. Irrigation wells (≅ 27% of the total) were considered active only during the irrigation months (from May to September). For pumping wells without information on the daily water-use permit, the average well discharge of the wells with the same use was assigned. Information on screen depth and/or well depth was lacking for 62.5% of the wells. To address this issue, the wells were first subdivided according to

homogeneous hydrogeological areas and then according to their use. The average screen/well depth was then assigned to each subgroup from the corresponding group of wells that had this information. For 12 public wells, information on actual well pumping rate was provided by Acque Bresciane S.r.l. SB. All the pumping wells have been categorized into 16 groups, as reported in Table S.7.4.

Table S.7.4 *– Total number of wells for each group category.*

Well Categories	Total number	Percentage (%)
Zootechnical	2475	33.33%
Irrigation	2012	27.00%
Industrial	746	10.05%
Hygienic	727	9.79%
Drinking	579	7.80%
Domestic	433	5.83%
Firefighting	131	1.76%
N.A.	123	1.66%
Other Uses	104	1.40%
Pisciculture	46	0.62%
Green/Sport area	23	0.31%
Drinking - Acque Bresciane	12	0.16%
Heat pump	11	0.15%
Energy production	2	0.03%
Street washing	1	0.01%
Drinking for private	1	0.01%

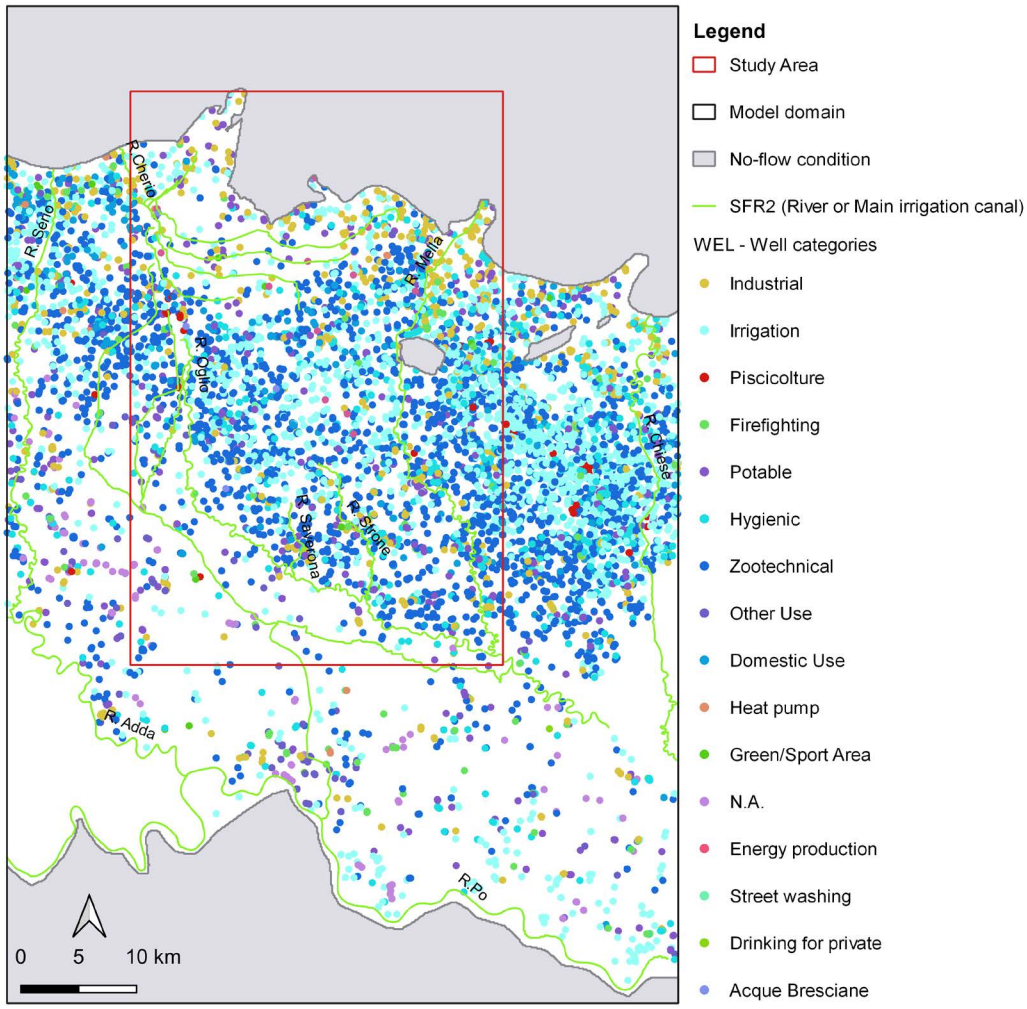

Figure S.7.3 *– Spatial distribution of the pumping wells, color-coded according to the 18 group categories.*

S.7.2.4.1 Hydrographic system

The complex hydrographic network of rivers and irrigation canals is represented by the Streamflow-Routing (SFR2) Package. This package calculates the exchange between surface-groundwater systems and routes the flow directly downstream along the hydrographic network (Niswonger and Prudic, 2010). Moreover, it allows for the simulation of disconnected stream-aquifer interaction, which was particularly important

in the higher plains, where rivers are not in direct contact with the water table (Rotiroti et al., 2019; Vassena et al., 2012). A sequence of 77 segments (8357 reaches) simulates both rivers (in a NW–SE order, including the Serio, Cherio, Oglio, Saverona, Strone, Mella, and Chiese rivers, as well as parts of the Adda and Po rivers) and the main artificial irrigation canals in the model area (see Fig. 7.4). Specifically, a detailed reconstruction of the Oglio River was conducted by dividing the river's course into 32 segments corresponding to the presence of tributaries or effluents. Each stream reach was characterized by specifying the following parameters: stream stage, bed elevation, channel width and length, streambed thickness and hydraulic conductivity, bed slope and roughness, as well as incoming flow for boundary segments. These information were identified or reconstructed through field campaign analysis, the Digital Terrain Model analyses (DTM, with spatial resolution of 100 m (Regione Lombardia, 2024)), and the information reported in the Oglio-Mella Consortium report (Consorzio di bonifica Oglio Mella, 2020). The streambed thickness was set to 1 m, and a rectangular channel was used to define the stream geometry in all model segments. The streambed slope was imposed equal to 0.001 to ensure that the stream channel altitude decreased in a downstream direction in each segment, while the streambed roughness of all segments was set at 0.037 (medium-low roughness) to simulate gravel–dominated substrates with gentle slopes (Arcement and Schneider, 1989; Barnes, 1967). A streambed hydraulic conductivity ranging from $8x10^{-8}$ m/d (representative of a nearly impermeable canal) to 1 m/d was assigned to the different segments, based on the lithology of the riverbed.. A median monthly inflow (Q) was imposed at the upstream boundary (first SFR cell) of each river segment to simulate flow propagation along the river network (Prudic et al., 2004). Specifically, the average monthly median flow released from the dam was introduced into the first SFR cell of the Oglio River, as well as the monthly volumes of water diverted into the four main irrigation canals for agricultural use were added in the first cell of each diversion. The dense network of secondary irrigation canals distributed in the model area was represented through the MODFLOW RIV package (a Cauchy boundary condition). The total number of 104921 RIV cells was assigned to Layer 1 to simulate the mechanism of collecting tailwater runoff (surface water runoff at the end of

a field) without forcing water out of the system (a passive mechanism). Finally, the MODFLOW DRN package (a Cauchy boundary condition) was used to represent the 385 lowland springs distributed within the model domain.

References

Arcement, G., Schneider, V., 1989. Guide for selecting Manning's roughness coefficients for natural channels and flood plains, Area. https://doi.org/10.3133/wsp2339

Barnes, H.H., 1967. Roughness characteristics of natural channels, U.S. Geological Survey Water-Supply Paper; Paper 1849. United States Government Printing Office, Washington, DC, USA.

Bonomi, T., Fumagalli, L., Rotiroti, M., Bellani, A., Cavallin, A., 2014. The hydrogeological well database TANGRAM©: a tool for data processing to support groundwater assessment. Acque Sotter. - Ital. J. Groundw. 3, 35–45. https://doi.org/10.7343/AS-072-14-0098

Consorzio di bonifica Oglio Mella, 2020. Piano Comprensoriale di Bonifica, Irrigazione e Tutela del territorio rurale. Delibera N.3357, Regione Lombardia. https://consorziodibonificaogliomella.com/piano-comprensorio-di-bonifica-irrigazione-e-tutela-del-territorio-rurale/

Martin, P.J., Frind, E.O., 1998. Modeling a complex multi-aquifer system: the Waterlo Moraine. Groundwater 36, 679–690.

Niswonger, R.G., Prudic, D.E., 2010. Documentation of the Streamflow-Routing (SFR2) Package to Include Unsaturated Flow Beneath Streams—A Modification to SFR1: U.S. Geological Survey Techniques and Methods 6-A13. US Geol. Surv. Tech. Methods 6 59.

Paradigm, 2009. Paradigm GOCAD 2009.1 User Guide. Houston, TX.

Prudic, D.E., Konikow, L.F., Banta, E.R., 2004. A new streamflow-routing (SFR1) package to simulate stream-aquifer interaction with MODFLOW-2000, U.S. Geological Survey, Open-File Report. https://doi.org/10.3133/ofr20041042

Redaelli, A., Bonomi, T., Sartirana, D., Sinatra, G., Rotiroti, M., Zanotti, C., 2025. The dual role of irrigation in the groundwater budget under baseline conditions versus the 2022 drought: Lessons for future climate adaptation. J. Hydrol. 658, 133211. https://doi.org/10.1016/j.jhydrol.2025.133211

Regione Lombardia, 2024. Lombardy Geoportal Metadata Download https://www.geoportale.regione.lombardia.it/en/home (accessed 10 September 2024).

Regione Lombardia & ENI Divisione AGIP, 2002. Geologia Degli Acquiferi Padani Della Regione Lombardia. Cipriano Carcano e Andrea Piccin. S.EL.CA, Florence, Italy.

Rotiroti, M., Bonomi, T., Sacchi, E., McArthur, J.M., Stefania, G.A., Zanotti, C., Taviani, S., Patelli, M., Nava, V., Soler, V., Fumagalli, L., Leoni, B., 2019. The effects of irrigation on groundwater quality and quantity in a human-modified hydro-system: The Oglio River basin, Po Plain, northern Italy. Sci. Total Environ. 672, 342–356. https://doi.org/10.1016/j.scitotenv.2019.03.427

Vassena, C., Durante, C., Giudici, M., Ponzini, G., 2008. The importance of observations on fluxes to constrain ground water model calibration. Phys. Chem. Earth 33, 1105–1110. https://doi.org/10.1016/j.pce.2008.01.004

Vassena, C., Rienzner, M., Ponzini, G., Giudici, M., Gandolfi, C., Durante, C., Agostani, D., 2012. Modeling water resources of a highly irrigated alluvial plain (Italy): Calibrating soil and groundwater models. Hydrogeol. J. 20, 449–467. https://doi.org/10.1007/s10040-011-0822-2

S.7.3 – Methodological Parameter Settings for S1 Scenario

In this section, a detailed description of the parameter setting necessary to develop S1 scenario is reported. The inflow to the Oglio River set for the baseline condition was replaced with monthly mean values of 2022 derived from daily discharge data obtained from the Consorzio dell'Oglio (2025). In addition, the abstraction rate of irrigation wells in the higher surface-water-fed irrigated plain was doubled to reflect the intensified withdrawals reported during drought conditions (ANBI Lombardia, 2023), used to compensate for the lack of surface water for irrigation. Recharge was also modified by applying multiplicative factors to its two main components: effective precipitation and irrigation return flow. For precipitation, twelve monthly factors were calculated as the ratio between the cumulative monthly precipitation in 2022 and the mean cumulative monthly precipitation over the 2016–2021 reference period. This time frame was selected to align with the reference period used by ANBI Lombardia (2023) for assessing irrigation well abstraction increment and the water diverted from the Oglio river in 2022. The resulting multiplier factors were applied uniformly to the three recharge macro-areas defined during model calibration. For irrigation return flow, since no real data were available, a proxy value corresponding to a 33% reduction in Oglio River derived-flows over the 2016–2021 reference period was adopted (ANBI Lombardia, 2023). This factor was applied to both the irrigated macro-area of the higher surface-water-fed irrigated plain and to the remaining portion of the plain, but only during the five irrigation months (May–September).

References

ANBI Lombardia, 2023. Report sulla stagione irrigua in Lombardia 2022.

Consorzio dell'Oglio, 2025. Daily Discharge Data. https://oglioconsorzio.it/dati-idrologici/dati-della-regolazione-del-lago-d-iseo/deflussi-giornalieri/ (accessed 10 July 2025).

S.7.4 – Calibration Results

In this section, Table S.7.5 reports the eight parameter groups, their descriptions, the number of parameters in each group, the ranges (minimum and maximum) of initial values obtained after manual trial-and-error calibration, the ranges (minimum and maximum) of applied bounds, and the final calibrated value ranges (minimum and maximum). For groups comprising different parameter types, additional subdivisions into subgroups are provided, together with the corresponding information. Moreover, a detailed description of the set of parameter values obtained by parameter estimation calibration performed through PEST is presented. Calibrated hydraulic conductivity in Aquifer Group A zones ranged from 0.02 to 265.38 m/d, while in Aquifer Group B zones it ranged from 0.17 to 396.47 m/d. Vertical anisotropy values were varied by ±4%. The calibrated Sy in the 3 considered zones was 0.062, 0.105, and 0.158, while Ss ranged respectively from 9.97×10^{-6} to 1×10^{-5} m^{-1} in Aquifer Group A and from 9.88×10^{-6} to 1×10^{-5} m^{-1} in Aquifer Group B. Streambed hydraulic conductivity ranged from 8×10^{-8} to 1.92 m/d. For the Oglio River (segments 1-32), calibrated values ranged between 3.77×10^{-3} and 1.92 m/d. The calibrated conductivity of the secondary irrigational canal network remained unchanged, while the calibrated drain conductivity was reduced by 56%. The calibrated inflows of the Oglio and Cherio Rivers were, on average, adjusted by ±4%. In the higher surface-water-fed irrigated plain, the calibrated recharge was consistently lower than pre-calibration values in every stress period, with multipliers ranging from 0.19 to 0.98. In contrast, in the lower groundwater-fed irrigated plain, recharge was increased in 47% of the stress periods, with multipliers ranging from 0.14 to 2. In the remaining portion of the plain, recharge was increased in 67% of the stress periods, with applied multipliers ranging from 0.17 to 2. Finally, abstraction rates for irrigation wells located upstream of the main irrigation canals and in the higher surface-irrigated plain were reduced in all stress periods, with a reduction ranging from 2% to 13% of the initial value. For wells in the medium-lower groundwater-fed irrigated plain and in the lower groundwater-fed plain, there was a decrease in the withdrawal rate in 73% and 53% of the total stress period, respectively. Specifically, for the wells located

in the medium-lower groundwater-fed plain, the multipliers ranged between 0.8 and 1.06, while for the wells located in the lower groundwater-fed plain, the multipliers ranged between 0.89 and 1.14.

Table S.7.5 *– List of the eight parameter groups, their descriptions, the numbers of parameters in each sub-group, ranges of initial values set after manual trial and error calibration (for each sub-group, the minimum and the maximum values of all parameters are reported), the ranges of the applied bounds (for each sub-group, the minimum and the maximum bounds of all parameters are reported), and the ranges of final values (for each sub-group, the minimum and the maximum final values of all the parameters are reported).*

Group	Description	N° of parameters	Min Initial Value	Max Initial Value	Min Lower Bound	Max Upper Bound	Min Final Value	Max Final Value
1	Hydraulic conductivity multiplier for the secondary canal beds	1	1	1	0.1	2	1.00	1.00
2	Streambed hydraulic conductivity values (m/d)	79	8.00E-08	1.00E+00	8.00E-09	1.00E+01	7.99E-08	1.92E+00
	Lowland spring hydraulic conductivity value (m/d)	1	5.00E+03	5.00E+03	1.00E-05	1.00E+06	2.22E+03	2.22E+03
3	Inflow in the first cell of the Oglio River (m^3/d)	36	2.23E+06	7.44E+06	2.01E+06	8.18E+06	2.01E+06	6.70E+06
	Inflow in the first cell of the Cherio River (m^3/d)	36	8.00E+03	2.21E+05	1.60E+03	1.11E+06	7.81E+03	2.27E+05
4	Recharge multipliers	108	1	1	0.1	2	0.14	2.00
5	Horizontal hydraulic conductivity values for Aquifer Group A (Layers 1-11) (m/d)	20	4.80E-02	1.99E+02	4.80E-03	1.99E+03	1.89E-02	2.50E+02

Group	Description	N° of parameters	Min Initial Value	Max Initial Value	Min Lower Bound	Max Upper Bound	Min Final Value	Max Final Value
	Horizontal hydraulic conductivity values for Aquifer Group B (Layers 12-16) (m/d)	20	4.80E-02	1.99E+02	4.80E-03	1.99E+03	1.69E-01	1.98E+02
6	Vertical anisotropy	20	1.00E+01	1.00E+01	1.00E+00	1.00E+03	9.68E+00	1.28E+01
7	Specific yield values (Sy)	3	7.00E-02	2.00E-01	1.00E-02	3.00E-01	6.24E-02	1.58E-01
	Specific storage values (Ss) for Aquifer Group A (Layers 1-11) (m^{-1})	3	1.00E-05	1.00E-05	1.00E-07	1.00E-02	9.97E-06	1.00E-05
	Specific storage values (Ss) for Aquifer Group B (Layers 12-16) (m^{-1})	3	1.00E-05	1.00E-05	1.00E-07	1.00E-02	9.88E-06	1.00E-05
8	Abstraction rate multipliers for the irrigation wells	144	1	1	0.8	1.2	0.80	1.14

S.7.5 – Annual storage variations

In this section, Figure S.7.4 shows the annual storage variation for a) the higher surface-water-fed irrigated plain and b) the lower groundwater-fed irrigated plain.

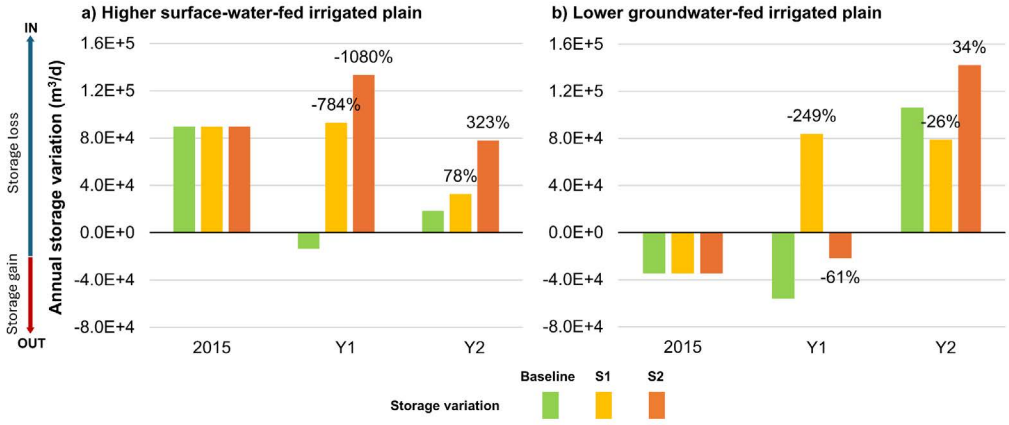

Figure S.7.4 *– Annual storage variation for* ***a)*** *the higher surface-water-fed irrigated plain and* ***b)*** *the lower groundwater-fed irrigated plain. The percentages refer to the annual storage variation in Y1 and Y2 of the two scenarios, S1 (yellow) and S2 (orange), compared to the baseline simulation (2015-2017, green). Y1 and Y2 refer to the first and the second year of the S1 and S2 scenarios. Positive storage variation indicates a loss of storage (blue arrow), while negative storage variation indicates a gain in storage (red arrow).*

Chapter 8: Conclusions

The main aim of this PhD project was to investigate the key processes governing the groundwater budget in a highly anthropized system characterized by intensive agricultural activities, with the ultimate goal of identifying and quantifying the main drivers of the system and their vulnerability in the context of a changing climate.

To achieve this goal and to provide practical support to decision-makers, two phases were followed, in particular:

1. A data-driven approach was applied to the groundwater level time series to investigate groundwater dynamics in different hydrogeological contexts in the Brescia province. The main aim of this phase was to develop a procedure to exploit dynamic data from active wells to identify the main processes governing the groundwater budgets under baseline conditions (2013-2021) and to compare their dynamics under critical conditions (2022 hydrogeological drought).
2. A model-based approach that led to the implementation of a basin-scale numerical groundwater flow model for the Oglio River basin. The main aim of this phase was to quantify the inputs and outputs of a highly human-influenced system with significant agricultural activity, and to perform a quantitative assessment of two synthetic scenarios of practical interest (i.e., meteorological drought and a change in irrigation practices as a potential result of reduced surface water availability), identifying the main driver of potential future aquifer depletion.

The development of this work allowed for different considerations that are summarized in the following paragraphs.

8.1 Data-driven approach

Findings from the analysis conducted in this first phase of this PhD thesis demonstrated how dynamic data collected from active wells, when properly managed, can represent a crucial resource. The proposed procedure offers valuable support to both researchers and water managers, providing a key tool for improving groundwater monitoring and management, and enabling the extraction of multiple groundwater level time series,

particularly useful in regions where monitoring networks are often missing or insufficient.

The extracted seasonal groundwater level time series from 61 wells were analyzed to investigate different hydrogeological contexts in the province of Brescia, including the Alpine area, the morainic amphitheaters of Lake Iseo and Lake Garda, the higher plain, the middle plain, and the lower plain, as well as different water management practices.

First, a cluster analysis was used to identify the typical seasonal patterns of the hydrogeological systems investigated under baseline conditions (2013-2021). The clusters were then analyzed to identify the average seasonal patterns and the associated recharge and discharge processes. Subsequently, the 2022 data were compared with the baseline data to quantify the effect of the hydrological drought.

Results highlighted the central role of irrigation on the groundwater budget of the main aquifer systems in the plain area, with different effects based on the water source (i.e., surface water or groundwater-fed irrigation).

Specifically, in the higher plain, the seasonal profile, with its summer rising, can be associated with recharge from surface-water-fed irrigation return flow. For this reason, surface water scarcity under hydrological droughts (as in 2022) can rapidly induce groundwater depletion due to the lack of recharge from irrigation return flow and the consequent increase in groundwater abstraction to compensate for the lack of surface water. In these regions, the transition toward more efficient irrigation practices, such as sprinkling or micro irrigation, would determine a significant reduction of aquifer recharge and would require compensation measures such as managed aquifer recharge during wet seasons.

Conversely, in the lower plain, where groundwater-fed irrigation is the main irrigation practice, a pluriannual trend with significant summer decreases was observed. Here, the increased irrigation needs under hydrological droughts (as in 2022) can lead to greater summer groundwater depletion than the average summer depletion observed under baseline conditions. Mitigation actions to reduce abstracted groundwater volumes, such

as transitioning to more efficient irrigation systems, could reduce groundwater vulnerability to climate change.

On the contrary, aquifer systems mainly governed by natural recharge and discharge processes (i.e., Alpine aquifers and Morainic aquifers) are more vulnerable to pluriannual variability associated with dry and wet years, while they are less affected by individual dry seasons than highly anthropogenic systems.

8.2 Model-based approach

Results from the second phase of this PhD thesis demonstrated that numerical models are effective tools for quantifying the volumes of water exchanged among the system's components, not only under baseline conditions but also under hypothetical scenarios.

During this second phase, a basin-scale numerical groundwater flow model (MODFLOW-NWT code) for the Oglio River basin was developed to quantify the inputs and outputs of two of the most important and productive compartments that characterize the Brescia province: the surface-water-fed irrigated plain and the lower groundwater-fed irrigated plain.

Using the MODFLOW's Hydrostratigraphic Unit (HSU) option, all the inflows and the outflows of the two main compartments were quantified. In the higher surface-water-fed irrigated plain, results indicated that the irrigation return flow (the main component of the vertical recharge) constituted the main component of the total inflow while the outflow was mainly generated by discharge to the lower plain aquifer. In the lower plain, the main inflow was the outflow from the higher plain, while aquifer outflow was generated by gaining rivers.

Subsequently, two synthetic hydrological scenarios of practical interest were simulated to assess the changes in the water budget caused by the two most significant potential stressors: 2-year droughts (S1 scenario) and a shift from traditional irrigation methods to more efficient techniques aimed at reducing irrigation return flow to cope with surface water scarcity (S2 scenario).

The comparison between baseline conditions and the two scenarios highlights the crucial role of surface-water-irrigation return flow in maintaining groundwater balance and the ecological functions of the groundwater-dependent system (e.g., lowland springs, baseflow to rivers). While 2-year drought conditions (S1) attenuated recharge mechanisms without significantly altering seasonal dynamics, the reduction in irrigation return flow (S2) induced a drastic change in the system, especially in the higher surface-water-fed irrigated plain, leading to the disappearance of the typical summer rise in groundwater, persistent loss in groundwater storage during the irrigation season, and a decrease in spring discharges.

Therefore, findings from the analysis conducted in this second phase of the thesis indicated that, if not tailored to the specific hydrological and hydrogeological context, the adaptation measures implemented by policymakers to address surface water scarcity induced by climate change may have a greater impact on groundwater resources than the direct effects of climate change itself. This emphasizes the importance of carefully selecting context-specific adaptation measures, supported by targeted research and improved communication between academia and policymakers, to ensure the sustainable management of water resources.

8.3 Final remarks

In conclusion, the research work and the results of this PhD led to the following considerations:

- Time series analysis proved to be an effective tool to perform data mining on groundwater level data. Particularly, a focus on seasonal patterns allowed for the identification of the main drivers governing groundwater availability over different hydrogeological contexts, providing insights into their vulnerability to climate change.
- Groundwater numerical flow models, on the other hand, have been demonstrated to be a valuable instrument for an actual quantification of the volumes exchanged among the system's components, taking into consideration all the

natural and anthropic elements of the system (e.g., surface water bodies, springs discharge, and well abstraction) and their modification induced by changes in climatic variables or human adaptation measures.

- Human processes play a significant role in the equilibrium of the aquifer systems, and therefore, human response to climate change in terms of water management can exacerbate the effects of climate change.
- Adaptation strategies' effects, if not implemented following local studies and specific needs, could exceed the magnitude of the direct climatic impacts on groundwater resources.

On the whole, the combination of all the proposed methodologies and tools provides a deeper knowledge of the aquifer systems, thus bringing valuable support to researchers, stakeholders, and decision makers, offering tools for more effective groundwater management in the context of climate change, particularly in regions where irrigation plays a central role.

Appendix A: Articles and Presentations

A.1 Articles

1. **Redaelli, A.**, Bonomi, T., Sartirana, D., Sinatra, G., Feinstein, D.T., Hunt, R.J., Rotiroti, M., Zanotti, C. *Changes in irrigation practices may bankrupt aquifers faster than meteorological droughts: a numerical modeling approach.* **Submitted**

2. **Redaelli, A.**, Bonomi, T., Sartirana, D., Sinatra, G., Rotiroti, M., Zanotti, C. (2025). *The dual role of irrigation in the groundwater budget under baseline conditions versus the 2022 drought: Lessons for future climate adaptation.* JOURNAL OF HYDROLOGY, 658 [10.1016/j.jhydrol.2025.133211]. https://dx.doi.org/10.1016/j.jhydrol.2025.133211

3. Sartirana, D., Zanotti, C., Rotiroti, M., Caschetto, M., **Redaelli, A.**, Bruno, S., Fumagalli, L., De Amicis, M., Bonomi, T. (2024). *Urban Water Management in Milan Metropolitan Area, a review.* ACQUE SOTTERRANEE, 13(3), 103-122 [10.7343/as-2024-763]. https://dx.doi.org/10.7343/as-2024-763

4. Zanotti, C; Palazzi, A; Bonomi, T; Fumagalli, L; **Redaelli, A**; Caschetto, M; Stano, C; Rotiroti M. (2024). *Mixing processes in wells tapping confined acquifers: quality and risks assessment for public drinking water supply.* In: Chenchouni, H., et al. Recent Advancements from Aquifers to Skies in Hydrogeology, Geoecology, and Atmospheric Sciences. MedGU 2022. Advances in Science, Technology & Innovation. Springer, Cham. https://dx.doi.org/10.1007/978-3-031-47079-0_10

5. Biasibetti, M., Longhi, E., Bozza, S., Zanotti, C., Rotiroti, M., Fumagalli, L., Caschetto, M., **Redaelli, A.**, Bonomi, T. (2024). *Climate-related risk assessment in water safety plans: the case study of Acque Bresciane (Italy).* JOURNAL OF WATER AND HEALTH, 22(1), 97-122 [10.2166/wh.2023.103]. https://dx.doi.org/10.2166/wh.2023.103

6. Zanotti, C., Rotiroti, M., **Redaelli, A.**, Caschetto, M., Fumagalli, L., Stano, C., Sartirana, D., Bonomi, T. (2023). *Multivariate Time Series Clustering of Groundwater Quality Data to Develop Data-Driven Monitoring Strategies in a Historically Contaminated Urban Area.* WATER, 15(1) [10.3390/w15010148]. https://doi.org/10.3390/w15010148

7. Sartirana, D., Zanotti, C., Rotiroti, M., De Amicis, M., Caschetto, M., **Redaelli, A.**, Fumagalli, L., Bonomi, T. (2022). *Quantifying Groundwater Infiltrations into*

Subway Lines and Underground Car Parks Using. MODFLOW-USG. WATER, 14(24), 1-23. https://doi.org/10.3390/w14244130

8. Bonomi, T; Toscani, L; Sartirana, D; Stefania, G.A; Zanotti, C; Rotiroti, M; **Redaelli, A.**, Fumagalli, L. (2022). *Modeling groundwater/surface water interactions in an industrial area (Mantua, Italy).* Acque sotterranee. https://doi.org/10.7343/as-2022-569

9. Zanotti, C; Rotiroti, M; Caschetto, M; **Redaelli, A**; Bozza, S; Biasibetti, M; Mostarda, L; Fumagalli, L; Bonomi, T (2022). *A cost-effective method for assessing groundwater well vulnerability to anthropogenic and natural pollutions in the framework of Water Safety Plans.* Journal of Hydrology. https://dx.doi.org/10.1016/j.jhydrol.2022.128473

A.2 Communication to conferences

1. **Redaelli, A**., Zanotti, C., Fumagalli, L., Arici, S., Procopio, G., Palazzi, A., Rotiroti, M. & Bonomi, T. (2025). *Hydrogeological characterization of the complex hydrogeological system of the Brescia metropolitan area (N Italy) in the framework of Water Safety Plan.* In 7th Edition of FLOWPATH the National Meeting on Hydrogeology. Conference Proceedings Book. (**Abstract and Poster presentation**)

2. Caschetto, M., Zanotti, C., Pinti, D., Sacchi, E., Sartirana, D., **Redaelli, A.**, Bruno, S., Fumagalli, L., Bonomi, T., Riparbelli, C., Brenna, S., Rotiroti, M. (2023). *Groundwater ages distribution along an alluvial basin aquifer: how age estimates can guide nitrate mitigation in groundwater?* International Symposium on Isotope Hydrology. (**Abstract and Oral Presentation**)

3. **Redaelli, A.**, Rotiroti, M., Bonomi, T., Fumagalli, L., Caschetto, M., Esposto, F., Sinatra, G., Olivieri, M., Bozza, S., Zanotti, C. (2023). *A reproducible procedure to elaborate long groundwater level and abstraction rate time series acquired from data logger, a present-day necessity.* In 6th Edition of FLOWPATH the National Meeting on Hydrogeology. Conference Proceedings Book (pp.14-14). (**Abstract and Oral Presentation**)

4. Sartirana, D., Zanotti, C., Rotiroti, M., De Amicis, M., Caschetto M., **Redaelli, A.**, Fumagalli L., Bonomi T. (2023). *A Local-Scale Numerical Model to Quantify*

Groundwater Infiltrations into Underground Infrastructures: The Case of Milan. In 6th Edition of FLOWPATH the National Meeting on Hydrogeology. Conference Proceedings Book (pp.81-81). (**Abstract and Poster Presentation**)

5. Rotiroti, M., Caschetto, M., Zanotti, C., **Redaelli, A.**, Bruno, S., Sartirana, D., Sacchi, E., Riparbelli, C., Brenna, S., Fumagalli, L., Bonomi, T. (2023). *Changes in shallow groundwater recharge due to drought impacting the Po River Basin.* In 6th Edition of FLOWPATH the National Meeting on Hydrogeology. Conference Proceedings Book (pp.67-68). (**Abstract and Oral Presentation**)

6. Caschetto, M., Zanotti, C., Pinti, D., Sacchi, E., Sartirana, D., **Redaelli, A.**, Bruno, S., Fumagalli, L., Bonomi, T., Riparbelli, C., Brenna, S., Rotiroti, M. (2023). *Groundwater age modelling to refine knowledge on the hydrogeological functioning of the shallow alluvial aquifer in the Po River Basin.* In 6th Edition of FLOWPATH the National Meeting on Hydrogeology. Conference Proceedings Book (pp.103-104). (**Abstract and Poster Presentation**)

7. Zanotti, C., Rotiroti, M., **Redaelli, A.**, Caschetto, M., Fumagalli, L., Stano C., Sartirana, D., Bonomi T. (2023). *Data-driven monitoring strategies for groundwater quality protection through time series clustering of groundwater pollution data.* In 6th Edition of FLOWPATH the National Meeting on Hydrogeology. Conference Proceedings Book (pp.23-24). (**Abstract and Poster Presentation**)